Modelling and Analysis of a District Heating Network

Marouf Pirouti

School of Engineering, Cardiff University

A thesis submitted for the degree of
Doctor of Philosophy

February 13, 2013

Acknowledgment

This research would not have been possible without the support of many people. First and foremost, I would like to thank my supervisors, Prof. Nick Jenkins and Dr. Jianzhong Wu who were abundantly helpful and offered invaluable assistance, support and guidance.

My deepest gratitude is due to Dr. Audrius Bagdanavicius and Dr. Janaka Ekanayake, whose advice and scientific guidance helped me greatly in conducting my research and developing this thesis.

I would like to thank members of the Energy Infrastructure group at CIREGS, who provided me with a great deal of additional insight during many hours of weekly meetings and discussions. Particular appreciation goes to Marc Rees and Meysam Qadrdan for their assistance both during my research and especially during the development of this thesis.

I also would like to thank staff in the research office, graduate office and EPSRC via SUPERGEN-HiDEF project for providing supporting activities and training.

Last but not the least; I would like to thank my loving family for all their support, patience and encouragement.

DECLARATION

This work has not previously been accepted in substance for any degree and is not concurrently submitted in candidature for any degree.

Signed .... (Candidate) Date ....

This thesis is being submitted in partial fulfilment of the requirements for the degree of PhD.

Signed .... (Candidate) Date ....

This thesis is the result of my own independent work/investigation, except where otherwise stated. Other sources are acknowledged by explicit references.

Signed.................................... .... (Candidate) Date ....

I hereby give consent for my thesis, if accepted, to be available for photocopying and for interlibrary loan, and for the title and summary to be made available to outside organisations.

Signed.. (Candidate) Date…..............................

Abstract

District heating systems have the potential to contribute to the UK renewable energy targets. However, there are a number of economic barriers which would have to be addressed in order to make district heating competitive in comparison with alternative heating technologies. The objective of this research was to model and analyse a district heating network and develop an optimisation method to calculate the minimum capital investment, heat losses and pump energy consumption.

Firstly, modelling and analysis of a district heating network was conducted to obtain district heating design cases with minimum annual total energy consumption, annual total exergy consumption and annualised cost. Then through the analysis, a two-stage programming model was developed which synthesised design and optimal operation of a district heating network. The optimisation was used to minimise annual total energy consumption, annual total exergy consumption or annualised cost of the heat network by selecting suitable pump and pipe sizes, taking into account different parameters such as target pressure loss, temperature regime and operating strategy. The optimisation technique was used to investigate two different case studies, with high and low heat density.

In all cases, a variable flow and variable supply temperature operating method was found to be beneficial. Design cases with minimum annual total energy consumption and annualised cost used rather small pipe diameters and large pressure drops. To achieve the minimum annual total exergy consumption a design case with larger pipe diameters and smaller pressure loss was found to be desirable. It was observed that by reducing the water temperature and increasing temperature difference between supply and return pipes, the annual total energy consumption, annual total exergy consumption and the annualised cost were reduced. It was also shown that district heating in an area with high heat density is more energy efficient and cost effective.

Publications

Journal

- M. Pirouti, A. Bagdanavicius, J. Wu, N. Jenkins and J. Ekanayake, "Modelling and optimisation of a district heating network," To be published.

- M. Pirouti, A. Bagdanavicius, J. Ekanayake, J. Wu, and N. Jenkins, "Energy consumption and economic analyses of a district heating network," *Energy (in press)*, 10.1016/j.energy.2013.01.065

Conference

- M. Pirouti, J. Wu, J. Ekanayake, and N. Jenkins, "Dynamic modelling and control of a direct-combustion biomass CHP unit," in *45th International Universities Power Engineering Conference (UPEC), August 31st -September 3rd, Cardiff, UK*, 2010, pp. 1–6.

- M. Pirouti, J. Wu, A. Bagdanavicius, J. Ekanayake, and N. Jenkins, "Optimal operation of biomass combined heat and power in a spot market," in *2011 IEEE PowerTech,19-23 June, Trondheim, Norway*, 2011, pp. 1–7.

- M. Pirouti, A. Bagdanavicius, J. Wu, and J. Ekanayake, "Optimisation of supply temperature and mass flow rate for a district heating network," in *The 25th International Conference on Efficiency, Cost, Optimization, Simulation and Environmental Impact of Energy Systems (ECOS), June 26-29, Perugia, Italy*, 2012, pp. 104–1–104–12.

- M. Pirouti, A. Bagdanavicius, J. Wu, N. Jenkins, and J. Ekanayake, "Optimal operation of a district heating system," in *The 7th Conference on Sustainable Development of Energy, Water and Environment Systems (SDEWES), July 1-7, Ohrid, Republic of Macedonia*, 2012, pp. 1–10.

- M. Pirouti, A. Bagdanavicius, J. Ekanayake, J. Wu, and N. Jenkins, "Selection of optimal pipe diameters in a district heating network using minimisation of annual total energy and exergy consumption," in *DHC13, the 13th International Symposium on District Heating and Cooling September 3rd to September 4th, Copenhagen, Denmark*, 2012, pp. 176–182.

- Y. Xing, A. Bagdanavicius, S. Lannon, M. Pirouti, and T. Bassett, "Low temperature district heating network planning with focus on distribution energy losses," in *International Conference on Applied Energy, ICAE 2012 - 5-8 July, Suzhou, China, 2012,* pp.1-10.

Contents

List of Figures

List of Tables

Nomenclature

Abbreviations

ASHP	Air source heat pump
CHP	Combined heat and power
CCGT	Combined cycle gas turbine
CF-CT	Constant flow and constant temperature
CF-VT	Constant flow and variable temperature
DH	District heating
EAC	Equivalent annual cost
EFW	Energy from waste
EU	European Union
EFTA	European Free Trade Association
GSHP	Ground source heat pump
HEX	Heat exchanger
MPL	Maximum pressure loss
NPV	Net present value
ST	Steam turbine
SLP	Sequential linear programming
TPL	Target pressure loss
VF-CT	Variable flow and constant temperature
VF-VT	Variable flow and variable temperature

Parameters

A	Annuity factor
b	Index for binary variable
C	Cost, £
c_p	Specific heat capacity, kJ/kg.K
d	Diameter, mm or m

D_d	Degree days, K.day
E	Energy, kWh or MWh
Ex	Exergy, kWh or MWh
$\dot{Ex}$	Exergy rate, kW or MW
f	Friction factor
h	Heat loss coefficient, kW/K
H	Head loss, m
i	Interest rate, %
l	Pipe length, m
$\dot{m}$	Mass flow rate, kg/s
p	Pressure, Pa or bar
Δp	Differential pressure, Pa or bar
P	Electrical power, kW or MW
Q	Thermal power, kW or MW
Re	Reynolds number
T	Temperature, °C or K
U	Heat transition coefficient, W/mK
u	Velocity, m/s
$\dot{V}$	Volume flow rate, m^3/s
V	Volume, m^3
ξ	Consumers pressure drop coefficient
v	Kinematic viscosity, m^2/s
η	Efficiency
ε	Pipe roughness, mm
ρ	Water density, kg/m^3
δ	Index for difference in differential pressure, Pa or kPa

Subscripts and superscripts

b	Boiler
chp	CHP
c	Consumer
e	Electricity

eq	Equivalent
$fuel$	Fuel
g	Ground
inl	Inlet
ind	Indoor
j	Index for pipe section
k	Index for node
$loss$	Heat losses
L	Index for load
min	Minimum
max	Maximum
M	Number of pipe section
N	Number of node
o	Time step 0
$outl$	Outlet
$outd$	Outdoor
p	Pump
r	Return
s	Supply
src	Source
st	Index for standard pipe size
SH	Space heating
t	Time step
th	Thermal
T	Total
w	Water
Y	Number of standard pipe sizes

CHAPTER 1- Introduction

1.1 Background

In the UK heat demand for homes, businesses and industrial processes accounts for around 49% of total energy demand and 47% of the carbon emissions[1]. The majority of domestic and none domestic buildings use individual heating systems such as gas boilers or electricity. Less than 0.5% of heat is from renewable sources [1].

The UK government has a target to reduce carbon emissions to at least 34% below the base year level[1] in 2020 [2], and to deliver 15% of the UK's energy consumption from renewable sources by 2020 [3]. Renewable heat is expected to contribute approximately a third of this overall renewable energy target. Therefore, to achieve the UK overall renewable energy target, around 12% of the total heat demand in 2020 will need to come from renewable energy [4]. Debates are now taking place on how to supply heat for buildings in future in order to reduce or completely avoid the use of fossil fuels [5–8].

District heating (DH) systems have the potential to contribute to the renewable energy targets. DH systems offer the primary energy savings, especially where heat and electricity are generated in a single unit (CHP) or waste heat from existing power

[1] The base year is 1990 for carbon dioxide, nitrous oxide and methane.

plants is recovered. In addition, DH has the flexibility to accommodate heat from a variety of renewable heat sources including: biomass, solar thermal and geothermal. A study conducted by BRE [9], shows that under the right conditions[1], DH could supply up to 14% of the UK's heat demand. It could be a cost-effective and viable alternative to individual heating technologies while reducing bills for consumers. According to the National Heat Map for England [10], 50% of the heat demand in England is concentrated with sufficient density to make a DH network worth investigating[2]. However, there are a number of economic barriers[3] (i.e. high capital investment, heat losses and pumping costs) which would have to be addressed in order to make DH competitive in comparison with alternative heating technologies.

1.2 Policy drivers for district heating in the UK

District heating has many benefits including the reduction of fuel poverty levels in the UK through achieving cost savings. Fuel-poor households spend more than 10% of their overall income on fuel [11]. DH also allows whole communities to be switched to new and emerging technologies fuelled by low and zero-carbon energy sources. The fuel flexibility of DH systems can lead to the integration of renewable technologies that are crucial to the overall reduction of carbon emissions.

As a consequence of the prevalence of fuel poverty (Figure 1-1 and Figure 1-2)[12], [13], as well as carbon reduction targets for buildings, and the Code for Sustainable Homes in particular [14], the role of DH as a low carbon solution is being increasingly considered in the UK.

[1] District heating is best suited to urban areas with high heat demand, with a mix of different building types.

[2] District heating becomes economically viable at heat density of 3000 kW/km^2 [10].

[3] Active government policy such as financial incentives also can increase the economic competitiveness of district heating compared with alternative heating technologies.

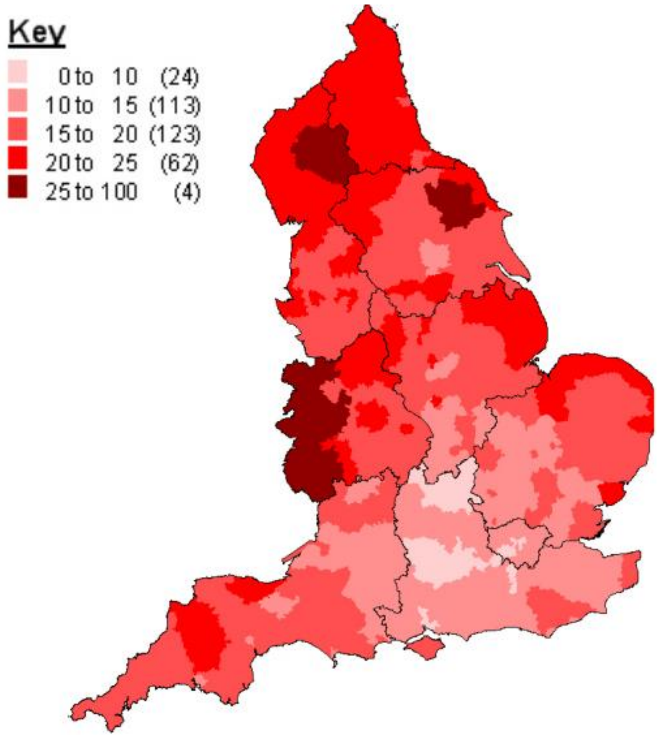

Figure 1-1 Percentage of households in fuel poverty at local authority level, England, 2010 [12]

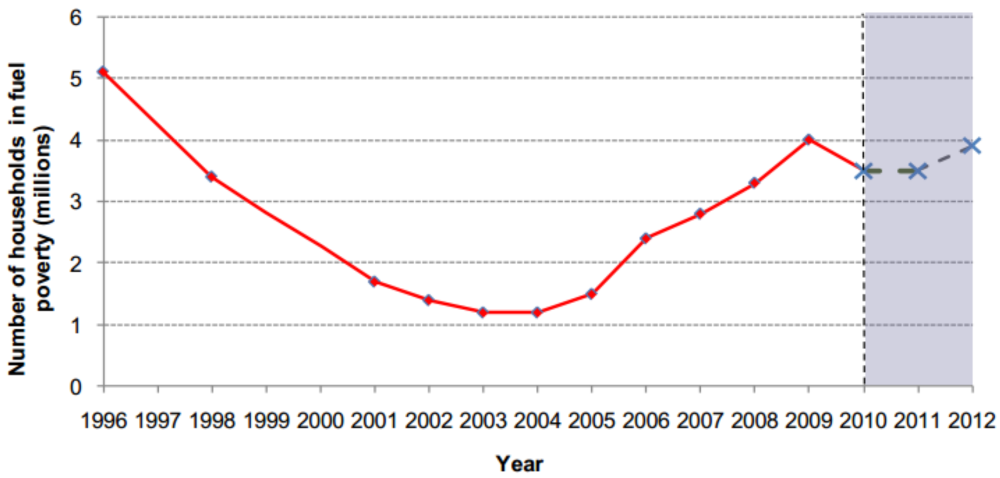

Figure 1-2 Number of households in fuel poverty 1996- 2010, and projections for 2011 and 2012, England [12]

There are current political considerations of DH as a heat delivery method in the UK. There is an increased interest in the DH networks from the UK government, as demonstrated by the Strategic Framework for Low Carbon Heat in the UK [10]. For instance, to achieve the higher levels of the Code for Sustainable Homes, the UK government guidelines on planning acknowledge the benefits that can be obtained by using energy-generating plants located closer to the end consumer (i.e. DH) [15]. These benefits include:

- The use of locally available energy sources including waste heat from adjacent sites where commercial or industrial activities may be dumping heat;
- The use of heat generated from renewable sources, e.g. biomass, geothermal and solar thermal heat;
- The use of heat from CHP plants.

Overall, the various drivers that are stimulating an increased use of DH include high targets set for CO_2 emission reduction, as well as the prevalence of fuel poverty [16], [17].

1.3 District heating systems

District heating is a means of delivering heat to multiple buildings from a central source as shown in Figure 1-3.

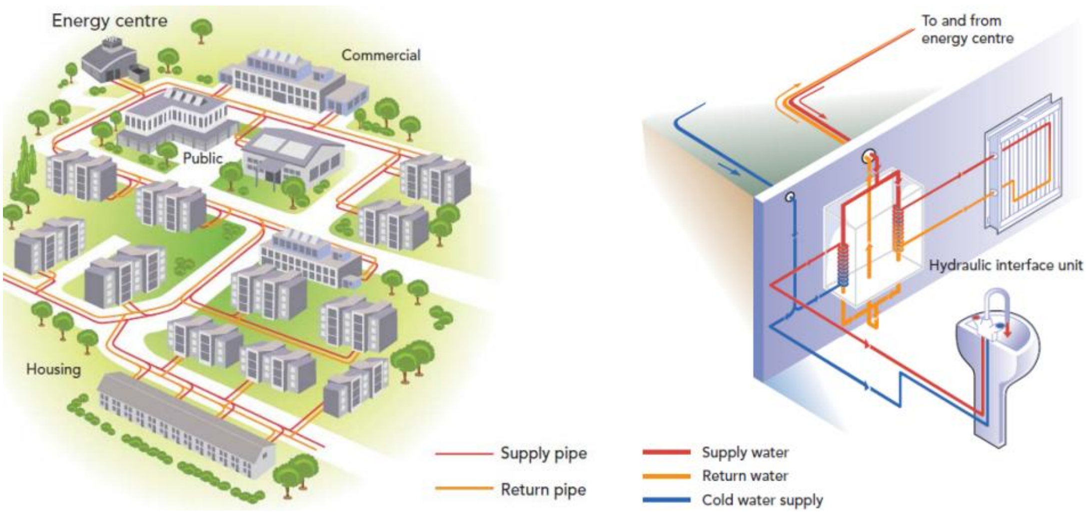

Figure 1-3 District heating pipe network (left) and the hydraulic interface unit (right) [18]

There are three basic parts in a DH system: an energy centre containing heat sources, a hydraulic interface unit for each customer (e.g., heat exchangers) and a network of pipes to connect the heat source to the consumers. The energy centre can include a range of technologies and fuels. Hot water from the energy centre is pumped through the pipe network to the individual buildings. In each dwelling, heat is conveyed via the hydraulic interface unit to the central heating radiators and to the hot water taps.

1.3.1 Development of district heating

District heating systems have been used in Europe since the 14th century, with one geothermal DH system (Chaudes-Aigues thermal station in France) which has been in continuous operation since that time. The US Naval Academy constructed the first DH service on its Annapolis campus in 1853 [19]. However, the American engineer Birdsill Holly is considered to be the founder of modern DH and was involved in the first commercially successful DH scheme at Lockport, New York in 1877 [11].

Nowadays, DH systems can be found in many countries but the level of expansion and market penetration varies between different states. For example, the share of DH for the supply of heat varies from 99% in Iceland to about 1% in the USA (Figure 1-4). Northern European countries are the main users of DH systems. DH systems currently cover around 12% of the European heat market for buildings in the residential and service sectors. The equivalent market share for the industrial sector is about 9% [20].

In Europe, DH systems have networks containing distribution pipes with a total trench length of almost 200,000 km. Total revenues for selling heat are about €30 billion per year [20]. The DH systems in EU15 and EFTA3[1] are expanding by about 2800 km annually. This is equivalent to about 3% of total installed trench length. This gives a demand of 5600 km of new distribution pipes per year [21].

[1] European Free Trade Association

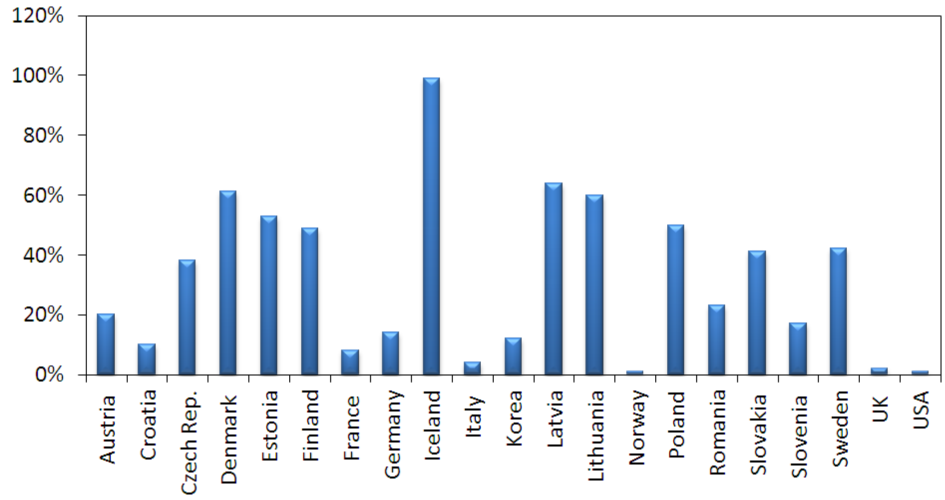

Figure 1-4 Share of citizens served by district heating [22]

District heating grew significantly in the UK during the council house building boom from the 1950s to 1970s. However it achieved a low market penetration and currently provides less than 2% of the UK heat demand (Figure 1-4), supplying 172,000 domestic buildings (predominantly social housing, tower blocks and public buildings) and a range of commercial and industrial applications [10]. The low level of DH deployment reflects past policy choices, most significantly the UK's decision to access natural gas from North Sea, which provides a cost effective and reliable source of heating [10]. Further, those systems were not well designed or maintained; and problems regularly arose with water penetration and pipe corrosion in the network. In addition, heat networks suffered from a poor reputation, where customers were unable to control their heat supply and bills, or where the efficiency of those networks was rather low[1]. Many were decommissioned because they failed to provide an adequate service [10], [15].

Within the UK, only a small number of cities have large DH networks. These include Nottingham, Southampton, Sheffield, Aberdeen, Birmingham and schemes like Citigen in London which serves the Barbican Centre.

Nottingham City is home to one of the largest DH networks in the UK. The 65 km heat network scheme has been running since 1972 and supplies around 3.5% of the city's entire heat demand. Another large DH scheme in the UK is in the Sheffield

[1] Modern district heating schemes give customers just as much control as individual gas boilers and could be very efficient.

City centre. Over 140 buildings are provided with heat through a network with a 50 km pipe line. The DH scheme in Southampton is connected to a geothermal well with a depth of one mile, and uses a CHP plant. This scheme is 14 km long and provides relatively low carbon heat [10].

All these DH schemes have already reduced residents' bills and contributed to the tackling of fuel poverty and CO_2 emission [10]. For example, the CHP district heating scheme in Aberdeen has reduced heating bills by 50% in an area where 70% of consumers were previously fuel-poor [10]. The CO_2 saving for the Nottingham and Sheffield DH networks are around 27,000 t/year and 21,000 t/year, respectively [10].

It is now widely recognised that the underlying rationale of DH is sound, and it can be a key component in delivering environmental objectives.

1.3.2 Technical features of district heating

District heating technologies are typically categorised as 1st, 2nd, 3rd and 4th generation. The 1st generation of DH systems used steam as the heat carrier. Almost all DH systems established before 1930 used this technology. Later, the 2nd generation with high temperature water, typically about 120 ºC, was introduced. The current generation (3rd), began in the 1970s. The heat carrier is pressurised water at a temperature of 90 ºC. The 4th generation of DH systems, currently under development, use a low supply temperature of 55-60 ºC, similar to that of domestic hot water systems [23], [24].

District heating can accommodate heat from a wide range of sources. These include fossil fuels, waste heat from industrial and electricity generation processes, electricity and renewable energy sources such as biomass, solar thermal and geothermal. The energy conversion system where CHP, boiler or heat pumps can be connected to the DH network directly or indirectly via a heat exchanger. For example, in Akureyri geothermal DH network in Iceland, hot water from geothermal wells is directly pumped to the consumers [25].

CHP plant connected to a DH network is one of the most cost effective ways of generating heat and it has a proven track record in many countries [26]. CHP generates heat and power simultaneously in a single unit. The main advantage of

CHP is the saving of primary energy without compromising the quality and reliability of the energy supply to the consumers (Figure 1-5).

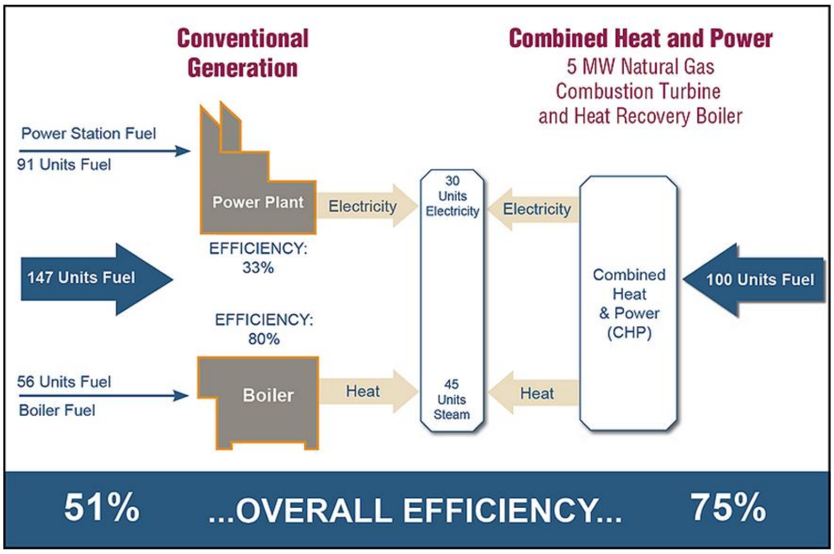

Figure 1-5 Energy efficiency comparison between combined heat and power and conventional generation systems [27]

The most common types of CHP technologies are listed in Table 1-1 [27]. CHP technologies shown in Table 1-1 can use a wide range of fuels, such as biomass, oil, gas and coal.

Table 1-1 CHP technologies

CHP Technologies	**Overall efficiency (%)**
Steam Turbine	80-90
Diesel Engine	70-80
Natural Gas Engine	70-80
Gas Turbine	70-75
Micro turbine	65-75
Fuel Cell	60-80

District heating systems also have the potential to deliver, heat derived from existing power plants and renewable energy sources. Waste heat from existing power plants, large scale ground source heat pumps (GSHP), solar thermal, geothermal and renewable energy conversion systems (e.g. biomass or biogas from anaerobic digestion) can be connected to DH networks (Table 1-2) [18].

Table 1-2 List of district heating systems

Scheme	Country	Supply technologies	Scale of the network
Sheffield	UK	Municipal waste CHP, gas and oil back-up	City centre, nondomestic and domestic
Southampton	UK	Gas CHP, deep geothermal heat, fossil fuel boilers	City centre, principally nondomestic
Barnsley	UK	Biomass boilers	Several small networks
Grosvenor, London	UK	Gas CHP, biomass, gas boilers	Small new-build residential
Chalvey, Slough	UK	ST[1], biomass, ASHP[2], GSHP	Research rig at 10 houses
VEKS	Denmark	Municipal waste CHP, gas/oil CHP, deep geothermal	Whole city
Hillerod	Denmark	Gas CHP, biomass, solar field	Town scheme
Eksta	Sweden	Biomass, individual dwelling solar thermal	Small new-build residential network
Malmo	Sweden	Building–integrated solar thermal, ground source heat pumps	New-build development with connection to city scheme

District heating networks consist of heat distribution systems which transport heat in the form of hot water to the consumers. Distribution networks can carry heat at variable temperatures and pressures. Heat distribution networks are categorised as:

- Primary network (long distance transport);
- Secondary network (distribution after heat exchange substation or building's internal heating system).

The size of DH networks can vary significantly, from supplying heat to a small number of buildings such as Edinburgh University DH network which provides heat for six halls of residence, to a substantial coverage of an entire city's heat demand for example Vienna DH network provides 35% of the city's heat demand[17].

A large DH network may use multiple interconnected subsystems. For example, the Copenhagen DH system (Figure 1-6) consists of a large interconnected pipe network, including a heat transmission network and numerous local DH distribution networks. Thermal power is transmitted from the high temperature transmission network to lower temperature DH distribution networks via heat exchangers

[1] Steam turbine
[2] Air source heat pump

[28].This resembles the relationship between high voltage electricity transmission systems and low voltage distribution networks.

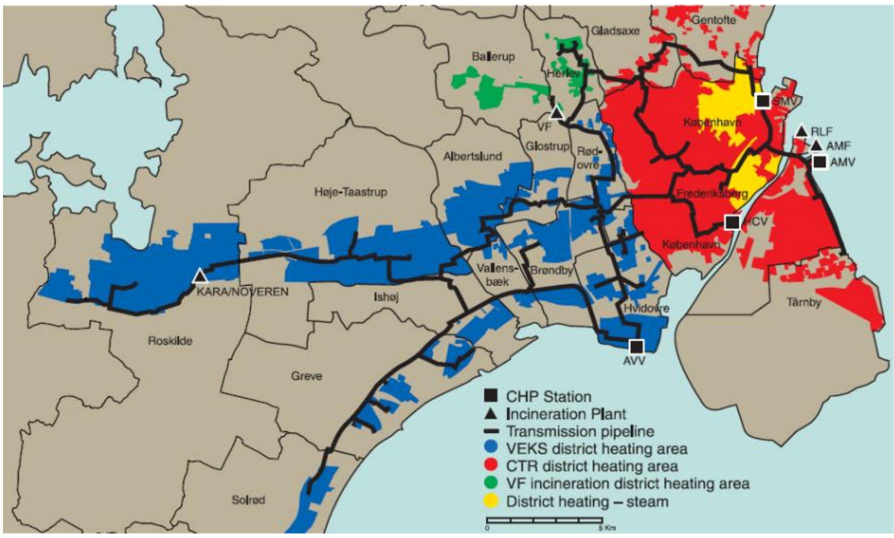

Figure 1-6 District heating system in the greater Copenhagen area [28]

Consumers may be connected to the DH distribution system directly or indirectly. Where the connection is indirect, heat exchangers (HEX) are used to separate DH hot water from the building's internal heating system (Figure 1-7)[29] rather than pump directly.

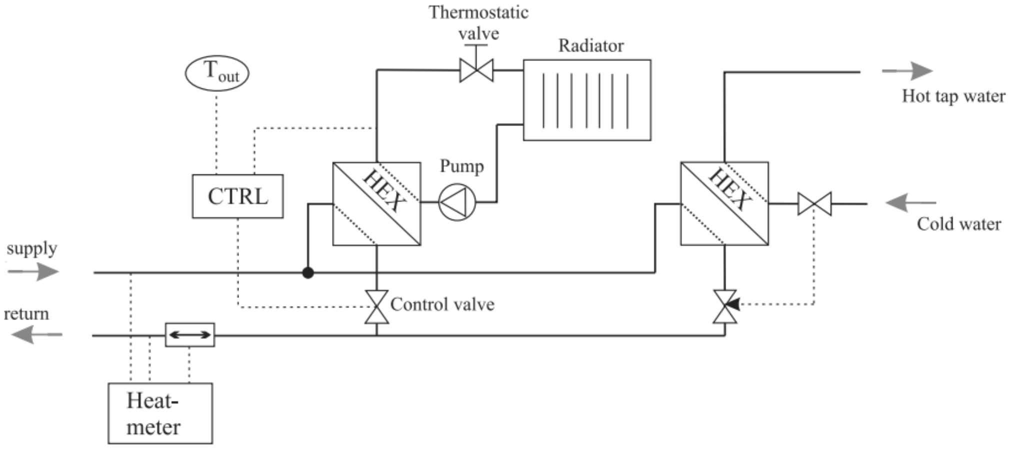

Figure 1-7 A typical consumer heating substation using an indirect connection [29]

1.3.3 Advantages and disadvantage of district heating

Heat can be generated in one large plant through the use of DH systems, a method which is usually more efficient than heat generation in multiple smaller units. Moreover, due to the possibility of using various energy sources within a DH network, the reliability of heat supply is increased. DH systems do not depend on specific heat generation technologies and this provides an opportunity to change heat supply sources to renewable energy sources at some point in the future. In summary DH networks provide the following direct benefits [11], [30]:

1. Allowing transportation and the use of heat for a wide range of users;
2. Enabling a diverse range of energy generation technologies to work together to meet heat demand;
3. Reducing the costs of energy generation;
4. Increasing fuel efficiency through the use of CHP;
5. Reducing labour and maintenance costs compared to individual heating systems.

These advantages in turn deliver a range of beneficial outcomes:

- Significant reduction in CO_2 emissions;
- Extending the reach of sustainable energy sources;
- Improving security of energy supply through fuel diversity.

Although there are many benefits of DH, there are also some disadvantages which can be summarised as follows:

- High investment costs;
- Challenges during installation (retrofitting, road digging and so forth);
- Heat losses in pipe networks and electrical energy consumption of the pump;
- Requirement to have an establishment to operate the system

When considering DH, the long term investment must be recognised. An example of cost comparisons between individual heating technologies and DH system is shown in Figure 1-8. The graph below illustrates the net present value (NPV) of Whole Life Cost (e.g. capital costs, replacement costs, operational costs and maintenance costs) of a community heating system with 500 dwellings using different schemes[1] [31], [32].

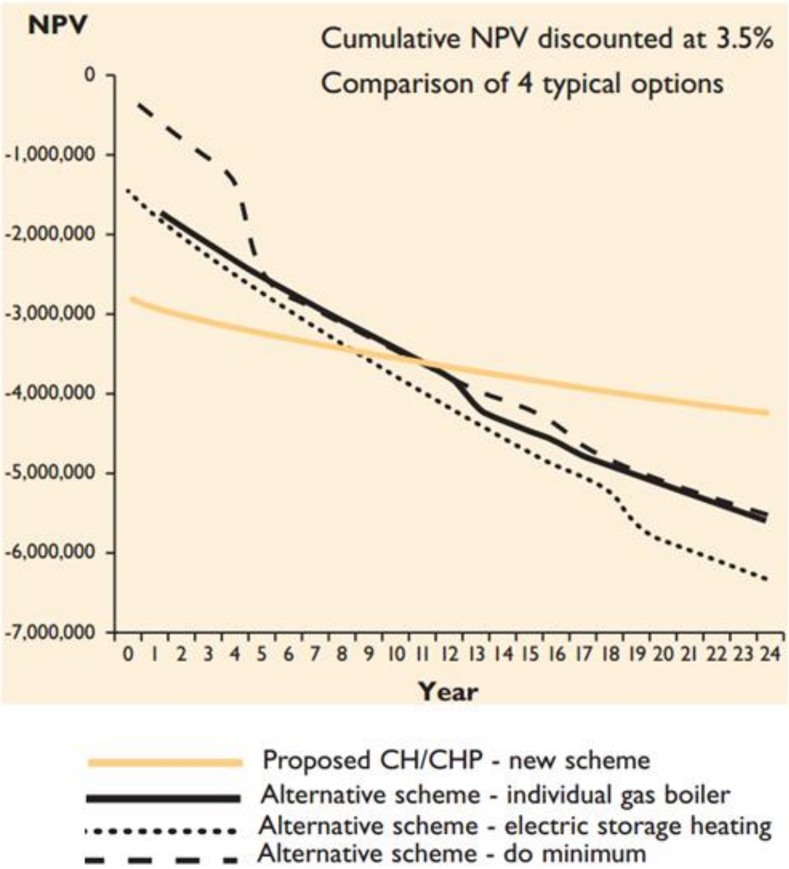

Figure 1-8 NPV of Whole Life Cost of a community heating system [31], [32]

As shown in Figure 1-8, the initial investment cost of a community heating/ district heating (CH/DH) scheme is around £3 million, almost twice those of other alternatives. The "do minimum" scheme represents the option of continuing with the existing system without significant changes. However, when net costs are calculated over 25 years at 3.5 % discount rate, the CH/DH scheme costs are about £4 million which is substantially less in comparison with the other options, which are close to £6 million. It worth noting, that changing discount rate would have impact on the NPV of Whole Life Cost of different heating schemes. For example, a higher discount rate increases the Whole Life Cost of the CH/DH, while a lower discount

[1] The Whole Life Cost varies for different district heating schemes and technologies.

rate reduces the Whole Life Cost of CH/DH compared to the other heating schemes[1]. Overall, the average cost of heat supply using DH is currently higher than alternative heating technologies in the UK. Hence, the main explanation of the low penetration of DH in the UK to date can be attributed to the high cost of heat provision using DH networks compared with conventional heating technologies such gas or electric boilers (Figure 1-9).

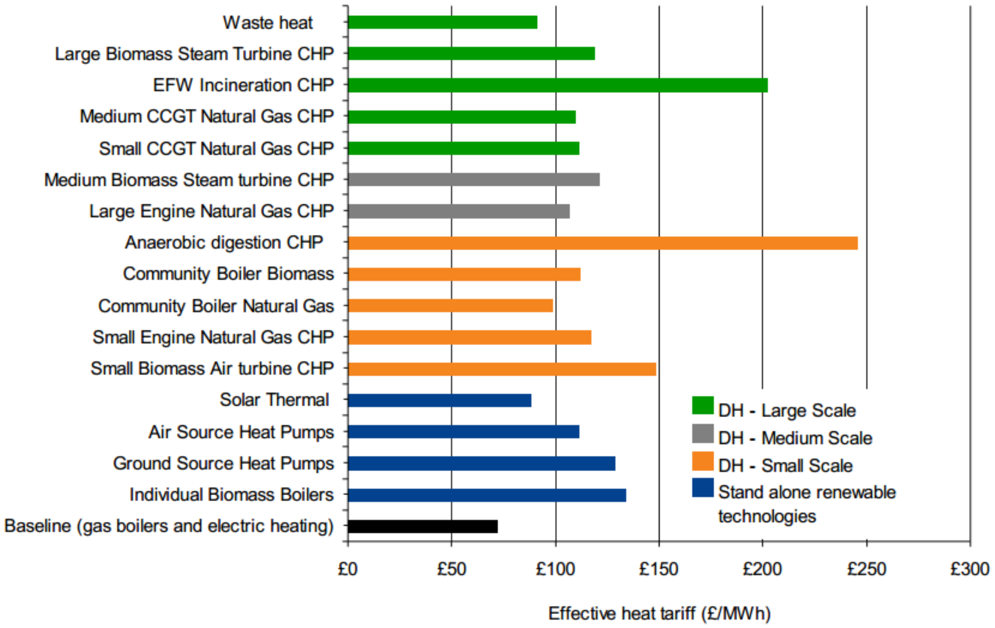

Figure 1-9 Cost of heat supply by technology (current market conditions, £/MWh) [1]

Figure 1-9 shows the average cost of heat supply for a range of DH options, stand-alone renewable heat technologies, gas and electric heating. The average cost of heat supply using DH is relatively high in comparison to the baseline (gas boiler and electric heating).

Digging roads and the traffic disruption should be taken into account when installing DH systems in established towns and cities. Heat losses and pump electrical energy consumption are other drawbacks, which need to be taken into consideration when designing a DH pipe network. The heat load of a DH network varies considerably over the course of the year, hence DH networks usually operate

[1] According to current policy the discount rate is around 6-10% in the UK [1].

in off-design (part load) conditions [33]. Operation of a DH network in off design condition reduces the efficiency as well as the profitability of the system. Finally, in comparison to individual heating systems, a DH requires a formal establishment, similar to the network operator for electricity system, which runs the system and provides service to the consumers [11].

1.3.4 Piping network design

Bringing down the cost of DH pipe infrastructure along with reducing heat losses and pump electrical energy consumption would reduce the capital costs and increase the economic competiveness of DH compared with other alternative technologies. The high cost of DH is mainly attributed to the capital cost of the hot water pipe network [1]. The investment in the DH pipe network mainly depends on pipe length and diameter [34]. An over-dimensioned DH network increases total installation and operating costs, while an under-dimensioned DH network may affect the supply of heat. DH systems, as mentioned, usually operate at part loading conditions hence a DH pipe network designed to carry full load in an area with low energy density is uneconomic [35].

The heat losses in a DH network are affected by pipe diameters and the insulation material used, as well as the temperature of the heat carrier medium in the supply and return pipes. Pipe diameters also have an impact on pressure loss in DH and consequently on the electrical energy consumption of pumps. The electrical energy consumption of pumps is also influenced by the flow rate of the heat carrier [36]. As a result, special attention needs to be paid to the determination of pipe diameters as well as the way the system is operated.

Pressure loss per unit length or target pressure loss (TPL) is a common design parameter used in DH pipe network design. Traditional methods of DH pipe size determination involve the use of a size searching algorithm in which the smallest pipe diameter is selected in accordance with the maximum TPL [37].

As a rule of thumb many DH networks in Denmark and in other European countries have been designed using TPL of 100 Pa/m [38–40]. Wide ranges of TPL were used in various studies to determine pipe diameters in DH networks as shown in Table 1-3.

Table 1-3 TPL used to determine pipe diameters in district heating networks

TPL (Pa/m)	Pipe network	References
30-70	Primary network	[41]
50-200	Primary network	[37], [42]
100	Primary network	[43], [44]
150	Primary network	[29]
200	Primary network	[45]
500	Primary network (main pipes)[1]	[46]
1500	Primary network (street pipes)	[46]
2000	Primary network	[34], [35]

When pipe sizes are determined, DH circulation pumps are another component which should be chosen to ensure sufficient flow circulation in the network. Traditionally, pumps are chosen using the maximum pressure difference for the most remote consumer.

Designing a DH pipe network according to the maximum TPL may result in an inefficient and unnecessary costly DH network. The risk of having an inefficient and unnecessary oversized pipe network can be reduced, by considering the variable TPL, the annual heating demand and DH operating strategy (or method) during design of the pipe network. However, the variation of TPL, heat demand and DH operating method contribute to the difficulty of the decision making process.

1.4 Research objectives

The objectives of this research are to develop a fundamental understanding of various designs of a DH pipe network and to develop a method which allows the planner to design an efficient and cost effective DH network. The following work has been undertaken in order to achieve these objectives:

- Investigated different DH network designs with different pipe and pumps sizes, based on various TPL and supply and return temperature regimes;
- Investigated the impacts of DH operating strategies and temperature regimes on annual energy and exergy performance as well as the annualised cost of DH;

[1] Main pipes: pipe sections along the route with maximum pressure drop, Street pipes: pipe sections in the other branches.

- Investigated the impact of heat sources on DH design and operation. DH connected with an ideal heat source, a boiler and a CHP were examined;
- Developed an optimisation model for the determination of optimal flow and supply temperature, as well as the optimal size of pipes and pumps in a DH network. Three different optimisation objectives were examined: 1) minimisation of annual total energy consumption; 2) minimisation of annual total exergy consumption; and 3) minimisation of the equivalent annual cost (EAC) or annualised cost of DH. Initially, for each optimisation objective, the optimal supply temperature and mass flow rate were calculated. Subsequently, the optimal annual total energy consumption, annual total exergy consumption and overall annual cost of the heat network installation and operation were determined. Finally, the optimal pipe and pump sizes were found;
- Investigated the impacts of the reduction of DH supply and return temperatures (low temperature DH network) on annual total energy consumption, annual total exergy consumption and the annualised cost of DH. Furthermore, the impact of reducing DH supply and return temperatures on optimal pipe and pump sizes were examined.

1.5 Thesis outline

Chapter 2 describes the energy consumption and economic analyses of a number of DH design cases when they are operated using different DH operating strategies. Firstly, a number of DH design cases with different pipe and pump sizes were designed and simulated. Then the operation of the design cases was investigated under several DH operating strategies such as constant flow and constant supply temperature (CF-CT), constant flow and variable supply temperature (CF-VT) and variable flow and constant supply temperature (VF-CT). Annual energy performance and overall annual cost of the design cases were compared.

In Chapter 3, the design cases obtained in Chapter 2 were operated under a variable flow and variable supply temperature (VF-VT) operating strategy. To obtain optimal flow and supply temperature, an optimisation model was developed using the FICO^{TM} Xpress optimisation suite. Further, the impact of a heat source on optimal solution of flow and supply temperature was examined. DH with an ideal heat source, a boiler and a CHP were compared. Annual energy performance and overall annual cost of the design cases were analysed, considering the impact of the heat source.

Chapter 4 describes an optimisation model for the determination of optimal pipe and pump sizes, flow and supply temperature in a DH network. The method combines the analysis procedures described in Chapters 2 and 3. The objective of the optimisation is to minimise annual total energy consumption, annual total exergy consumption as well as the annualised cost of the DH network. Exergy analysis and the impact of the reduction of supply and return temperatures in a DH network were also investigated.

Chapter 5 presents the conclusions drawn, the main findings and recommendations for future work.

CHAPTER 2- Energy Consumption and Economic Analyses of a District Heating Network

2.1 Introduction

The determination of pipe and pump sizes using the maximum TPL method may result in an unnecessarily costly DH pipe network. The risk of having an inefficient and a costly pipe network can be reduced by taking into account different TPL values, annual heating load and DH operating strategy during design.

In this chapter energy and economic analyses of a number of DH design cases using different operating strategies are investigated. The PSS SINCAL software tool was used to model different cases. First, design cases were simulated at a maximum heating load using different supply and return temperature regimes and TPL. Then their operation was performed under different operating strategies according to annual heating load.

Annual pump energy consumption and heat losses were calculated and then an economic evaluation of the design cases was conducted using the annualised cost of the heat network in Microsoft Excel. Annual total energy consumption (heat losses plus pump energy consumption) and the annualised cost of the design cases were compared. The design cases with minimum annual total energy consumption and minimum cost were determined.

2.2 Methods

First, a number of design cases were simulated. Then annual energy performance along with the annualised cost of the design cases were investigated when design cases were operated, under varying conditions of outside air temperature using different operating methods.

2.2.1 District heating topology

First, the topographical configuration of the DH network was determined. A real redevelopment project in South Wales, UK was used (Figure 2-1) [47]. For the sake of simplicity, the consumers within a geographical area were aggregated and they are represented by a cluster, shown in Figure 2-1. The consumers within a cluster may have different building sizes and occupancy patterns. It was assumed that consumers were connected to the network using heating substations.

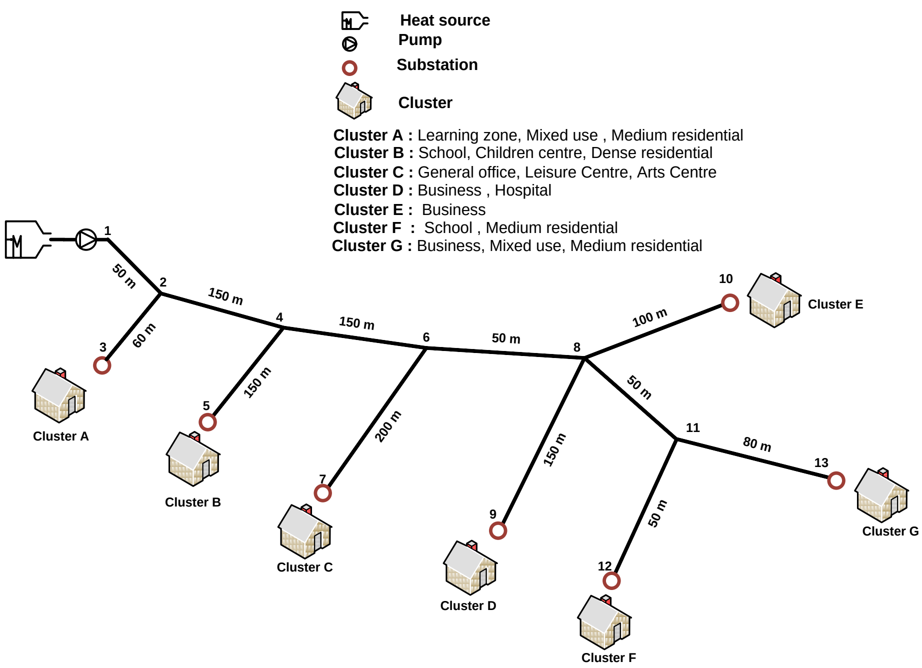

Figure 2-1 Simplified diagram of the Ebbw Vale district heating project

2.2.2 Calculation of energy use in buildings

Maximum heat demand was calculated for each consumer. Energy demand for space heating and domestic hot water were found based on the estimated area and heat-load density (W/m^2)[1] for each building [48], [49].

In order to calculate the annual heating load, it was assumed that the energy requirement for domestic hot water system was constant over the year. Variation of space heating over the year depends on the outdoor temperature. The variable heating load over the year for space heating was calculated using the concept of heating degree days.

Degree days are simplified representation of outside air-temperature data. They show how much (in degrees), and for how long (in days), the outside air temperature was lower than a specific "base temperature"[2] [50], [51]. As the outdoor air temperature changes, the temperature difference between indoor and outdoor creates a proportional change in heat demand.

When degree days of a location are known daily energy demand is calculated:

$$E_{SH} = 24hD_d \tag{2.1}$$

where E_{SH} is daily energy demand, D_d is degree days and h is overall heat loss coefficient. The overall heat loss coefficient was calculated using the maximum demand for space heating and maximum difference between indoor and outdoor temperatures:

$$h = \frac{Q_{SH,max}}{T_{ind} - T_{outd,min}} \tag{2.2}$$

where $Q_{SH,max}$ is the maximum space heating demand. T_{ind} and $T_{outd,min}$ are indoor and minimum outdoor temperatures respectively.

[1] CIBSE Guide F benchmark for new buildings

[2] Base temperature is the outdoor temperature at which the heating is not required in order to maintain comfortable conditions. Degree days have traditionally come in a limited range of base temperatures such as 15.5 °C and 18.5 °C.

The total energy demand over the year was calculated by summing energy demand for hot water and space heating systems.

2.2.3 District heating design cases

To obtain design cases, maximum supply temperature at the heat source and return temperature at the consumer's heating substations were assumed to be known[1][52]. Several regimes of supply and return temperatures were considered. For each temperature regime, maximum mass flow rate (or volume flow rate) was calculated at maximum heating load assuming initial pipe diameters[2] in the network, using the calculation procedure shown in appendix A. Pressure loss was calculated using the maximum flow rate. A range of TPL values was taken into account and the pipe diameter of each section was calculated at maximum flow rate based on each TPL. The pipe diameters were calculated using the following equation:

$$d_j = \sqrt[5]{\frac{8 f_j \dot{m}_{j,max}^2}{\left(\frac{\Delta p_j}{l_j}\right) \rho \pi^2}} \qquad j = 1 \ldots M \tag{2.3}$$

where d and l are pipe diameter and pipe length, f is the frication factor, $\dot{m}$ is mass flow rate and Δp is pressure loss.

A pipe diameter calculated based on the TPL value may be different from those available on the market. Therefore, the pipe with a diameter closest to the calculated pipe diameter was selected. By repeating the calculation with actual pipe diameters, the actual maximum pressure loss (MPL) in the network was obtained.

Pump size was calculated to overcome loss of pressure along the route with maximum pressure drop in the network. The pump power in kW was calculated using the following equation [53]:

---

[1] Return temperature depends in a non-linear way on the heat load, supply temperature and consumer behaviour. For the sake of simplicity, return temperature was assumed to be known at the consumer's heating substations.

[2] Initial pipe diameters were assumed and they were used to calculate flow rate in each pipe section of the network.

$$P_p = \frac{\Delta p_p \dot{m}}{1000 \rho \eta_p} \tag{2.4}$$

where η_p is the pump's overall[1] efficiency and Δp_p is pump differential pressure. It was assumed that pump efficiency was 80% [54], [55]. Pump differential pressure was calculated by:

$$\Delta p_p = \sum_j (\Delta p_{sj} + \Delta p_{rj}) + \Delta p_c \tag{2.5}$$

where Δp_{sj} and Δp_{rj} are pressure drop in pipe sections of supply and return, respectively. Δp_c is the pressure drop in the consumer's heating substation and it was calculated using the following equation:

$$\Delta p_c = \xi \dot{m}^2 \tag{2.6}$$

where ξ is the consumer's pressure drop coefficient and it was calculated by assuming that the maximum pressure drop at the consumer's heating substation is 50 kPa [29], at maximum heating load and maximum flow rate.

2.2.4 District heating operating strategies

The DH design cases were operated for one year using several operating strategies. In a DH system intended to supply a consumer's energy requirement, two parameters can be controlled: supply temperature and flow rate[2] [56]. Therefore, the following four different operating strategies were investigated:

1. CF-CT: System operated at the maximum heating load, maximum temperature and maximum flow rate.

[1] Mechanical and electrical efficiency
[2] Return temperature was assumed to be known at the consumer's heating substations.

2. CF-VT: Flow rate was assumed to be constant and system supply temperature was controlled according to variable heat demand.
3. VF-CT: Supply temperature was assumed constant, but the flow rate varied according to the heat demand over the year. Therefore, the pressure drop and the required pump head varied accordingly.
4. VF-VT: The VF-VT is the combination of CF-VT and VF-CT operating methods. Control variables, flow and supply temperature were adjusted simultaneously with respect to the variation of heat demand.

In the CF-CT method it was assumed that the DH network is operating at the maximum load (peak demand) over the whole year. In the other three cases it was assumed that the load alters over the year according to the variation of heat demand. For all four operating methods, it was assumed that the DH network was fed by an ideal heat source (*ideal-DH*). The ideal heat source was defined as a heat source which has negligible operating costs, and is capable of delivering required amount of heat. The best example of an ideal source is geothermal[1].

Using each operating strategy, the DH network parameters including annual pump energy consumption and heat energy losses and the annual capital and operational costs of the design cases were calculated and compared.

In this Chapter the results of the first three operating methods are presented, using PSS SINCAL. The VF-VT operating method is described in detail in Chapter 3.

2.2.5 Modelling and analysis of district heating using PSS SINCAL

PSS SINCAL was used for modelling and simulation of the DH network [57]. Using the Hardy Cross method [58], PSS SINCAL allows simulation of large and complex DH pipe networks. An example of heat flow calculation for two simple cases of DH is given in Appendix A. All required parameters such as temperature, mass flow rate and pressure were calculated at the steady state condition.

Using the PSS SINCAL the main pipe network (primary network) was modelled, including supply and return pipes. It was assumed that return pipes have the same

[1] Assuming the future trend toward the development of low-cost electricity generation in the UK due to high penetration of renewable energy sources, heat pump can be considered as an ideal heat source.

diameters and length as the supply pipes. Pipes were laid in the ground. An average ground temperature of +7 ℃ over the whole year was assumed [59], [60]. Standard size pre-insulated single steel pipes with pressure rating up to 25 bar and temperature rating up to 140 ℃ were used. Pipe roughness (ε) of 0.4 mm was used in calculations [61]. The typical range of pre-insulated steel pipes are given in Table B2-1(appendix B) [62].

Four different regimes of maximum supply temperature at the heat source and return temperature at the consumer's heating substations were assumed for the analysis, $T_{s,max}/T_{r,max}$: 120/70 ℃, 110/70 ℃, 100/70 ℃ and 90/70 ℃ [63]. A range of TPL values were assumed in which the maximum differential pressure of pump is less than or equal to 16 bar[1] [63]. Supply and return pipe diameters and pump sizes were calculated for a range of TPL values and temperature regimes at the maximum heating load. The design cases were operated using different operating strategies according to annual heating load. The overall block diagram of the study is shown in Figure 2-2.

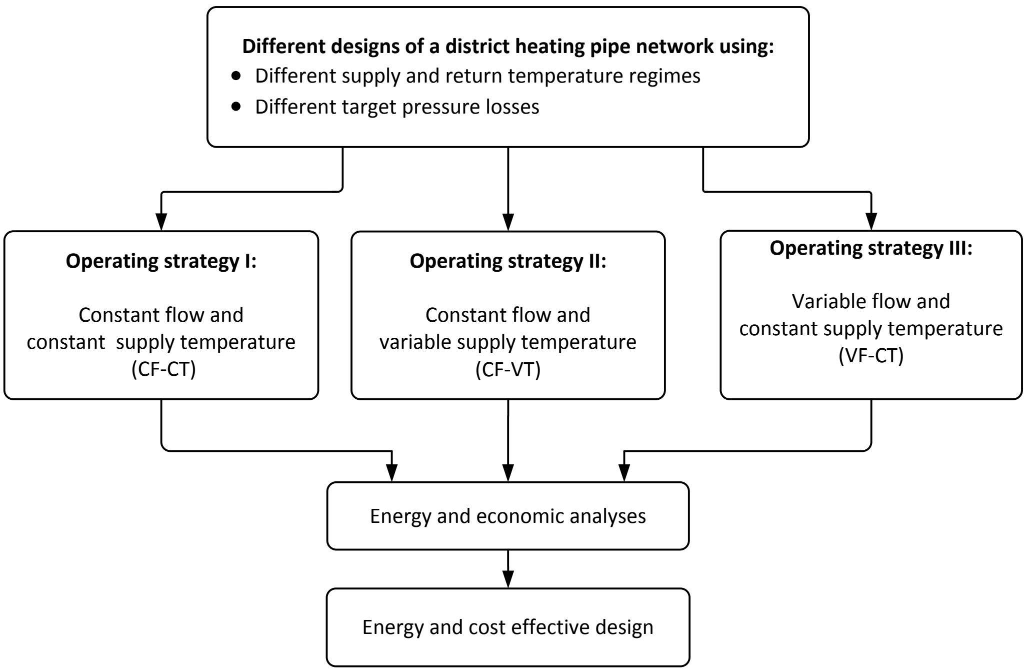

Figure 2-2 Block diagram of the study

[1] The majority of district heating systems in Scandinavian countries are designed to withstand 16 bar pressure.

2.3 Case study: Ebbw Vale district heating

A real redevelopment project in South Wales, UK, was used as the basis of a case study to analyse the DH network (Figure 2-1). For the calculation of annual heating load, minimum outdoor temperature was -3 ℃ and the base temperature was assumed to be +15.5 °C. The degree days were calculated based on the weather data for Cardiff, South Wales, UK. The daily space heating energy requirement was calculated for each day of the year (see section 2.2.2 and equations 2.1-2.2). Annual total heat demand was obtained (space heating plus domestic hot water), for the case study shown in Figure 2-1. The calculated annual heating load over the year (left) and load duration curve (right) in MW are shown in Figure 2-3.

It was observed (Figure 2-3) that annual total heat load is divided into two main seasons (summer and winter). It was assumed that the winter season lasts for 182 days, which includes demand for space heating and domestic hot water. For the rest of the year (summer season) only demand for domestic hot water was taken into account.

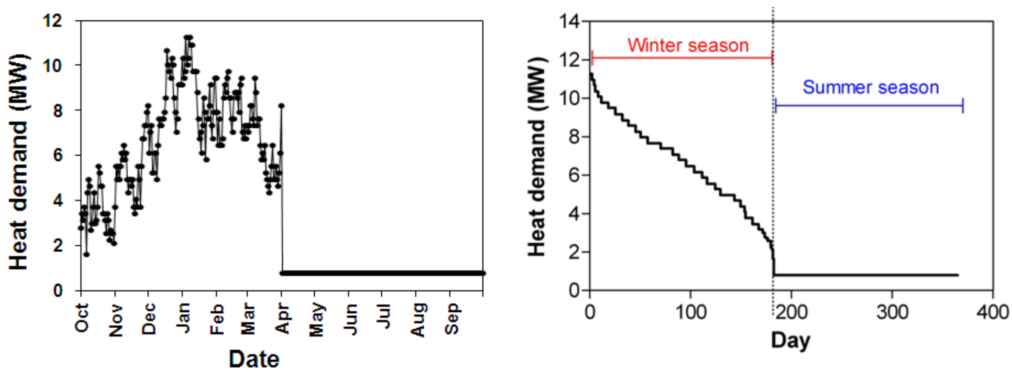

Figure 2-3 Annual heat demand (left), load duration curve (right)

For the DH network (Figure 2-1), a number of design cases with different sizes of pipes and pumps were obtained, using varying temperature regimes and TPL values at maximum heating load. The MPL obtained using this procedure is discussed in section 2.2.3, and different design cases are presented in Table 2-1. The physical and heating parameters of the design cases are given in Table B2-2 (appendix B).

Table 2-1 Design cases with obtained maximum pressure loss

	Temperature regimes :$T_{s,max}/T_{r,max}$ ℃							
	120/70		110/70		100/70		90/70	
TPL (Pa/m)	DH case	MPL (Pa/m)	DH case	MPL (Pa/m)	DH case	MPL (Pa/m)	DH case	MPL (Pa/m)
50	DH 1	52	DH 19	45	DH 37	51	DH 55	55
100	DH 2	99	DH 20	99	DH 38	101	DH 56	97
150	DH 3	156	DH 21	153	DH 39	143	DH 57	152
200	DH 4	214	DH 22	196	DH 40	191	DH 58	197
250	DH 5	248	DH 23	262	DH 41	269	DH 59	244
300	DH 6	304	DH 24	304	DH 42	299	DH 60	318
350	DH 7	339	DH 25	331	DH 43	345	DH 61	367
400	DH 8	407	DH 26	402	DH 44	382	DH 62	389
450	DH 9	448	DH 27	470	DH 45	462	DH 63	425
500	DH 10	483	DH 28	524	DH 46	536	DH 64	496
550	DH 11	552	DH 29	576	DH 47	582	DH 65	577
600	DH 12	592	DH 30	630	DH 48	723	DH 66	667
700	DH 13	661	DH 31	694	DH 49	828	DH 67	748
800	DH 14	790	DH 32	748	DH 50	923	DH 68	851
900	DH 15	847	DH 33	800	DH 51	1015	DH 69	948
1000	DH 16	977	DH 34	854	DH 52	1110	DH 70	1029
1100	DH 17	1276	DH 35	1023	DH 53	1223	DH 71	1195
1200	DH 18	1403	DH 36	1312	DH 54	1318	DH 72	1297

Different design cases (see Table B2-2) consist of different set of pipes with different diameters. For the sake of simplicity in presentation of different design cases, the concept of equivalent pipe diameter (d_{eq}) was introduced. The equivalent pipe diameter represents all pipes as a single pipe and it was calculated using the equation:

$$d_{eq} = \sqrt{\frac{4V^T}{\pi l^T}} \tag{2.7}$$

where V^T is the total volume of the pipe network. This was calculated using the following equation:

$$V^T = \sum_j V_j \tag{2.8}$$

l^T is the total length of the pipe network and it was calculated using equation:

$$l^T = \sum_j l_j \tag{2.9}$$

Maximum heat losses and pump power for different design cases using different temperature regimes and TPL were calculated (see Table B2-2). Maximum pump power and heat losses versus equivalent pipe diameter are shown in Figure 2-4.

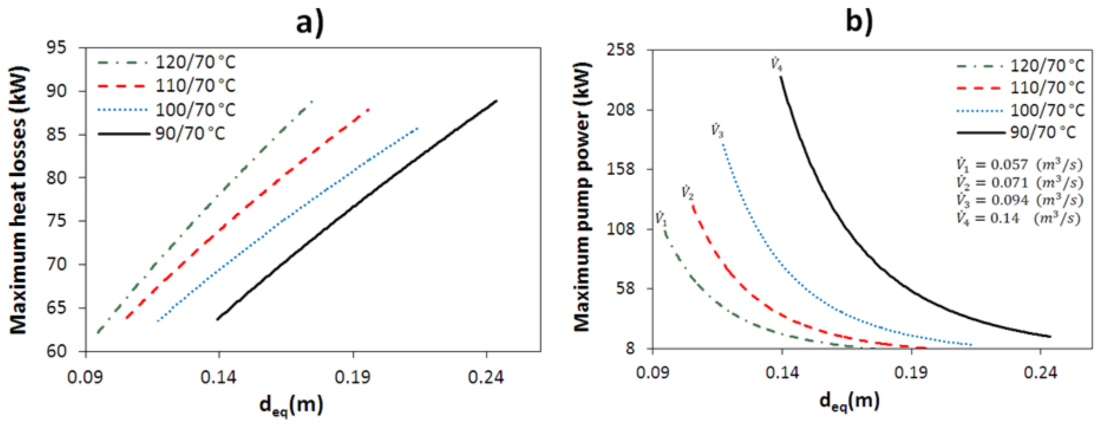

Figure 2-4 a) Maximum heat losses b) maximum pump power, vs. equivalent pipe diameter

It can be seen in Figure 2-4 a) that when the equivalent pipe diameter increases the heat losses in the network increase, since the pipe diameters increase the heat transition coefficient (see Table B2-1). Therefore, heat losses within the network increase correspondingly (see appendix A). The maximum heat losses decrease along with any reduction in pipe's supply temperature.

Figure 2-4 b) shows that the change in equivalent pipe diameter and temperature regime has a significant impact on pump power. Maximum pump power increases rapidly ($P_p \approx \frac{1}{d_{eq}^5}$) (see equations 2.4 and A.11 (appendix A)), as the equivalent pipe diameter is reduced. Due to the reduction in temperature difference between supply and return pipes the maximum pump power increases considerably. Reducing temperature difference between supply and return pipes increases flow rate which in turn increases pump power (see equation 2.4).

2.4 Analysis of energy consumption and heat losses

The DH design cases using the methodology described in section 2.2.3 were operated over the year, using different operating methods explained in section 2.2.4.

2.4.1 CF-CT method

For the CF-CT method, using a temperature regime of $T_{s,max}/T_{r,max}$= 120/70 °C, the supply temperature at the heat source and the return temperature at the consumer's substations were fixed at 120°C and 70°C over the year. Since the simulation was carried out under maximum load the flow rate was maximum.

The pump electrical energy consumption and heat losses for all four temperature regimes shown in Table 2-1 were obtained when the DH network was operated using the CF-CT operating method. The results obtained for the design cases based on the temperature regime of $T_{s,max}/T_{r,max}$= 120/70 °C are shown in Figure 2-5.

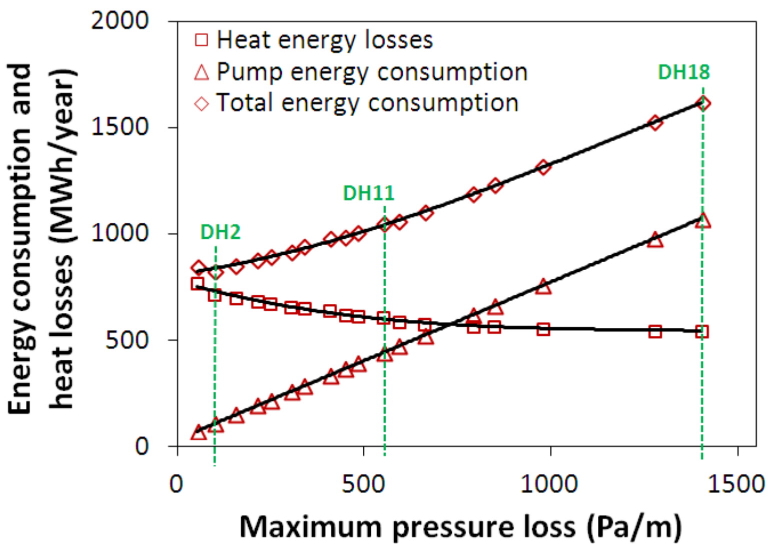

Figure 2-5 Annual pump energy consumption and heat losses obtained by the CF-CT method

Figure 2-5 demonstrates that annual pump energy consumption and heat losses changes when the CF-CT method is used, depending on the design case presented in Table 2-1 (design cases are indicated as red mark). By increasing the MPL the annual pump energy consumption increases whereas heat energy losses decrease. The annual total energy consumption (pump energy consumption plus heat energy losses) increases along with the MPL. The annual total energy consumption is minimum when the *DH2* (MPL: 99 Pa/m) design case is used.

2.4.2 CF-VT method

The temperature and flow rate using the CF-VT method for the temperature regime of $T_{s,max}/T_{r,max}$= 120/70 °C are shown in Figure 2-6.

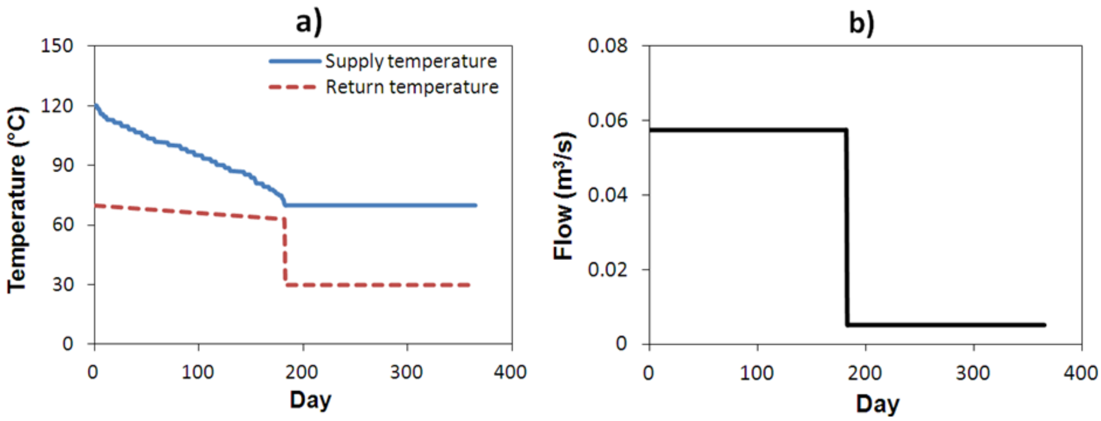

Figure 2-6 a) Temperature b) flow, CF-VT method

It is shown in Figure 2-6 that flow rate is constant for the winter and summer seasons. Supplying the consumer's energy requirement during winter season requires the variation of supply and return temperatures between assumed limits, according to annual heat demand (see Figure 2-3). For the summer season there is only demand for domestic hot water hence, system temperature is fixed at its minimum level.

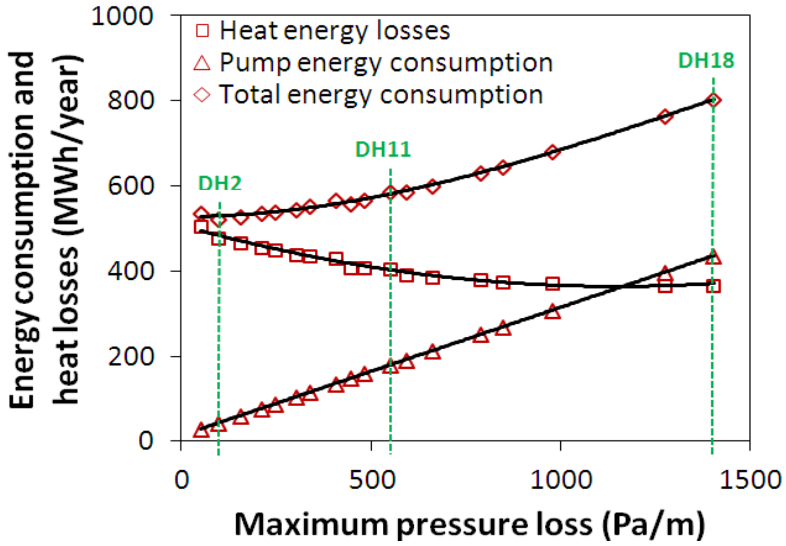

Figure 2-7 Annual pump energy consumption and heat losses obtained by the CF-VT method

The annual pump energy consumption and heat losses are shown in Figure 2-7. It is seen that as the MPL increases pump energy consumption increases while heat energy losses decrease. For the CF-VT method, the minimum annual total energy consumption occurs for the design case *DH2* (MPL: 99 Pa/m).

2.4.3 VF-CT method

Figure 2-8 shows the temperature and flow rate for the VF-CT method, using the temperature regime of $T_{s,max}/T_{r,max}$= 120/70 °C.

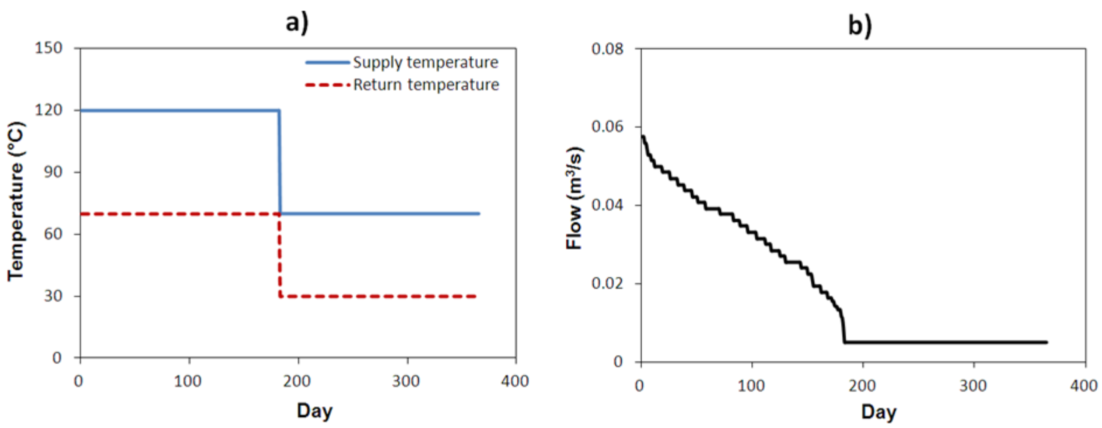

Figure 2-8 a) Temperature b) flow, VF-CT method

It can be observed from Figure 2-8 that supply and return temperatures are fixed for the winter and summer seasons. Flow rate is varied according to annual heat load in order to supply the consumer's energy demand.

Annual pump energy consumption and heat energy losses are shown in Figure 2-9. As the MPL increases the pump electrical energy consumption increases and heat losses decrease. However, due to the variation of flow rate during operation, it is seen that annual pump energy consumption is considerably less in comparison with annual heat energy losses. The *DH12* (MPL: 592 Pa/m) design case displays minimum annual total energy consumption using the VF-CT method. This case has a relatively higher pressure loss compared with the case *DH2*, which was chosen as the best design case for the CF-CT and CF-VT operating methods.

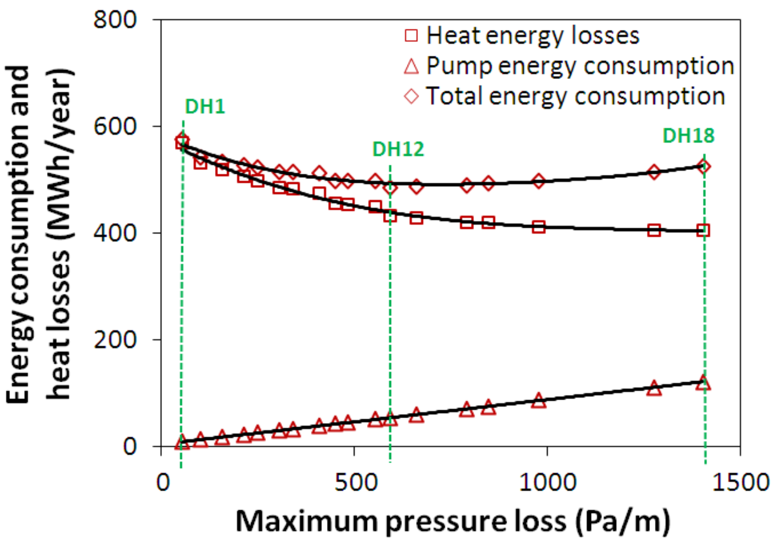

Figure 2-9 Annual pump energy consumption and heat losses obtained by the VF-CT method

2.5 Economic analysis

All DH design cases were examined using EAC. The annualised cost comprises both capital and operating costs of the DH pipe network. The capital costs include pipe and pump investment costs.

Pipe investment costs consist of:

a. The price of pre-insulated steel pipes including fittings, site joints and termination seals: this is based on the price list obtained from reference [64]. The prices of DH pipes are given in Table B2-3 (appendix B);
b. The cost of civil works: this depends on the pipe size, ground condition and method of digging. The ground condition and digging type were assumed to be the same for all pipes. Civil work costs between 700-1000 (£/m) [65], [66] were assumed according to the pipe size.

Pump investment costs: these consist of costs for two pumps, one for the winter season and one for the summer season. It was assumed that the pumps were equipped with variable speed drives. Prices of the pumps were taken from [67], and prices of variable speed drives were found in [68]. The prices are given in Table B2-4 (appendix B).

Operating costs of a DH network: pumping costs (costs of electricity consumption and CO_2) and costs associated with heat losses were taken into consideration. The EAC was calculated using the following equation:

$$EAC = \frac{NPV}{A} \tag{2.10}$$

Net present value (NPV), considering the life time of the systems (n years), were calculated using the equation:

$$NPV = \sum_{t} \left(\frac{C_t}{(1+i)^t} + C_o \right) \tag{2.11}$$

Annuity factor (A) was obtained using the following equation:

$$A = \frac{(1+i)^t - 1}{i\,(1+i)^t} \tag{2.12}$$

The data used to calculate EAC are given in Table 2-2.

Table 2-2 Physical and economic data

			Reference from where data were taken
Operating time	8760	hour/year	
Pump life time	15	year	
Pipe network life time	30	year	
Pump overall efficiency	80	%	
Discount rate	7	%	[69]
Inflation rate	5	%	[70]
Electricity price	95	£/MWh	[69], [71]
Heat price	70	£/MWh	[1]
CO_2 emission linked to the grid electricity	0.422	kgCO2/kWh	[69]
CO_2 price	22	£/tCO2	[1]

2.5.1 CF-CT method

The annualised cost of different design cases using different operating methods was calculated using equations 2.10- 2.12. The EAC of different designs using the CF-CT method under temperature regime of $T_{s,max}/T_{r,max}$=120/70 °C is shown in Figure 2-10.

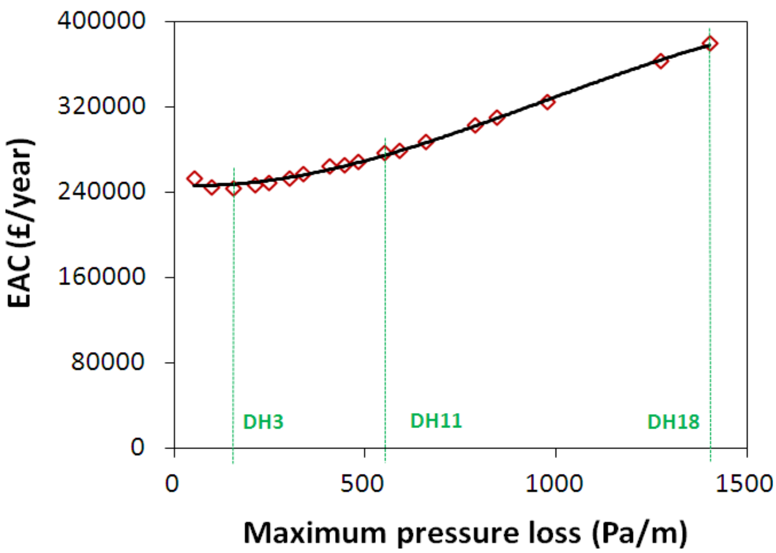

Figure 2-10 Equivalent annual cost of design cases obtained by the CF-CT method

For the CF-CT method the case with minimum EAC is the *DH3* (MPL: 156 Pa/m) design case. As the MPL increases further, the EAC of the design cases (indicated in red) also increases rapidly.

2.5.2 CF-VT method

The EAC of different design cases for the CF-VT method under temperature regime of $T_{s,max}/T_{r,max}$= 120/70 °C is shown in Figure 2-11.

By using the CF-VT method the EAC is minimum for the *DH4* (MPL: 214 Pa/m*)* design case. As the MPL increases further, the EAC of the design cases increases gradually.

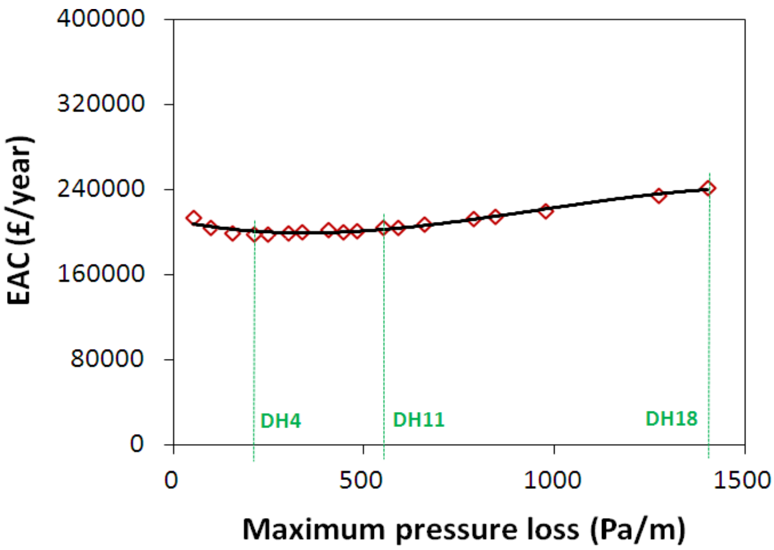

Figure 2-11 Equivalent annual cost of design cases obtained by the CF-VT method

2.5.3 VF-CT method

The EAC of different design cases for the VF-CT method under temperature regime of $T_{s,max}/T_{r,max}$= 120/70 °C is shown in Figure 2-12.

For the VF-CT operating method, the EAC is minimum using the *DH12* (MPL: 592 Pa/m) design case. For the *DH12,* the pressure loss is relatively higher compared to the design cases obtained for the CF-CT and CF-VT methods. The reason is associated with the variation of flow rate during operation. Variation of flow rate during operation reduces annual pump energy consumption. Therefore, by using the VF-CT method the annual pumping cost was reduced compared to the CF-CT and CF-VT methods. Consequently, a design case with much higher pressure loss was found.

It can be observed that using the VF-CT method the differences between the EAC of design cases *DH12-DH18* is small. These occur due to the decrease of pipe diameters, pressure loss in the system increases and consequently pumping energy demand increases. Therefore, pipe investment costs decrease while pump investment and operating costs increase. In addition, when using smaller pipe sizes, the costs of heat losses reduce.

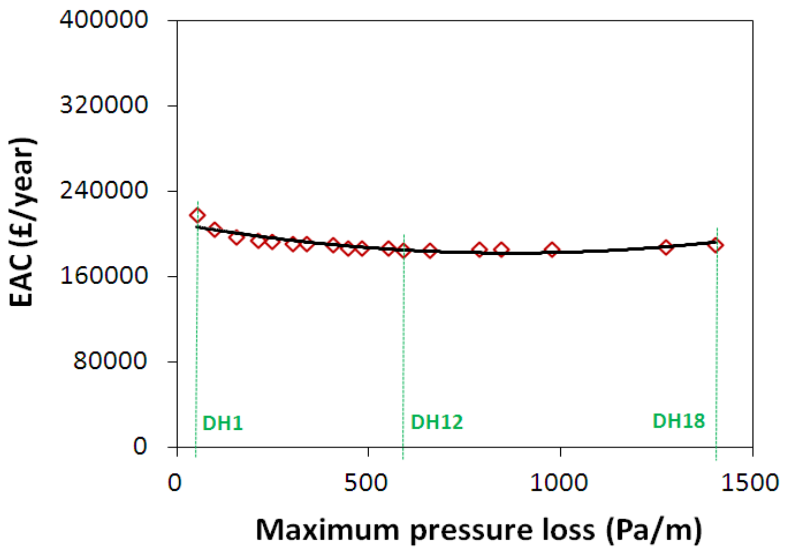

Figure 2-12 Equivalent annual cost of design cases obtained by the VF-CT method

2.6 Comparison

The annual heat energy losses and pump energy consumption and the EAC were calculated using different temperature regimes and operating methods. Table 2-3 and Table 2-4 summarise the DH design cases with minimum annual total energy consumption and minimum EAC for each temperature regime and operating method.

From Table 2-3, it is clear that when different temperature regimes are used the minimum annual total energy consumption changes. Reducing temperature difference between supply and return pipes increases the system flow rate which in turn increases the annual pump energy consumption.

Table 2-3 Design cases with minimum annual total energy consumption, using different temperature regimes and operating methods

Operating method	**CF-CT**		**CF-VT**		**VF-CT**	
$T_{s,max}/T_{r,max}$ ℃	**DH case**	**$E_{T,min}$ (MWh/year)**	**DH case**	**$E_{T,min}$ (MWh/year)**	**DH case**	**$E_{T,min}$ (MWh/year)**
120/70	DH2	823	DH2	522	DH12	486
110/70	DH20	839	DH20	546	DH26	518
100/70	DH37	884	DH38	580	DH42	527
90/70	DH55	953	DH55	646	DH62	577

These results indicate that the VF-CT method achieves a better energy performance of the DH network compared with other operating methods. Using this operating method, much smaller pipes can be designed with much larger pressure loss in comparison to the results obtained for the other operating methods.

Table 2-4 Design cases with minimum EAC, using different temperature regimes and operating methods

Operating method	**CF-CT**		**CF-VT**		**VF-CT**	
$T_{s,max}/T_{r,max}$ ℃	**DH case**	**EAC_{min} (£/year)**	**DH case**	**EAC_{min} (£/year)**	**DH case**	**EAC_{min} (£/year)**
120/70	DH3	242969	DH4	197805	DH12	184211
110/70	DH22	252703	DH22	204802	DH27	193429
100/70	DH38	270556	DH40	218403	DH45	200336
90/70	DH55	301220	DH66	248320	DH63	218346

From Table 2-4, it is observed that when using DH cases with less temperature difference between supply and return pipes, the EAC is increased. Due to the reduction of temperature difference between supply and return pipes the flow rate in the system increases. Design cases with larger flow rates require pipes and pump with larger sizes. Therefore, investment and operating costs will increase commensurately.

The EAC was divided by the annual total energy demand (32602 MWh/year) and the cost of heat transmission per MWh was obtained, given in Table 2-5. The cost of heat transmission is associated to the capital and operational costs of the DH network.

It is shown in Table 2-5 that using the VF-CT operating method, for the design case with smaller pipe sizes as well as larger temperature difference between supply and return pipes, the lowest cost of heat transmission is achieved.

Table 2-5 Design cases with minimum cost of heat transmission, using different temperature regimes and operating methods

Operating method	**CF-CT**		**CF-VT**		**VF-CT**	
$T_{s,max}/T_{r,max}$ ℃	**DH case**	**Cost (£/MWh)**	**DH case**	**Cost (£/MWh)**	**DH case**	**Cost (£/MWh)**
120/70	DH3	7.45	DH4	6.07	DH12	5.65
110/70	DH22	7.75	DH22	6.28	DH27	5.93
100/70	DH38	8.30	DH40	6.70	DH45	6.14
90/70	DH55	9.24	DH66	7.62	DH63	6.70

Comparison of the results presented in Table 2-3 and Table 2-4 shows that both energy and cost analyses present somewhat similar results. The difference seen in Table 2-3 and Table 2-4 is due to pipe and pump investment costs as well as heat losses and pump operating costs. However, both energy and economic analyses shows that the VF-CT operating method has a better performance. The minimum annual total energy consumption and EAC using the VF-CT method was observed when smaller pipe diameters and larger pressure loss were selected in comparison with results found for the other operating methods.

2.7 Conclusions

A DH network was modelled using PSS SINCAL, then energy and economic analyses of 72 DH design cases were investigated. First, a number of DH design cases with different pipe diameters and pump sizes were designed. Then performance of the design cases using three DH operating strategies (CF-CT, CF-VT and VF-CT), were examined over one year. Annual pump energy consumption and heat losses as well as the EAC of the design cases were found and compared.

The results showed that the DH operating method and temperature regime of the supply and return pipes have a substantial impact on the annual energy performance and operational costs of DH network. Due to the selection of different operating methods and different temperature regimes, the flow and temperature in the system varied. Consequently, pump energy consumption and heat losses changed. Hence, the design cases with minimum annual total energy consumption as well as minimum annualised cost were different under these conditions.

It was found that, for the VF-CT operating method, the annual total energy consumption and the annualised cost of the design cases were less when compared to the CF-VT and CF-CT methods. For the VF-CT method, the design case with minimum annual total energy consumption and minimum annualised cost was observed using a much larger pressure loss. This indicates that the reduction of annual total energy consumption and annualised cost can be achieved by reducing the diameter of the pipes and increasing the pump size.

A comparison of design cases with different temperature regimes showed that, due to the reduction of temperature difference between supply and returns pipes, the annual total energy consumption and annualised cost of a DH network increase. The flow rate in DH network increases due to the reduction of temperature difference between supply and return pipes. Hence, it is more beneficial to increase temperature difference between supply and return pipes and to reduce the system flow rate in order to reduce the annual total energy consumption and the annualised cost of the heat network installation and operation.

CHAPTER 3- Energy Consumption and Economic Analyses of a District Heating Network using a Variable Flow and Variable Supply Temperature Operating Strategy

3.1 Introduction

In Chapter 2 the annual pump energy consumption and heat losses as well as the EAC of different DH design cases, using different operating methods and temperature regimes, were compared. This chapter presents energy and cost analyses of the design cases, shown in Table 2-1 and Table B2-2 (appendix B) using the VF-VT operating method.

The energy supply changes according to the change of energy demand for heating. Energy supply to consumers can be regulated by varying mass flow rate and supply temperature independently or simultaneously. Using the VF-VT operating method, both control variables were adjusted simultaneously. However, the variation of both parameters increases the complexity of the system. Hence, an optimisation model was developed.

To obtain optimal flow and supply temperature for each design case according to annual heating load, an optimisation was used. The objective of the optimisation was to minimise annual total energy consumption and annual total operating costs. Optimal annual pump energy consumption and heat losses were calculated and compared alongside the annualised cost of the design cases. Subsequently, for each optimised design case, the optimal flow and supply temperature were obtained. The optimisation model was developed, using the FICO^{TM} Xpress optimisation suite.

Modelling and operation of a DH network is addressed in a number of studies [52], [72–76]. An optimisation model, which takes into account the dynamic performance of the network, was developed to minimise operational costs [52], [72]. A simple (aggregated) model of a DH system for simulation and operational optimisation was developed in [73]. Additionally, an equivalent model of a DH network was developed for on-line optimisation of the operational costs of complete DH system [74]. In [75], the formulated optimisation model accounted for the dynamic character of the DH network, in order to minimise operating costs and maximise the profit of the system. Reference [76] specifically addresses the modelling and optimal operation of a Microgrid system.

3.2 Optimisation model

For the operating methods discussed in Chapter 2, it was assumed that the DH network was fed by an ideal heat source (*ideal-DH*). Using the VF-VT operating strategy the impact of the heat source on the optimal solution of the flow and supply temperature, according to annual heating load, was investigated. Hence, in addition to the *ideal-DH*, the DH network with a boiler (*boiler-DH*) and CHP plant (*CHP-DH*) as the heat source was examined. The optimisation was based on the minimum annual total energy consumption and annual total operating costs. The following objective function was used to minimise annual total energy consumption of the system:

$$min \sum_{t} \left(E^{t}_{src,fuel} + E^{t}_{p} + E^{t}_{loss} \right) \tag{3.1}$$

where E_p and E_{loss} are pump electrical energy consumption and heat energy losses. $E_{src,fuel}$ is the fuel energy consumption of the heat source. Fuel consumption is zero for an ideal source.

In the case of optimisation based on cost, the following objective function was used:

$$min \sum_{t} \left(C^{t}_{src,fuel} + (-C^{t}_{chp,e}) + C^{t}_{p} + C^{t}_{loss} \right) \tag{3.2}$$

where C_p and C_{loss} are pumping cost and cost associated with heat losses. $C_{src,fuel}$ is the fuel cost. Fuel cost is zero for an ideal source. In the case of CHP the electricity revenue, $C_{chp,e}$ (given within parentheses), was added as a negative cost to the objective function [72], [77]. The constraints used for both optimisation approaches are:

$$T_{s,min} \leq T_{s,t} \leq T_{s,max} \tag{3.3}$$

$$\dot{m}_t \leq \dot{m}_{max} \tag{3.4}$$

$$\Delta p_{p,t} \leq \Delta p_{p,max} \tag{3.5}$$

where T_s is the supply temperature. $\dot{m}$ and Δp_p are mass flow rate and pump differential pressure.

3.2.1 Heat source

Assuming that the boiler is a heat source, fuel consumption was calculated using the following equation:

$$Q_{b,fuel} = \frac{Q_b}{\eta_b} \tag{3.6}$$

where $Q_{b,fuel}$, Q_b and η_b are respectively fuel consumption, thermal output and efficiency of the boiler.

For the CHP plant, fuel consumption was calculated as follows:

$$Q_{chp,fuel} = \frac{Q_{chp} + P_{chp}}{\eta_{chp,th} + \eta_{chp,e}} \tag{3.7}$$

where Q_{chp} , P_{chp} , $\eta_{chp,th}$ and $\eta_{chp,e}$ are thermal output, electrical output and the thermal and electrical efficiency of the CHP.

CHP with back pressure steam turbine was assumed in this study. Electricity generation by the CHP plant was described using the model proposed by Savola et al. [33], [44]. This depends on the heat power output of the CHP plant and DH supply temperature:

$$P_{chp} = a.Q_{chp} + b.T_s + d \tag{3.8}$$

The CHP power production coefficients of a = 0.444, b = -0.0351 and d =1.99 were considered [33], [44]. The relationship between CHP electricity generation, CHP heat output and DH supply temperature is shown in Figure 3-1.

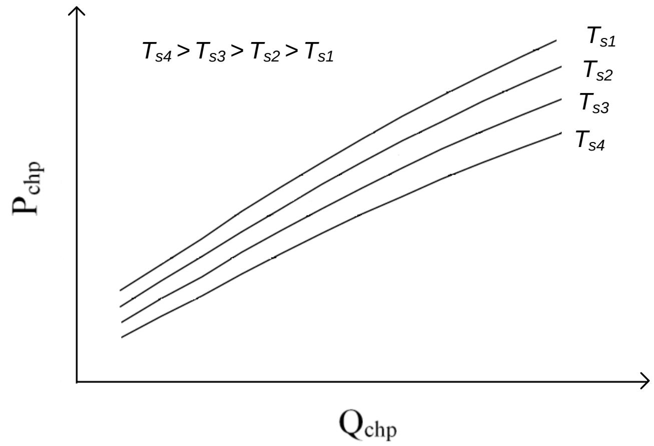

Figure 3-1 Power production in CHP with different district heating supply temperature

The impact of part-load efficiency on the variable heat source fuel energy consumption and cost was taken into account. For the sake of simplicity, the part load efficiency was modelled using a linear approximation shown in Figure 3-2.

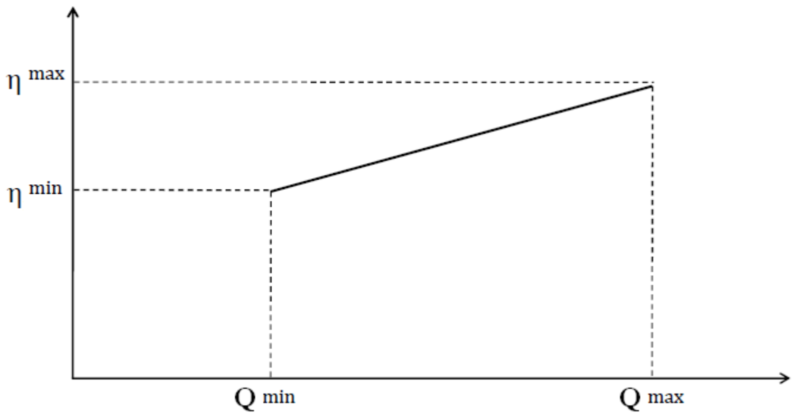

Figure 3-2 Linear approximation of part load efficiency of heat sources

Boiler efficiency was assumed to be between a maximum of 90% and a minimum of 60%, corresponding to the maximum and minimum thermal output [48]. The total efficiency of a CHP varied between a maximum of 90% and a minimum of 45% according to the maximum and minimum heat output of the CHP [27]. For the calculation of fuel cost, a price of 43£/MWh was used [78].

3.2.2 Calculation of heat flow

The concept of graph theory was used to describe the heating pipe network topology [79]. A graph is commonly defined as a combination of:

- A set of nodes;
- A set of branches, and
- Incidence relation.

Each branch within a graph connects a pair of nodes. A node is the starting or ending point of a branch. A heat network can be treated as a network graph. The heat source, pipes and loads are represented as branches; nodes symbolise points where branches divide or connect. The incidence matrix was created with N nodes and M flows (branches). The incidence matrix (A) which is a ($N \times M$) matrix, containing the element ($a_{k,j}$):

$a_{k,j}$ =-1 If pipe j starts at node k

$a_{k,j}$ =1 If pipe j ends at node k

$a_{k,j}$ =1 If source j ends at node k

$a_{k,j}$ =-1 If load j starts at node k

$a_{k,j}$ =0 Otherwise

The incidence matrix has one column for each flow stream in the system, and one row for each node. The case study shown in Figure 2-1 (Chapter 2) was used. The case study with its incidence matrix is shown in Figure 3-3.

The incidence matrix was used to calculate flow in branches. The numbers coloured in red represent the flow rate in heat source and loads. Accordingly, flow rates in return pipes are calculated in the same manner as those found in the supply pipes. For the calculation of flow in return pipes, the incidence matrix was multiplied by -1.

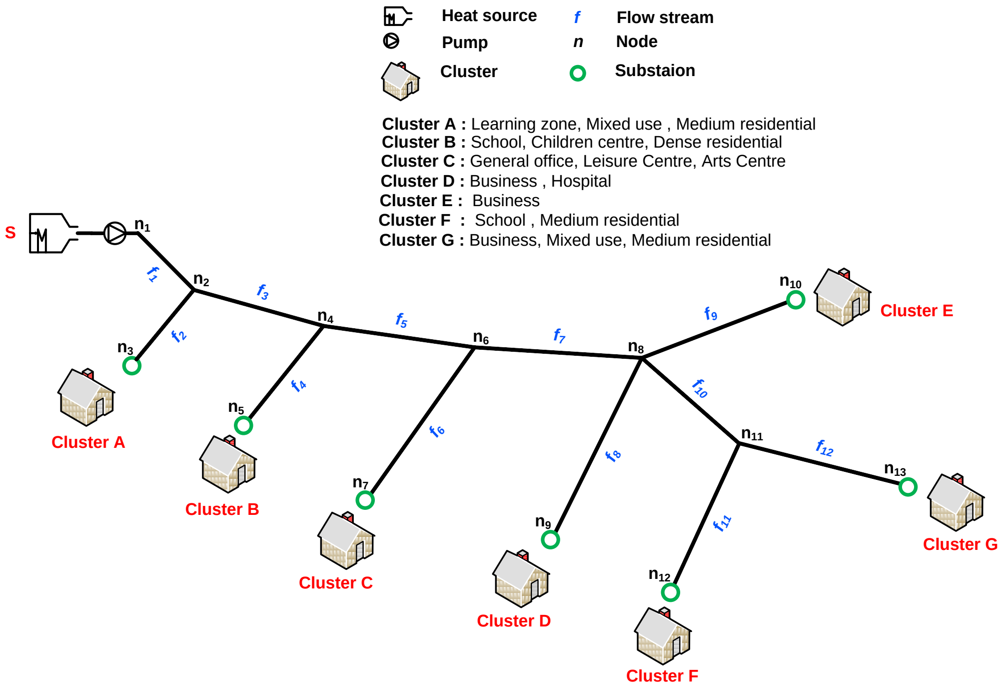

$$A = \begin{array}{cc} & \begin{array}{cccccccccccccccccccc} S & f_1 & f_2 & f_3 & f_4 & f_5 & f_6 & f_7 & f_8 & f_9 & f_{10} & f_{11} & f_{12} & A & B & C & D & E & F & G \end{array} \\ \begin{array}{c} n_1 \\ n_2 \\ n_3 \\ n_4 \\ n_5 \\ n_6 \\ n_7 \\ n_8 \\ n_9 \\ n_{10} \\ n_{11} \\ n_{12} \\ n_{13} \end{array} & \begin{bmatrix} 1 & -1 & 0 & 0 & 0 & 0 & 0 & 0 & 0 & 0 & 0 & 0 & 0 & 0 & 0 & 0 & 0 & 0 & 0 & 0 \\ 0 & 1 & -1 & -1 & 0 & 0 & 0 & 0 & 0 & 0 & 0 & 0 & 0 & 0 & 0 & 0 & 0 & 0 & 0 & 0 \\ 0 & 0 & 1 & 0 & 0 & 0 & 0 & 0 & 0 & 0 & 0 & 0 & 0 & -1 & 0 & 0 & 0 & 0 & 0 & 0 \\ 0 & 0 & 0 & 1 & -1 & -1 & 0 & 0 & 0 & 0 & 0 & 0 & 0 & 0 & 0 & 0 & 0 & 0 & 0 & 0 \\ 0 & 0 & 0 & 0 & 1 & 0 & 0 & 0 & 0 & 0 & 0 & 0 & 0 & 0 & -1 & 0 & 0 & 0 & 0 & 0 \\ 0 & 0 & 0 & 0 & 0 & 1 & -1 & -1 & 0 & 0 & 0 & 0 & 0 & 0 & 0 & 0 & 0 & 0 & 0 & 0 \\ 0 & 0 & 0 & 0 & 0 & 0 & 1 & 0 & 0 & 0 & 0 & 0 & 0 & 0 & 0 & -1 & 0 & 0 & 0 & 0 \\ 0 & 0 & 0 & 0 & 0 & 0 & 0 & 1 & -1 & -1 & -1 & 0 & 0 & 0 & 0 & 0 & 0 & 0 & 0 & 0 \\ 0 & 0 & 0 & 0 & 0 & 0 & 0 & 0 & 1 & 0 & 0 & 0 & 0 & 0 & 0 & 0 & -1 & 0 & 0 & 0 \\ 0 & 0 & 0 & 0 & 0 & 0 & 0 & 0 & 0 & 1 & 0 & 0 & 0 & 0 & 0 & 0 & 0 & -1 & 0 & 0 \\ 0 & 0 & 0 & 0 & 0 & 0 & 0 & 0 & 0 & 0 & 1 & -1 & -1 & 0 & 0 & 0 & 0 & 0 & 0 & 0 \\ 0 & 0 & 0 & 0 & 0 & 0 & 0 & 0 & 0 & 0 & 0 & 1 & 0 & 0 & 0 & 0 & 0 & 0 & -1 & 0 \\ 0 & 0 & 0 & 0 & 0 & 0 & 0 & 0 & 0 & 0 & 0 & 0 & 1 & 0 & 0 & 0 & 0 & 0 & 0 & -1 \end{bmatrix} \end{array}$$

Figure 3-3 The case study with its incidence matrix

The energy flow and flow rate at each branch and the temperature and pressure at each node of the network were calculated using equations found in thermal engineering text books [57], [80] (see appendix A).

Heat supplied to the network was calculated using the following equation:

$$Q_s = c_p\, \dot{m}(T_s - T_r) \tag{3.9}$$

Heat supply to each branch was obtained using Kirchhoff's rule at each node.

$$\sum_j Q_{jk} = 0 \qquad j = 1 \ldots M\,, \qquad k = 1 \ldots N \tag{3.10}$$

A linear approximation of the exponential decay of temperature (equation A.7, appendix A) was used to calculate temperature at the outlet of the pipes [76].

$$T_{j,outl} = \begin{cases} \left(T_{j,inl} - T_g\right)\left(1 - \dfrac{U_j l_j}{c_p \dot{m}_j}\right) + T_g & \dfrac{U_j l_j}{c_p \dot{m}_j} \leq 1 \\ T_g & \dfrac{U_j l_j}{c_p \dot{m}_j} \geq 1 \end{cases} \tag{3.11}$$

where U is the heat transition coefficient and T_g is the ground temperature.

At a node with more than one branch or supply source, the node temperature was calculated in terms of the temperature of the mixed incoming streams [57], [79]. For example, if pipe 1 receives hot water from pipe 2 and 3, then temperature at node l was calculated using the equation:

$$T_k = \frac{\sum_j \dot{m}_j T_{j,outl}}{\sum_j \dot{m}_j} = \frac{\dot{m}_2 T_{2,outl} + \dot{m}_3 T_{3,outl}}{\dot{m}_2 + \dot{m}_3} \tag{3.12}$$

Heat loss in each pipe section was obtained using the equation:

$$Q_{j,loss} = c_p\, \dot{m}_j (T_{j,inl} - T_{j,outl}) \tag{3.13}$$

Total heat losses in the heat network were the sum of the heat loss in each pipe section of the supply and return pipes:

$$Q_{loss} = \sum_j Q_{j,loss} \tag{3.14}$$

Flow rate in each pipe was calculated using Kirchhoff's rule at each node.

$$\sum_j \dot{m}_{jk} = 0 \tag{3.15}$$

Differential pressure of a variable speed pump was obtained using the equation [53]:

$$\Delta p_p = \left(\frac{\dot{m}}{\dot{m}_{max}}\right)^2 \Delta p_{p,max} \tag{3.16}$$

The electrical power of the pump (in kW) was calculated using equations 2.4-2.6.

The FICO Xpress Optimisation suite was used to solve the optimisation problem. The non-linearity of the heat network equations was dealt with through Sequential Linear Programming (SLP)[81].

Using the VF-VT operating method, for design cases based on temperature regime of $T_{s,max}/T_{r,max}$: 120/70 °C (see Table 2-1), the supply temperature was constrained at the heat source between a maximum of 120°C for the winter season and a minimum of 70 °C for the summer season. Similarly, for the design cases based on temperature regimes of $T_{s,max}/T_{r,max}$: 110/70 °C, 100/70 °C and 90/70 °C, maximum supply temperature of 110°C, 100°C and 90°C and minimum supply temperature of 70 °C were considered. For the summer season, when there is only demand for domestic hot water, the supply temperature was fixed at 70 °C on the heat source, within all temperature regimes.

It was assumed that return temperature was known at the consumer's heating substations. For the sake of simplicity, a constant return temperature of 40 °C for the winter season and 30 °C for the summer season were assumed at the consumer's heating substations, using all temperature regimes.

3.2.3 Model validation

Model validation is an essential part if the model be accepted and used to support decision making. Hence, the thermal and hydraulic calculations of the optimisation model developed in FICO Xpress were validated using the commercial software PSS SINCAL. For this purpose, physical and heating data of the design case *DH12* (MPL: 592 Pa/m), shown in Table 2-1 and Table B2-2 (appendix B), were used.

Using daily heat demand (Figure 2-3) the design case was optimised for the *ideal-DH*, by minimising annual total energy consumption over the year. Optimum flow rate and supply temperature were obtained at each time step over the year. Consequently, the optimal heat losses and pump power were calculated. Using the obtained flow rate and temperature data as input to the PSS SINCAL model, the heat losses and pump power were calculated at each time step. Calculated heat losses and pump power were compared with those obtained using the FICO Xpress optimisation model. Validation results are shown in Figure 3-4 a) and b).

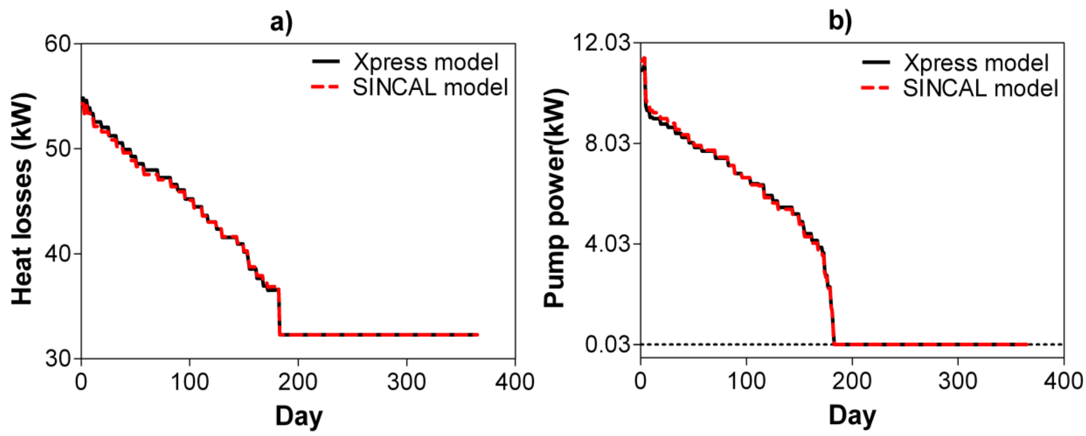

Figure 3-4 a) Heat losses b) pump power, FICO Xpress and PSS SINCAL model

The FICO Xpress model was shown to provide the same result as the PSS SINCAL model.

3.3 Calculation of optimal energy consumption and heat losses

Optimal flow, supply temperature and optimal annual pump energy consumption and heat losses of the DH design cases were compared. Optimisation results based on the minimum annual total energy consumption are presented.

3.3.1 Ideal-DH

For the *ideal-DH*, the objective function given in equation 3.1 includes pump energy consumption and heat energy losses in the pipes. Using the objective function and constraints given in equations 3.3-3.5 the optimum supply temperature and flow rate were calculated for all design cases, as shown in Table 2-1 and Table B2-2 (appendix B). Consequently, optimum annual pump energy consumption and heat energy losses were determined. Optimal flow and supply temperature for the design cases based on temperature regime of $T_{s,max}/T_{r,max}$: 120/70 °C are depicted in Figure 3-5 (only a few are shown and the rest can be obtained by correlating with those shown in Table 2-1).

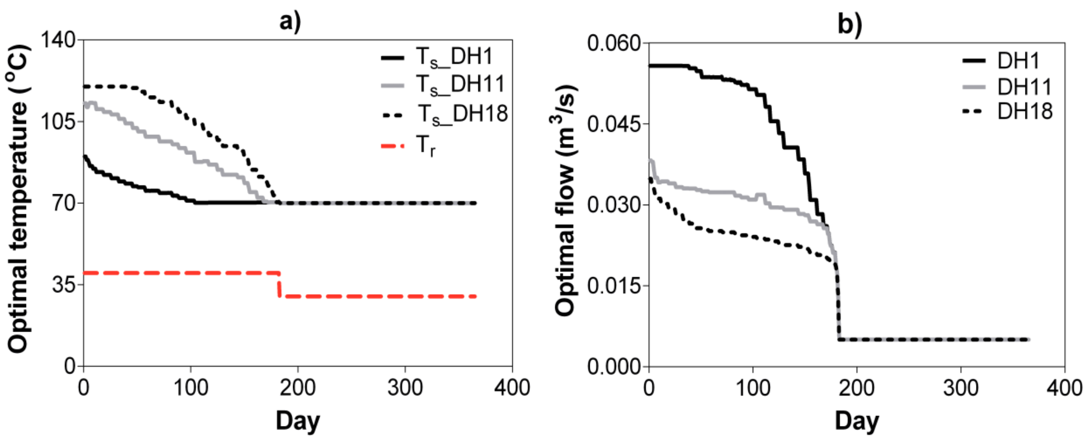

Figure 3-5 a) Optimal supply temperature b) optimal flow rate based on minimisation of the annual total energy consumption, *Ideal-DH*

From Figure 3-5, it is seen that for various design cases, different values of optimum supply temperature and flow rate are obtained over the course of the year. For *DH1* (MPL: 52 Pa/m) the supply temperature is the lowest over the whole year but the flow rate is the highest compared with other design cases. When MPL is low, smaller pump size is required to overcome flow resistance. However, since pipe diameters are larger, heat losses are consequently higher. Hence, the optimal annual total energy consumption was achieved when the supply temperature is lower and the flow rate is larger compared to the other design cases.

Using a design case based on a larger MPL, for instance *DH18* (MPL: 1403 Pa/m), due to the smaller pipe diameters and larger pump size, the annual pump energy consumption is higher while the annual heat energy losses are less compared with the other cases. Therefore, to achieve the optimal annual total energy consumption, optimum supply temperature was obtained larger and flow rate lower in comparison with other cases.

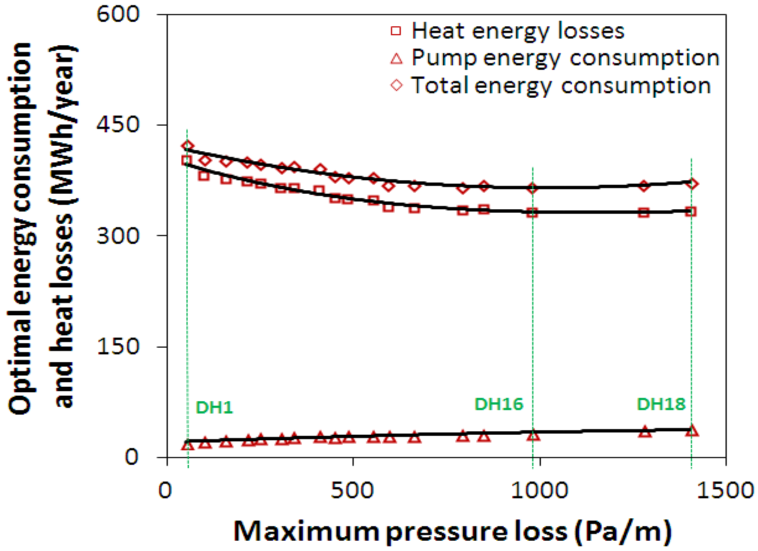

Figure 3-6 Optimal annual pump energy consumption and heat losses, *Ideal-DH*

Optimal annual pump energy consumption and heat losses are shown in Figure 3-6. From Figure 3-6, it can be observed that annual pump energy consumption and heat energy losses for different design cases are vary, due to differences in design, obtained supply temperature and flow rate. Optimal annual pump energy consumption is noticeably less than the optimal annual heat energy losses. The pump electrical energy consumption increases along with the MPL whereas the heat losses decrease. The optimal annual total energy consumption is minimum when *DH16* (MPL: 977 Pa/m) is used.

3.3.2 Boiler-DH

For *boiler-DH*, the objective function (equation 3.1) includes pump energy consumption, heat energy losses in the pipes and fuel consumption in the boiler. The objective of the optimisation is to minimise annual total energy consumption (including boiler fuel consumption). Using the optimisation, first optimal supply temperature and flow rate were determined and then the optimum annual pump energy consumption and heat energy losses were found for all design cases. Optimal flow rate and supply temperature for the design cases based on temperature regime of $T_{s,max}/T_{r,max}$: 120/70 °C are depicted in Figure 3-7.

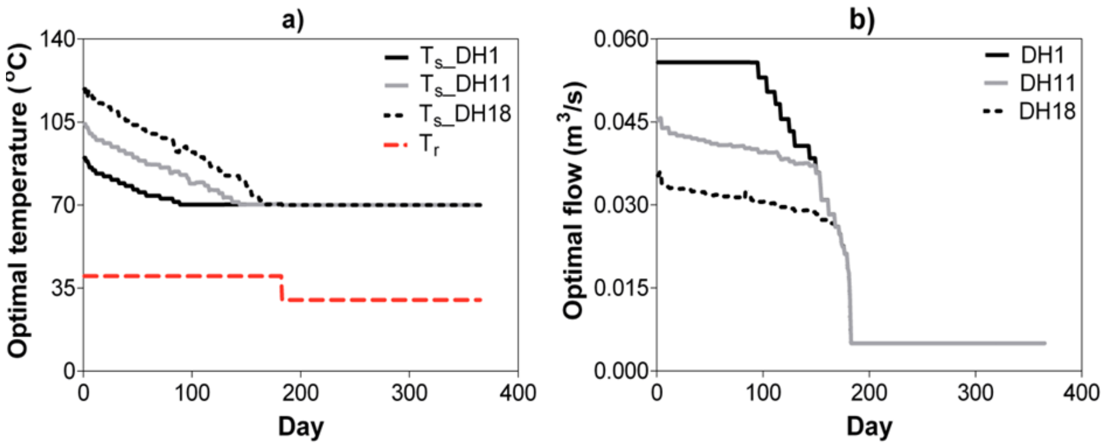

Figure 3-7 a) Optimal supply temperature b) optimal flow based on minimisation of the annual total energy consumption, *Boiler-DH*

Figure 3-7 shows that changes of optimum supply temperature and flow rate over the year are different for different design cases. For *DH1* (MPL: 52 Pa/m), due to the selection of pipes with larger diameters, the electrical energy consumption of the pump is lower and heat energy losses are higher compared with other cases. Therefore, in order to reduce the heat losses the optimum supply temperature was obtained lower and flow rate higher in comparison to the other design cases. By using *DH1* case the optimiser uses variable supply temperature and constant flow to reduce annual total energy consumption when demand is high. Later, when demand decreases and supply temperature reaches its minimum level, the flow starts to decrease at a constant minimum supply temperature.

In the *DH18* (MPL: 1403 Pa/m) case, in order to achieve minimum annual total energy consumption the optimal flow rate is less and the supply temperature is larger in comparison to other design cases.

Optimal annual pump energy consumption and heat losses are shown in Figure 3-8. It is shown that the minimum optimal annual total energy consumption (excluding boiler fuel consumption, although the impact of the boiler as a heat source was taken into account for the optimisation), occurs when using *DH16* (MPL: 977 Pa/m).

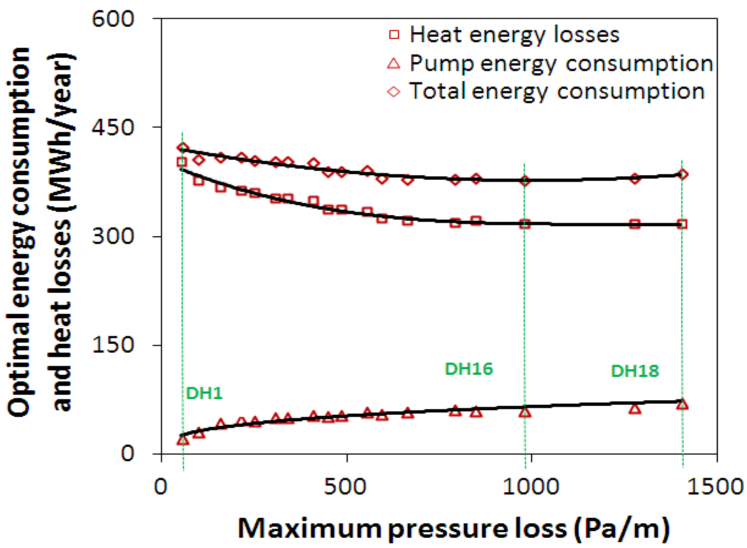

Figure 3-8 Optimal annual pump energy consumption and heat losses, *Boiler-DH*

3.3.3 CHP-DH

For *CHP-DH*, the objective function includes pump energy consumption, heat energy losses in the pipes and fuel consumption in CHP (equation 3.1). The objective of the optimisation is to minimise annual total energy consumption. Optimal flow and supply temperature for the design cases based on temperature regime of $T_{s,max}/T_{r,max}$: 120/70 °C are depicted in Figure 3-9.

Figure 3-9 shows that for *CHP-DH*, the optimal supply temperature and flow rate are the same using all design cases. This is related to the interaction of heat losses, pump energy consumption and fuel consumption in *CHP-DH* (equation 3.1).

When heat demand was high (approximately 100 days per year) the minimum annual total energy consumption was achieved by varying flow rate at relatively high constant supply temperature. This is because electricity generation is high when heat production in the CHP is also high (see equation 3.9). Therefore, the optimiser reduces electricity generation in the CHP by increasing the supply temperature (see Figure 3-1). Due to the reduction in electricity generation of the CHP, the fuel consumption decreases (equation 3.8). Further, increased supply temperature results in the reduction of the flow rate. Therefore, heat losses are increased while pump energy consumption is decreased. Overall annual total energy consumption was reduced.

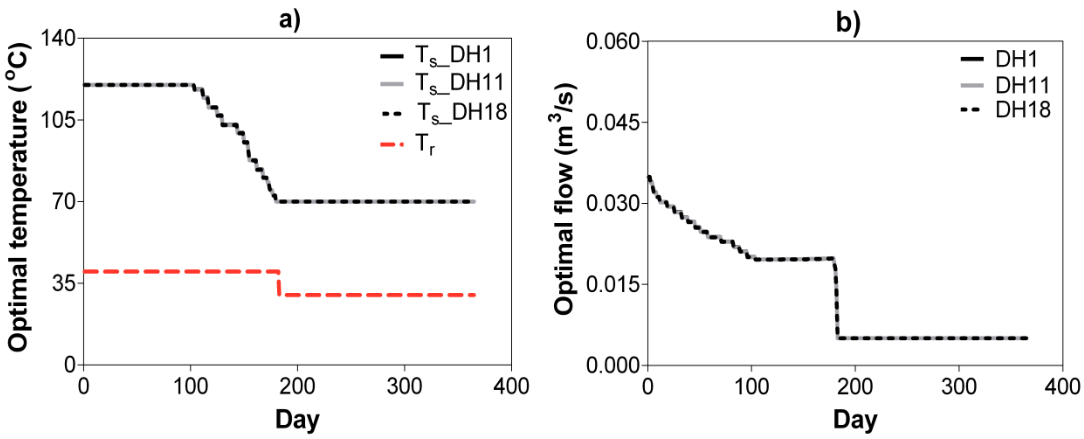

Figure 3-9 a) Optimal supply temperature b) optimal flow based on minimisation of the annual total energy consumption, *CHP-DH*

As heat demand reduces, electricity generation in CHP reduces accordingly (equation 3.9 and Figure 3-1). Hence, the effect of electricity generation on fuel consumption becomes less important and the role of heat losses becomes more significant. At this stage, the optimiser starts to reduce supply temperature at a constant flow rate. Due to the reduction of supply temperature, heat losses reduced and as a result the overall annual total energy consumption is decreased.

Optimal annual pump energy consumption and heat losses are shown in Figure 3-10. Due to the small flow rate, annual pump energy consumption has reduced substantially as shown in Figure 3-10. The minimum optimal annual total energy consumption (excluding CHP fuel consumption) happens when *DH16* (MPL: 977 Pa/m), is used.

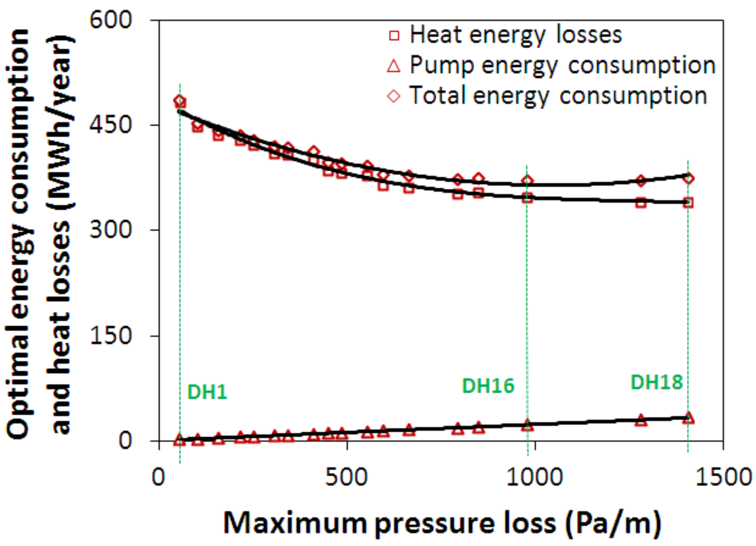

Figure 3-10 Optimal annual pump energy consumption and heat losses, *CHP-DH*

3.4 Economic analysis

Using the objective function given in equation 3.2 and constraints in equations 3.3-3.5 the optimisation was conducted to minimise annual total operating costs. At first the optimal supply temperature and flow rate were obtained for all DH design cases. Optimal annual pumping cost and heat losses cost were determined. Using the data given in section 2.5, the EAC of the design cases were calculated and compared.

3.4.1 Ideal-DH

For the *ideal-DH*, the objective function (equation 3.2) includes pumping cost and cost associated to the heat losses in the pipes. Using optimisation the optimal supply temperature and flow rate were determined. The optimal annual pumping cost and heat losses cost was found and finally the EAC was calculated. Optimal flow and supply temperature for the design cases based on temperature regime of $T_{s,max}/T_{r,max}$: 120/70 °C are depicted in Figure 3-11 (only three design cases are shown and the rest can be found by correlating with those shown in Table 2-1).

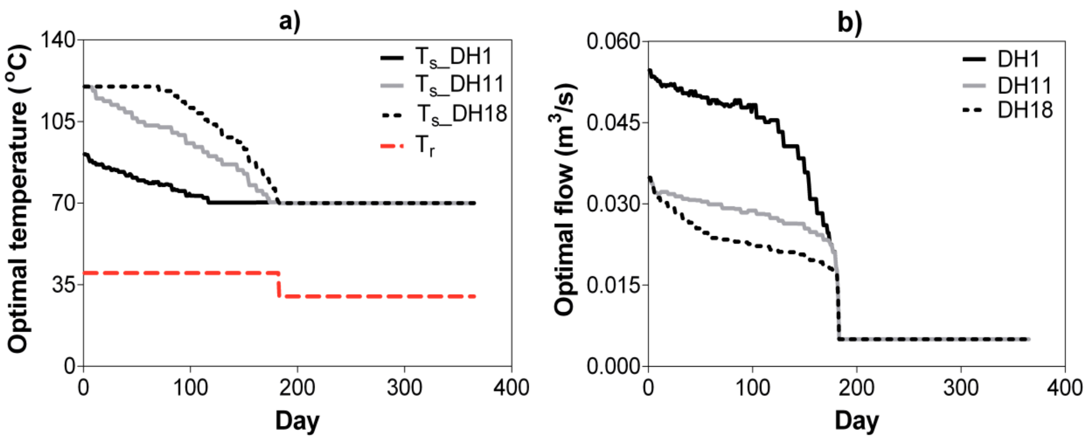

Figure 3-11 a) Optimal supply temperature b) optimal flow based on minimisation of the operational costs, *Ideal-DH*

Figure 3-11shows that for different design cases, optimal supply temperature and flow rate are different. For *DH18* (MPL: 1403 Pa/m), optimal supply temperature is the highest and flow rate is the lowest compared to the other design cases. Whilst for *DH1* (MPL: 52 Pa/m), the optimal supply temperature is the lowest and flow rate is the highest in comparison to the other cases. As previously explained, this is because the pipe diameters and pump size are different in different design cases.

For *DH18* (MPL: 52 Pa/m) pipe diameters are smaller and pump size is larger than the other design cases. Therefore, pump energy consumption is larger and heat losses are less. Hence, to avoid excessive pumping cost and to achieve minimum annual total operating costs, higher supply temperature and lower flow rate were obtained. For *DH1* (MPL: 52 Pa/m), pipes with larger diameters and smaller size pump were chosen compared with the other design cases. As a result, the optimiser reduces supply temperature and increases flow rate to achieve the minimum annual total operating costs.

The EAC shown in Figure 3-12 is minimum when the *DH17* (MPL: 1276 Pa/m) design case, which has a rather high pressure loss, is used.

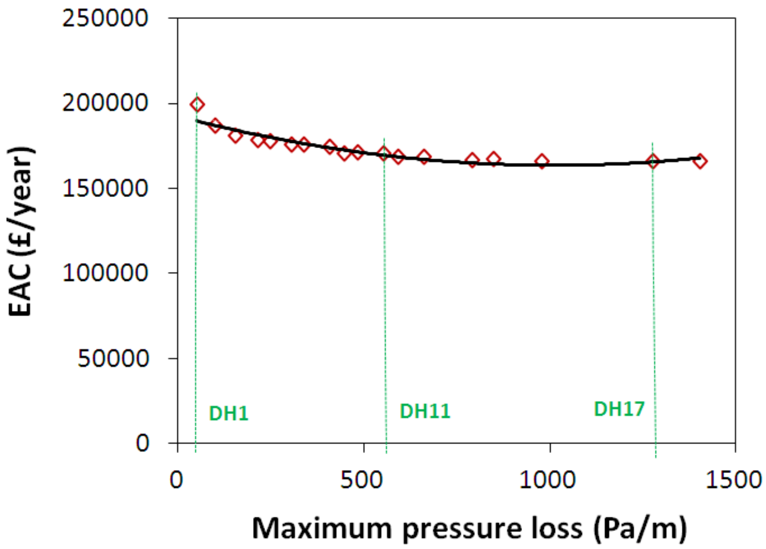

Figure 3-12 Equivalent annual cost, *Ideal-DH*

3.4.2 Boiler-DH

For *boiler-DH* the objective function (equation 3.2) includes pumping costs, costs associated with heat losses in the pipes and fuel consumption in the boiler. The objective of optimisation was to minimise annual total operating costs. First, optimal supply temperature and flow rate were determined. Then, the optimal annual pumping and heat losses costs were found and the EAC was calculated. Optimal flow and supply temperature are depicted in Figure 3-13 for the design cases based on temperature regime of $T_{s,max}/T_{r,max}$: 120/70 °C.

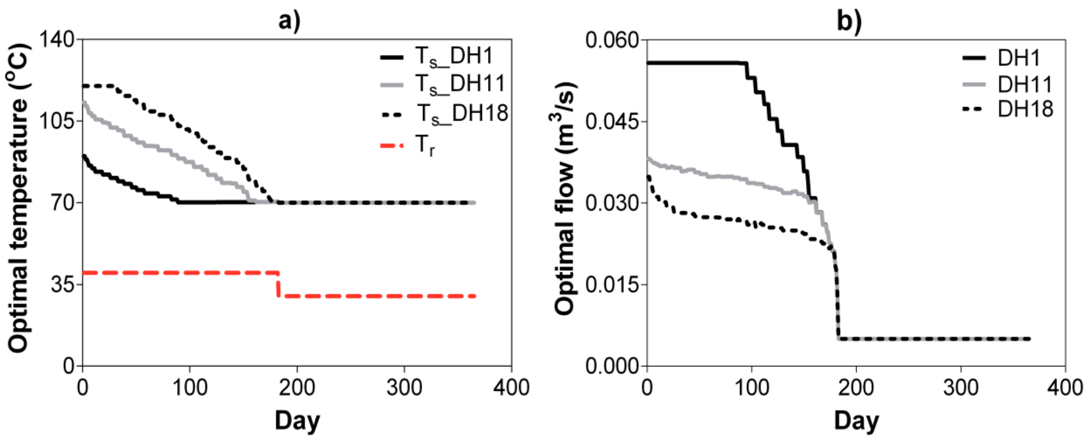

Figure 3-13 a) Optimal supply temperature b) optimal flow based on minimisation of the operational costs, *Boiler-DH*

Figure 3-13 shows that for different design cases the optimal supply temperature and flow rate are different. As explained previously this relates to the difference in pipe and pump sizes within the design cases.

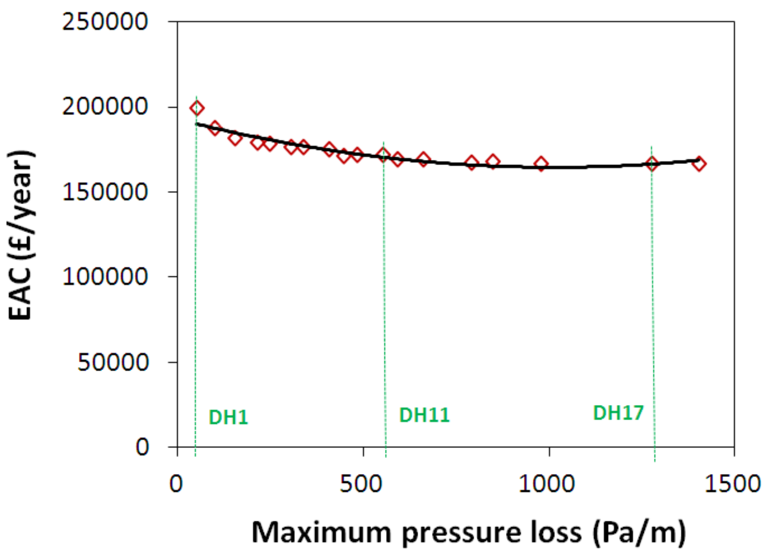

Figure 3-14 Equivalent annual cost, *Boiler-DH*

The EAC is shown in Figure 3-14. It is seen that the EAC is minimum when *DH17* (MPL: 1276 Pa/m), is used.

3.4.3 CHP-DH

Total operational costs of the *CHP-DH* consist of fuel cost, and costs associated with the pump energy consumption and heat energy losses. The CHP generates heat and electricity in a single unit which means that there is also a revenue stream from selling electricity to the grid. Therefore, to achieve the optimal operation of the *CHP-DH*, the revenue of selling electricity to the grid was added as negative cost to the objective function (equation 3.2). Using optimisation, the optimal supply temperature and flow rate were determined first. Then, the optimal annual pumping and heat losses costs were found and the EAC was calculated. Optimal flow and supply temperature for the design cases based on temperature regime of $T_{s,max}/T_{r,max}$: 120/70 °C are shown in Figure 3-15.

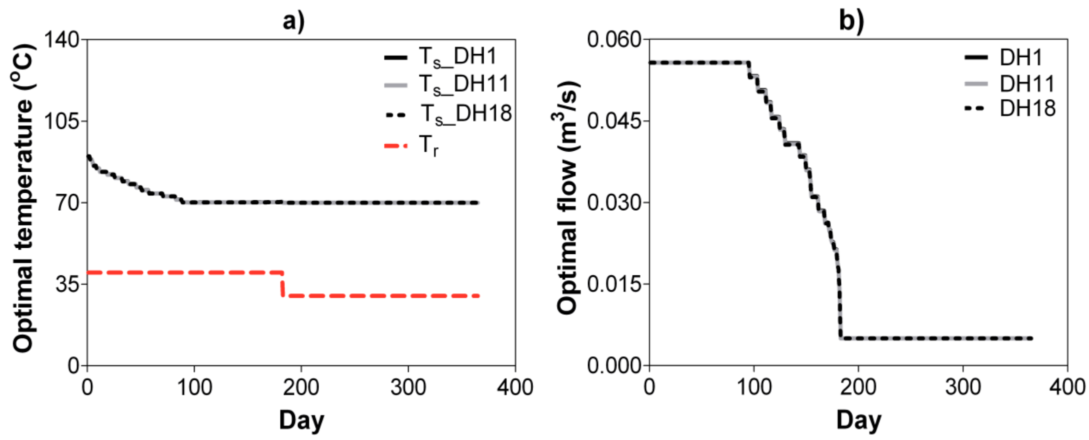

Figure 3-15 a) Optimal supply temperature b) optimal flow based on minimisation of the operational costs, *CHP-DH*

Fig 3-15 shows that the optimal supply temperature and flow rate are the same using all design cases. This is due to the fact that heat and electricity are generated in the CHP, and the effect of electricity revenue is added as negative cost to the objective function (equation 3.2).

When demand was high (around 100 days per year) the minimum annual total operating costs were obtained by varying supply temperature at a constant high flow rate. When demand was high, electricity generation in CHP was high (equation 3.9).

Therefore, the optimiser increased electricity generation in CHP by reducing supply temperature (equation 3.9 and Figure 3-1). Due to the reduction of supply temperature, heat losses decrease, electricity generation increases and the revenue from selling electricity also increases. Since flow rate is high, pump energy consumption increases, but the overall annual total operating costs decreases.

As heat demand reduces further, and supply temperature reaches its minimum level, the effect of supply temperature on electricity generation and heat losses reduces. Therefore, the optimiser supplies heat demand by varying flow rate at constant minimum supply temperature.

The EAC (excluding CHP fuel cost) is shown in Figure 3-16. The EAC is minimum for *DH9* (MPL: 448 Pa/m).

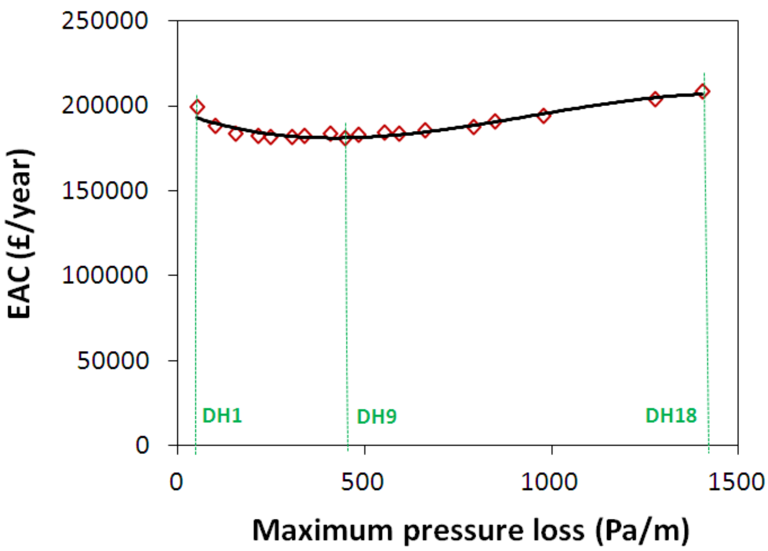

Figure 3-16 Equivalent annual cost, *CHP-DH*

3.5 Comparison

All the design cases were operated using the VF-VT operating method. The design cases with minimum optimal annual total energy consumption and minimum EAC are summarised in Table 3-1 and Table 3-2 respectively.

Table 3-1 shows that the minimum optimal annual total energy consumption is lowest for the design cases based on a temperature regime of $T_{s,max}/T_{r,max}$: 120/70 °C (see Table 2-1), when using the VF-VT operating method. The design case *DH16* (MPL: 977 Pa/m) has minimum optimal annual total energy consumption for all investigated types of heat sources. Further, as the temperature difference between supply and return pipes decreases, due to the increase in system flow rate, the annual total energy consumption increases.

Table 3-1 Design cases with minimum optimal annual total energy consumption, using different temperature regimes and the VF-VT operating method

System	***Ideal-DH***		***Boiler-DH***		***CHP-DH***	
$T_{s,max}/T_{r,max}$ ℃	**DH case**	**$E_{T,min}$ (MWh/year)**	**DH case**	**$E_{T,min}$ (MWh/year)**	**DH case**	**$E_{T,min}$ (MWh/year)**
120/70	DH16	367	DH16	377	DH16	371
110/70	DH35	378	DH35	390	DH35	383
100/70	DH44	389	DH44	395	DH44	394
90/70	DH68	389	DH68	393	DH68	400

Similarly, from results given in Table 3-2, it is observed that for the temperature regime of $T_{s,max}/T_{r,max}$: 120/70 ℃, the minimum EAC is lowest when using the VF-VT operating method. The design case *DH17* (MPL: 1276 Pa/m) was found to be the most cost effective design when boiler or an ideal heat source was considered. *DH9* (MPL: 448 Pa/m) was the cost effective design case when CHP was chosen as the heat source. Moreover, as the temperature difference between supply and return pipe decreases due to the increase in flow rate, the annualised cost of the heat network installation and operation increases accordingly.

Table 3-2 Design cases with minimum EAC, using different temperature regimes and the VF-VT operating method

System	***Ideal-DH***		***Boiler-DH***		***CHP-DH***	
$T_{s,max}/T_{r,max}$ ℃	**DH case**	**EAC_{min} (£/year)**	**DH case**	**EAC_{min} (£/year)**	**DH case**	**EAC_{min} (£/year)**
120/70	DH17	165501	DH17	166289	DH9	180475
110/70	DH36	170463	DH36	171259	DH23	183780
100/70	DH54	175852	DH54	176525	DH45	185773
90/70	DH68	184339	DH68	184814	DH67	188480

The EAC was divided by the annual total energy demand (32602 MWh/year) and the cost of heat transmission per MWh was obtained. This is given in Table 3-3.

Table 3-3 Design cases with minimum cost of heat transmission, using different temperature regimes and VF-VT operating method

System	***Ideal-DH***		***Boiler-DH***		***CHP-DH***	
$T_{s,max}/T_{r,max}$ ℃	**DH case**	**Cost (£/MWh)**	**DH case**	**Cost (£/MWh)**	**DH case**	**Cost (£/MWh)**
120/70	DH17	5.08	DH17	5.10	DH9	5.54
110/70	DH36	5.23	DH36	5.25	DH23	5.64
100/70	DH54	5.39	DH54	5.41	DH45	5.70
90/70	DH68	5.65	DH68	5.67	DH67	5.78

Comparison of results presented in Table 3-1 and Table 3-2 shows that the major difference between energy and cost effective design cases is observed when using CHP as the heat source. The difference, as previously explained, is related to the impact of electricity generation in *CHP-DH*. It indicates that in order to achieve economical operation of a *CHP-DH,* larger pipe diameters have to be chosen. For the *ideal-DH* and *boiler-DH,* the difference seen in Table 3-1 and 3-2 is due to the pipe investment costs, and the cost of heat losses to the pump investment costs and the cost of pump electricity consumption. An economic evaluation of the *ideal-DH* and *boiler-DH* found that the optimum solution corresponds to smaller pipe diameters.

Results obtained from energy and cost investigations when using the VF-VT operating method suggest using rather large TPL values for the design of a DH pipe network. Determination of pipe diameters using large TPL values in a DH network implies the use of relatively small pipe diameters and a large pump size. Therefore, the annual total energy consumption will reduce along with the annualised cost of the heat network installation and operation.

Results obtained in this Chapter for the VF-VT operating method are compared with those obtained in Chapter 2 using the VF-CT method. Comparing results obtained in Table 2-3 and Table 3-1 show that minimum annual total energy consumption of the design cases are reduced when using the VF-VT operating method compared to the VF-CT. The minimum annual total energy consumption is reduced by approximately 23% for the *ideal-DH*, *boiler-DH* and *CHP-DH* when using the VF-VT compared to the VF-CT operating strategy. Similarly, from Table 2-4 and Table 3-2, minimum EAC is reduced for the VF-VT operating method. The EAC is reduced by about 10% for the *ideal-DH* and *boiler-DH* when using the VF-VT operating method. Due to the impact of electricity generation in *CHP-DH*, the EAC is reduced about 2% when using the VF-VT compared to the VF-CT method. Overall, it indicates that a better performance of a DH can be achieved by using the VF-VT operating method.

3.6 Conclusions

Performance analysis of the DH design cases was conducted over the year using the VF-VT operating method and different supply and return temperature regimes. The annual pump energy consumption, heat losses and the EAC of the design cases were calculated and compared.

When using the VF-VT operating method the annual total energy consumption and the EAC were reduced in comparison with other operating strategies explained in Chapter 2. The most economical design also depended on the type of heat source. For *CHP-DH*, it was economically beneficial to have larger pipe diameters and a smaller size pump compared to the *ideal-DH* and *boiler-DH*. For the VF-VT operating method, the most energy and cost effective design cases of DH pipe used smaller pipe diameters and larger pressure drops.

A comparison of design cases with different temperature regimes showed that in order to achieve energy efficient and cost effective design of a DH pipe network, it was more advantageous to reduce system flow rate by increasing temperature difference between supply and return pipes. Due to the reduction of flow rate, the annual total energy consumption and the annualised cost of the heat network installation and operation were reduced.

CHAPTER 4- Modelling and Optimisation of a District Heating Network

4.1 Introduction

Investigation of the operation of DH design cases (Tables 2-1 and Table B2-2), using different operating strategies has been presented in Chapters 2 and 3. A better energy performance was achieved for DH using the VF-VT operating method. In addition, using the VF-VT operating method the EAC of DH was reduced compared to the other operating strategies. Using the analysis procedures described in Chapters 2 and 3, a two-stage programming model was developed to obtain the optimal flow, supply temperature, pipe and pump sizes in a DH network. The two-stage programming model synthesises both design and optimal operation of a DH network to obtain the optimal solution.

For the assessment of design cases, energy, exergy and cost analyses were used. Using energy analysis, the heat energy losses and electrical energy consumption of the pump were considered. Therefore, an optimal solution is based on the minimisation of the annual total energy consumption (pump energy consumption plus heat energy losses) of a DH network.

Exergy is a measure of quality of energy defined as the maximum amount of work which can be produced by a quantity of energy or a flow of matter when it comes to equilibrium with a reference environment [82]. Using exergy analysis, it was assumed that the quality of heat energy is lower than that of electrical energy. Hence, optimal solution is based on the minimisation of the annual total exergy consumption (pump exergy consumption and heat exergy losses) of a DH network.

In some studies, exergy analysis has been used to analyse the performance of buildings [83] and DH networks [84–86]. A key review on exergetic analysis and assessment of renewable energy resources is given in [87]. The concept and application of exergy analysis for low temperature heating and high temperature cooling is given in [88]. Generally, exergy analysis is recognised as an efficient technique to reveal whether or not, and by how much it is possible to design more efficient energy systems by reducing the inefficiencies in existing systems [89].

The cost analysis takes into account the capital investments and operating costs of a DH network. Using cost analysis, the design of a DH network is based on the minimisation of the annualised cost or the EAC of a DH network.

4.2 Optimisation model

The two-stage optimisation model was developed using the FICO™ Xpress optimisation suite. Microsoft Access linked to the FICO™ Xpress was used as the database to feed data as input and receive results from the optimisation. The non-linearity of the heat network equations was dealt with through SLP.

The structure and the flow chart of the optimisation process are shown in Figure 4-1 and Figure 4-2.

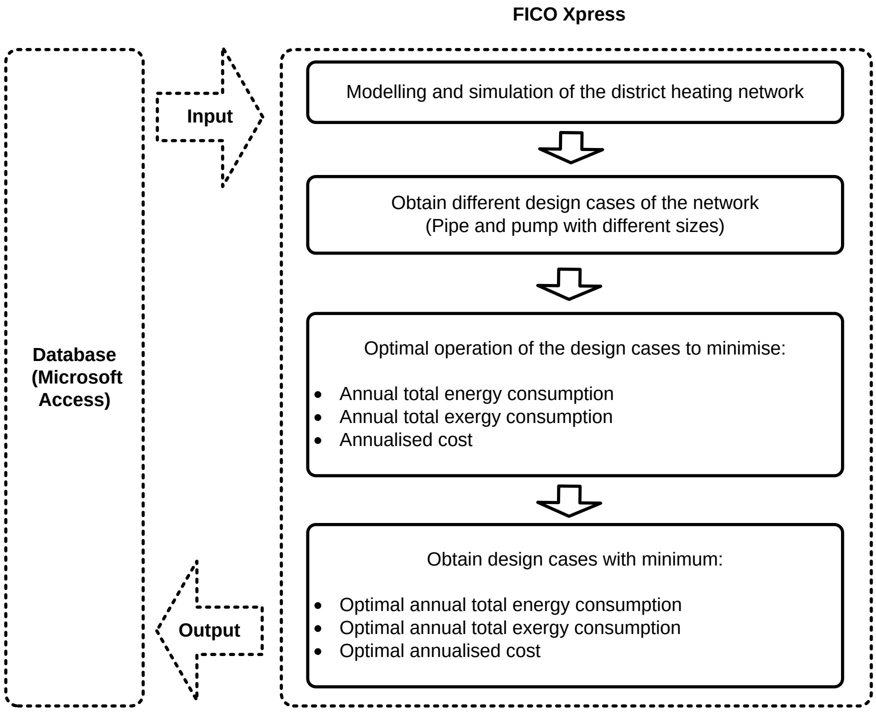

Figure 4-1 The structure of the optimisation process[1]

As shown in Figure 4-1 and Figure 4-2 the optimisation process includes several steps:

Step 1: Firstly, data required for optimisation model is collected and fed to the optimisation suite through a Microsoft Access data base (as in Figure 4-1). It includes:

- Topological configuration of the network;
- CO_2 and energy (heat, electricity and fuel) prices;
- Pipe and pump investment costs;
- Standard pipe sizes in the market;
- Maximum and variable heating load over a year;
- Maximum and minimum supply temperature at the heat source and return temperature at the consumer's heating substations;
- Maximum and minimum of TPL as well as TPL step change (ΔTPL).

[1] The process is automated.

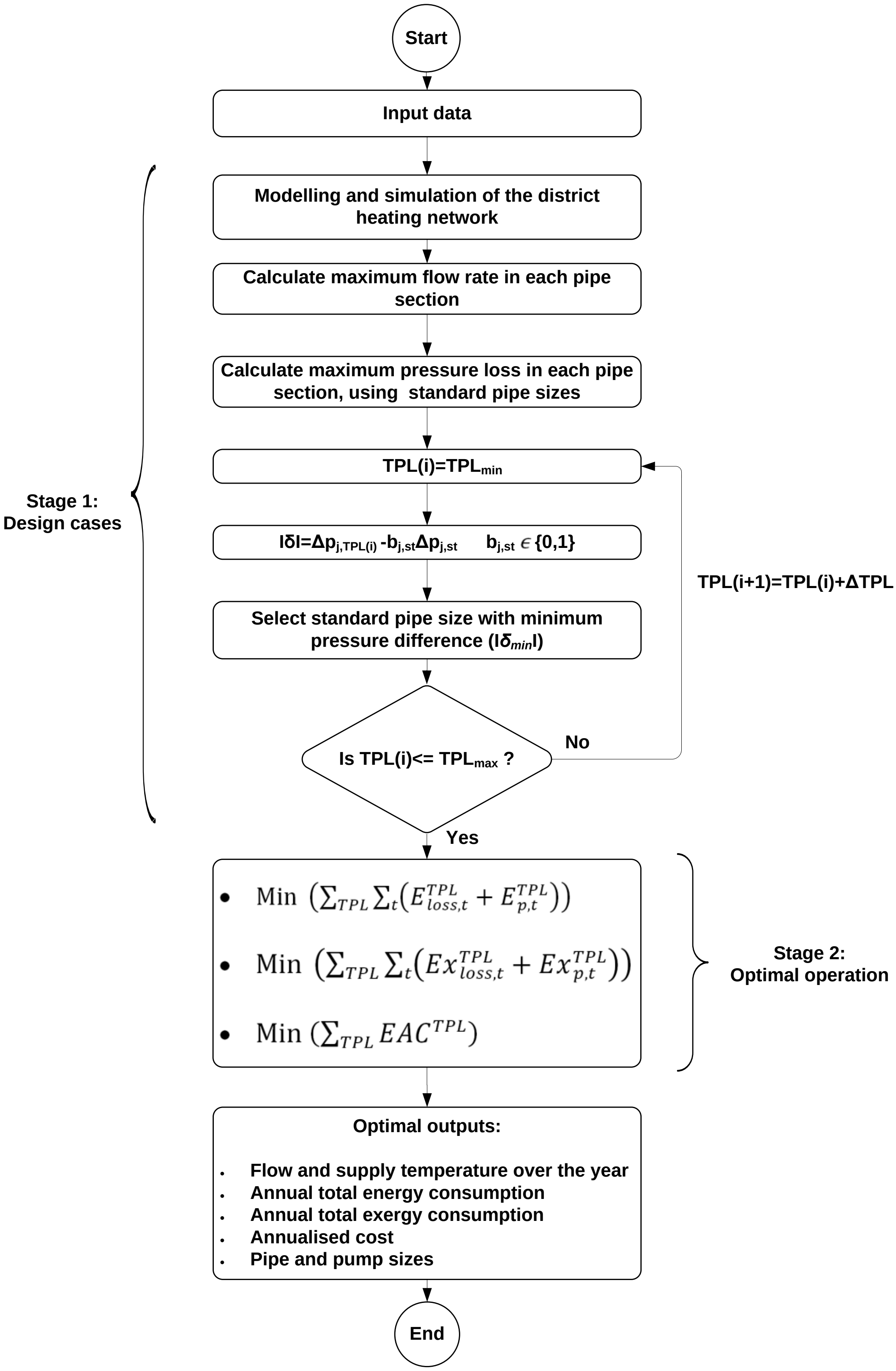

Figure 4-2 The flow chart of the optimisation process

Step 2: At this stage the incidence matrix of the DH network topology was created, using the concept of graph theory (see section 3.2.2).

Step 3: Initial pipe diameters were assumed. Following from Table B2-1, an average standard pipe size with d=137 mm, U=0.33 W/mK and ε=0.4 mm was considered for all pipes. The maximum flow rates were calculated in each pipe section of the network, using the maximum heating load, maximum supply temperature at the heat source and maximum return temperature at the consumer's heating substations (as described in appendix A).

Step 4: Using the maximum flow rate at each pipe section, MPL and maximum velocity using each standard pipe size in the market (see Table B2-1) were calculated:

$$\Delta p_{j,st} = 8 f_{j,st} \frac{l_j}{d_{st}^5} \frac{\dot{m}_j^2}{\rho \pi^2} \qquad j = 1 \dots M \quad st = 1 \dots Y \tag{4.1}$$

Friction factor f was evaluated as a function of Reynolds number Re and pipe roughness ε using the Colebrook formula [80] for turbulent flows.

$$\frac{1}{\sqrt{f_{j,st}}} = -2log_{10}\left(\frac{\varepsilon}{3.71 d_{st}} + \frac{2.51}{Re_{j,st}\sqrt{f_{j,st}}}\right) \tag{4.2}$$

where Reynolds number was calculated as follows:

$$Re_{j,st} = \frac{u_{j,st} d_{st}}{v} \tag{4.3}$$

Water velocity u in each pipe section was obtained using the following equation:

$$u_{j,st} = \frac{4\dot{m}_j}{\rho \pi d_{st}^2} \tag{4.4}$$

Step 5: The MPL obtained for each pipe section using standard pipe sizes, was compared with the pressure loss calculated according to the TPL values provided in the database. For each pipe section of the network, a standard pipe size with pressure loss closest to the pressure loss obtained according to the TPL was selected. The process was repeated for all TPL values until reaching the maximum TPL.

$$|\delta| = \Delta p_{j,TPL} - b_{j,st}\Delta p_{j,st} \qquad b_{j,st} \epsilon \{0,1\} \tag{4.5}$$

Pressure loss in each pipe section was compared with the pressure loss obtained based on TPL values using the selection of each standard pipe size. The standard pipe with minimum absolute pressure difference $|\delta_{min}|$ was selected. Therefore the value of $b_{j,st}$ is 1 otherwise 0.

Step 6: Pump size was determined following selection of standard pipe sizes corresponding to each TPL. For this purpose, the route with maximum pressure drop in the network was chosen. An extra 10% was approximately added on the calculated pressure loss to include the pressure drop in the pipe fittings, such as bends, tees and reducers [90]. Maximum differential pressure of pump and maximum pump power were calculated using equations 2.4-2.6.

Step 7: Finally, optimal operation of the design cases obtained in steps 5 and 6 was conducted for one year according to variations in the annual heating load. It was assumed that the DH network was fed by an ideal heat source (*ideal-DH*)[1] (see section 2.2.4). In addition, three objectives were examined. The objectives of the optimisation were to 1) minimise annual total energy consumption; 2) minimise annual total exergy consumption; or 3) minimise the annualised cost of the heat network.

The objective function based on minimisation of the annual total energy consumption is:

$$min \sum_{TPL} \sum_{t} \left(E^{TPL}_{loss,t} + E^{TPL}_{p,t} \right) \tag{4.6}$$

[1] The ideal heat source was defined as a heat source which has negligible operating costs, and is capable of delivering required amount of heat. The closest real word model is geothermal.

For the *ideal-DH,* only the heat energy losses E_{loss} and pump energy consumption E_p of the network were taken into account. Pump energy consumption and heat losses at each time step and for each design case were calculated using the equations 2.4-2.6 and 3.9-3.16.

The objective function based on minimisation of the annual total exergy consumption is:

$$min \sum_{TPL} \sum_{t} \left(Ex_{loss,t}^{TPL} + Ex_{p,t}^{TPL} \right) \tag{4.7}$$

Heat exergy losses Ex_{loss} and pump exergy consumption Ex_p were considered. Exergy loss associated with heat loss in each pipe section was calculated using the following equation [82]:

$$\dot{Ex}_{j,loss} = \left(1 - \frac{T_g}{T_{j,w}} \right) Q_{j,loss} \tag{4.8}$$

It was assumed that the pipes are laid underground and ambient temperature around the pipes ($T_g + 273$ in Kelvin) was assumed equal to the ground temperature. An average ground temperature of +7 ℃ was assumed over the year (see section 2.2.5). Hot water temperature (T_w in Kelvin) in each pipe section of the supply and return was assumed as the average temperature of the pipe inlet and pipe outlet temperature.

$$T_{j,w} = \left(\frac{T_{j,inl} + T_{j,outl}}{2} \right) \tag{4.9}$$

Pump exergy rate in (kW) was assumed to be equal to the pump power:

$$\dot{Ex}_p = P_p \tag{4.10}$$

The objective function based on minimisation of the EAC is:

$$min \sum_{TPL} EAC^{TPL} \tag{4.11}$$

For calculation of the EAC, impact of heat source on optimal solution of the supply temperature and flow rate was examined[1]. Therefore, DH connected to an ideal heat source (*ideal-DH*), a boiler (*boiler-DH*) and CHP (*CHP-DH*) were investigated.

The data required for calculation of the EAC, pipe investment costs including civil works and pump investment costs including the cost of variable frequency drive were taken from Table 2-2, Table B2-3 and Table B2-4 (appendix B). Pipe and pump estimated costs are shown in Figure B4-1 and Figure B4-2 (appendix B).

For each optimisation approach, the main DH network parameters such as temperature, flow rate and pressure loss in the pipe network were constrained (see equations 3.3-3.5).

District heating with high and low temperatures were investigated. For high temperature DH, maximum and minimum supply temperatures at the heat source were assumed to be 120 ℃ and 70 ℃ respectively. Similarly, maximum and minimum return temperature of 70 ℃ and 30 ℃ were considered at the consumer's heating substations. During operation, supply temperature at the heat source was constrained between maximum and minimum limits (VF-VT operating strategy). For the sake of simplicity, it was assumed that the return temperature was known at the consumer's heating substations according to annual heat demand. A linear change of return temperature between maximum and minimum limits was assumed corresponding to the maximum and minimum heat demand [75].

For a low temperature DH network, supply and return temperatures were reduced to the minimum level[2]. Supply temperature of 60°C at the heat source and return temperature of 25 ℃ at the consumer's heating substations were used. During

[1] In chapter 3, it was found that the type of heat source has an impact on optimal solution of the flow and supply temperature based on minimisation of the annual total operating costs.

[2] Low temperature district heating is defined as a system with temperature close to the temperature of domestic hot water system. The temperature setting for domestic hot water is usually between 55-60 ℃, to kill bacteria such as legionella.

operation supply and return temperatures were kept constant at minimum level over the year. Hence, flow was varied to supply consumer's energy requirement for all design cases (VF-CT operating strategy).

Furthermore, a minimum TPL of 50 Pa/m was assumed and maximum TPL was decided by the program. The maximum differential pressure was specified to be equal or less than 16 bar. The TPL step change (ΔTPL) of 50 Pa/m was taken into consideration.

The design cases with minimum optimal annual total energy consumption, minimum optimal annual total exergy consumption and minimum EAC were found as the optimal solution. The optimal outputs of the optimisation study were:

- Flow and supply temperature[1], over the year;
- Annual heat energy losses and pump energy consumption;
- Annual heat exergy losses and pump exergy consumption;
- Annualised cost;
- Pipe and pump sizes.

4.3 Case study: the Barry Island district heating network

The optimisation technique was used to analyse Barry Island's DH network [91]. The schematic diagram of this system is shown in Figure 4-3.

It was assumed that consumers are connected to the DH network using heating substations. Energy demand for space heating and domestic hot water was calculated using the concept of heating degree days (as explained in section 2.2.2). Two main seasons for the heat load were assumed. The winter season, which required demand for space heating and domestic hot water was assumed to last for 182 days. For the rest of the year (the summer season) only the energy demand for domestic hot water was taken into consideration. The annual total heat demand and load duration curve are shown in Figure 4-4. The annual total energy demand is 6893 MWh/year.

[1] For high temperature district heating, optimal flow and supply temperature were obtained according to the annual heating load. For low temperature district heating, since supply and return temperatures were fixed at minimum level, flow rate was simply calculated for the purpose of supplying the consumer's energy demand.

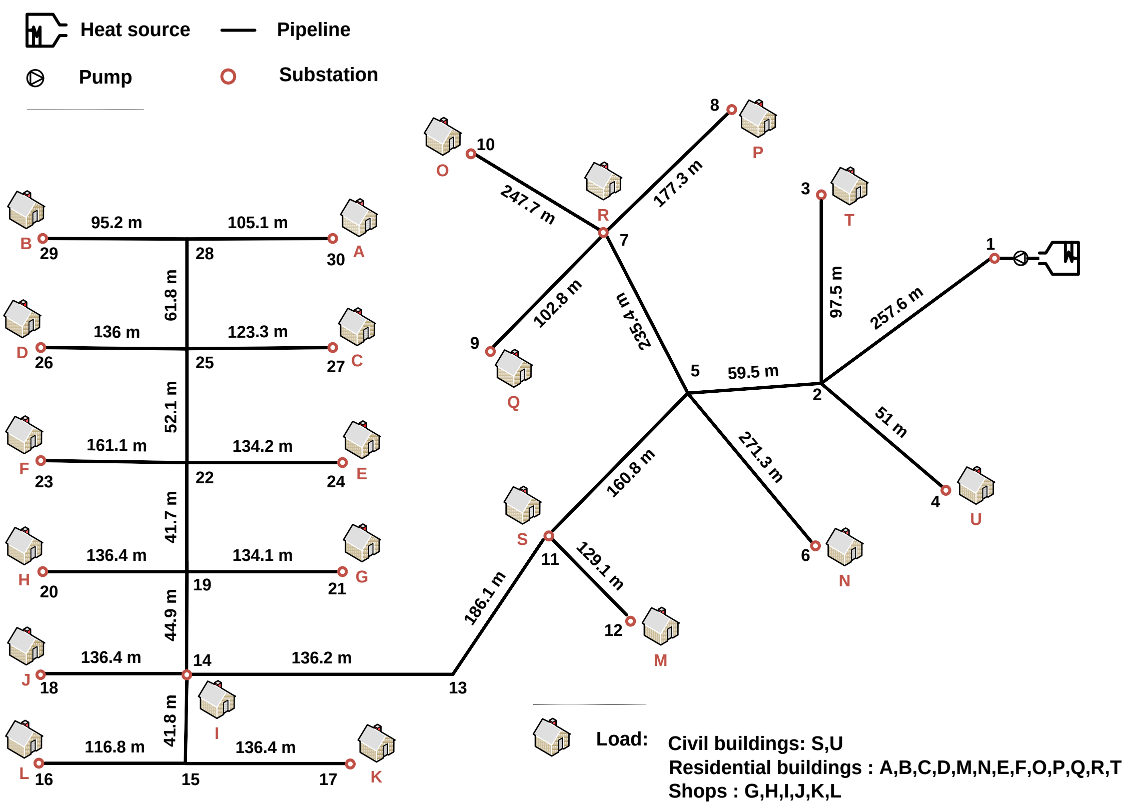

Figure 4-3 Schematic diagram of the case study

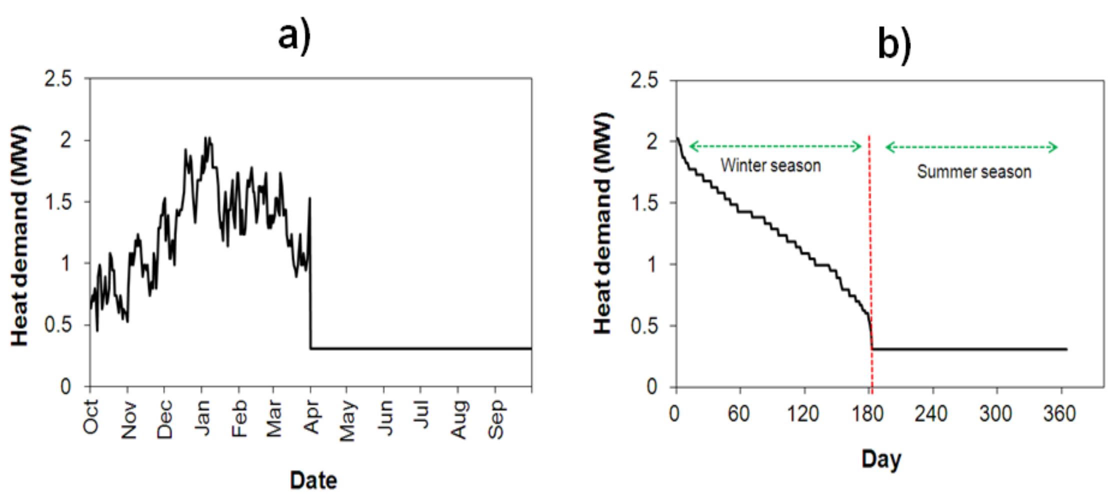

Figure 4-4 a) Annual heat demand b) and annual load duration curve

4.3.1 High temperature district heating

Optimisation results based on minimisation of the annual total energy consumption, annual total exergy consumption or the annualised cost were calculated, using a high temperature DH system.

A. Minimisation of the annual total energy consumption

For the *ideal-DH*, annual total energy consumption of DH includes annual pump energy consumption and heat energy losses. Accordingly, optimisation was carried out using the objective function given in equation 4.6. The optimal annual pump energy consumption and heat losses are shown in Figure 4-5.

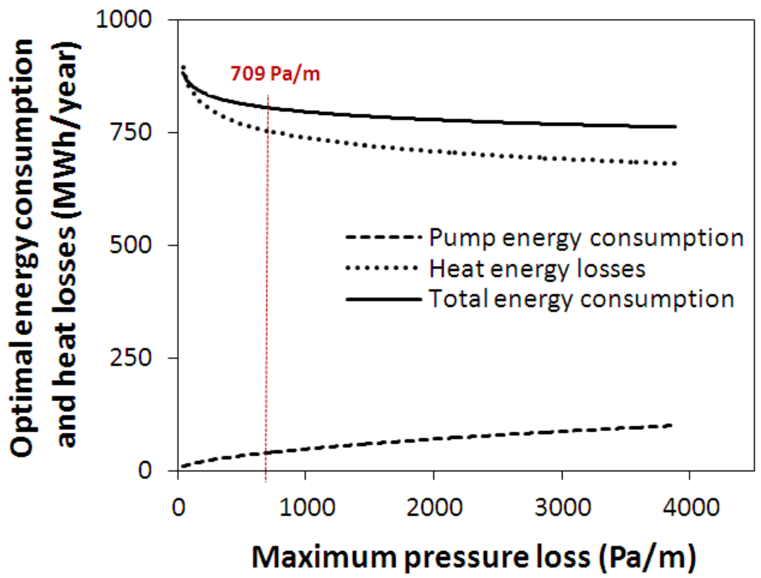

Figure 4-5 Optimal annual energy consumption and losses, high temperature district heating

In Figure 4-5, it is evident that heat energy losses are much higher in comparison with pump energy consumption. Therefore, the design cases with larger pressure drops are more energy efficient. As MPL increases, the heat energy losses decrease while pump energy consumption increases. Overall, the optimal annual total energy consumption decreases with increasing MPL. Markedly, the design case with MPL of 709 Pa/m has the minimum optimal annual total energy consumption. It should be noted that since the impact of the heat losses is more significant than pump energy consumption, the design cases with larger pressure losses than 709 Pa/m have less optimal annual total energy consumption. However, the total pressure loss in the network for those design cases is beyond the permissible range[1] hence, the design case with MPL of 709 Pa/m was considered. The obtained physical and heating parameters of the design case based on MPL of 709 Pa/m such as pipe and pump sizes, pressure loss, velocity and pump differential pressure are presented in Table B4-1 (appendix B).

B. Minimisation of the annual total exergy consumption

In this case, annual total exergy consumption included heat exergy losses and pump exergy consumption. Optimisation was carried out using the objective function given in equation 4.7. Results are presented in Figure 4-6.

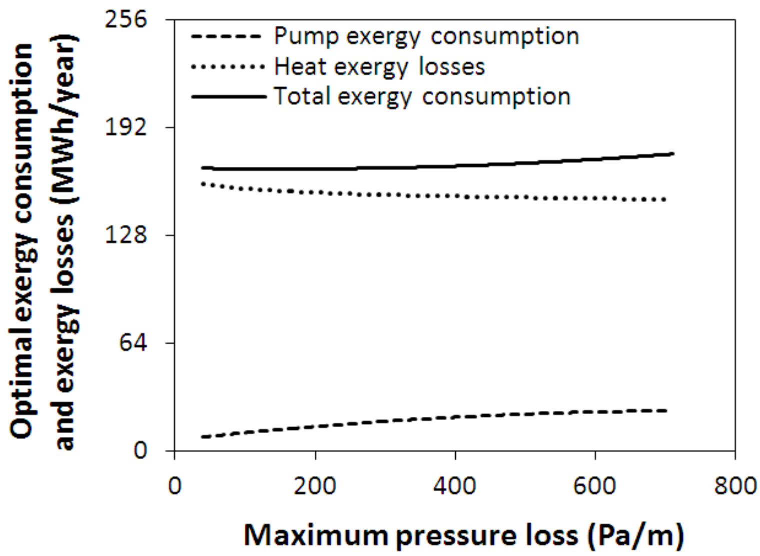

Figure 4-6 Optimal annual exergy consumption and losses, high temperature district heating

It is shown that heat exergy losses are significantly higher compared to the pump exergy consumption. As MPL increases, the heat exergy losses decrease gradually while pump exergy consumption increases. It is worth mentioning that the reduction of heat exergy losses along with increasing MPL is very small. The reason relates to the fact that as the MPL increases pipe sizes reduce while pump size increases. Therefore, for the design cases based on larger MPL values, the optimiser increases

[1] Maximum pressure loss in the network was considered to be equal or less than 16 bar.

supply temperature while reducing flow rate in order to reduce the impact of the pump exergy consumption. Reducing pipe sizes reduces heat exergy losses, while increasing supply temperature increases heat exergy losses. Overall, heat exergy losses decrease gradually. Altogether, the optimal annual total exergy consumption increases when MPL increases. The optimal annual total exergy consumption is minimum for the design case where MPL is around 126 Pa/m. The obtained physical and heating parameters of the design case are presented in Table B4-2 (appendix B).

C. Minimisation of the equivalent annual cost

For minimisation of the EAC, as previously explained, the impact of the heat source on an optimal solution of flow and supply temperature was examined. Optimisation was carried out for the *ideal-DH*, *boiler-DH* and *CHP-DH*, using the objective function given in equation 4.11. Results are presented in Figure 4-7.

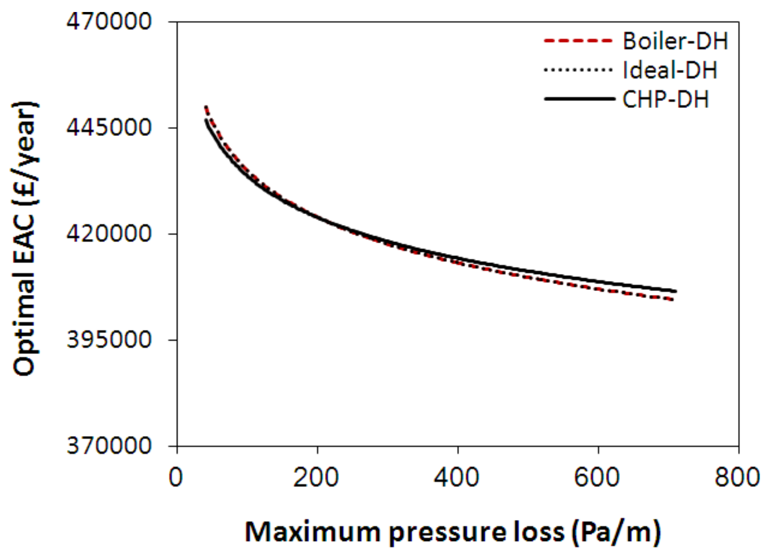

Figure 4-7 Optimal equivalent annual cost, high temperature district heating

The annualised cost of the heat network installation and its operation (excluding the investment and operational costs of the heat source), is comparatively equal using different types of heat sources. As MPL increases, the EAC decreases using all types of heat sources. This is related to the impact of pipe investment costs and the costs of heat losses rather than pump investment and operating costs. When MPL increases, pipe investment costs as well as the costs of heat losses decrease. However, pump investment and operating costs increase. For all types of heat sources, the design case based on MPL of 709 Pa/m has the minimum optimal EAC. As a result of the impact of pipe investment costs and the costs of heat losses, the design cases with larger pressure drops than 709 Pa/m have less EAC. However, since the total pressure loss in the network for those design cases is larger than 16 bar these design cases were not considered. The obtained physical and heating parameters of the design case with MPL of 709 Pa/m are presented in Table B4-3 (appendix B).

4.3.2 Low temperature district heating

An investigation of the low temperature district heating system was conducted.

A. Minimisation of the annual total energy consumption

Using low temperature DH, supply and return temperatures were kept constant at minimum level over the year for all design cases. Annual pump energy consumption and heat energy losses were considered. The investigation was carried out using the objective function given in equation 4.6. The results are shown in Figure 4-8.

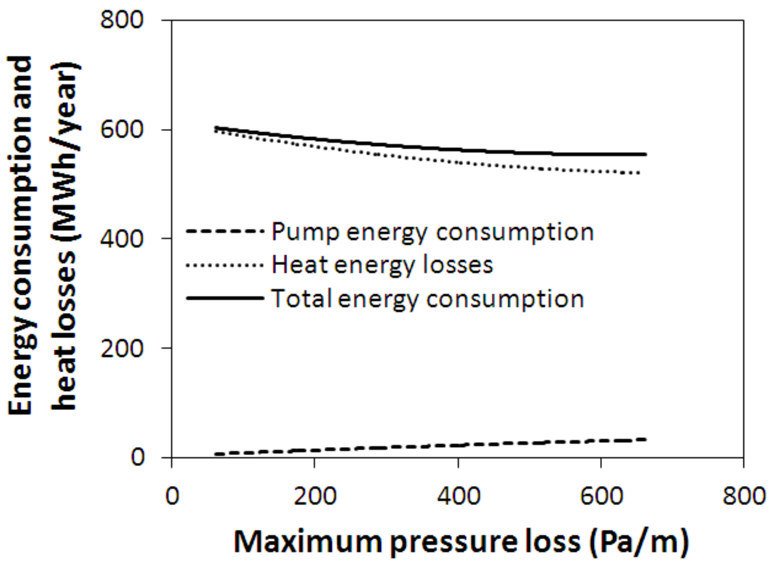

Figure 4-8 Annual energy consumption and losses, low temperature district heating

Figure 4-8 shows that as the MPL increases, heat energy losses decrease while pump energy consumption increases. It is clear that DH with smaller pipe sizes (larger MPL) has lower annual heat energy losses. Annual pump energy consumption in comparison to the annual heat energy losses is small. Therefore, pump energy consumption has little effect on the annual total energy consumption. Consequently, design cases with larger pressure drops have less annual total energy consumption. However, due to pressure limit the case with minimum annual total energy consumption is the DH design case based on MPL of 662 Pa/m. The obtained physical and heating parameters of the design case are presented in Table B4-4 (appendix B).

B. Minimisation of the annual total exergy consumption

The annual exergy consumption of pump and annual heat exergy losses were taken into account. Using the objective function in equation 4.7 and a set of equations 4.8-4.10, investigation was carried out to minimise annual total exergy consumption of DH. Results are shown in Figure 4-9.

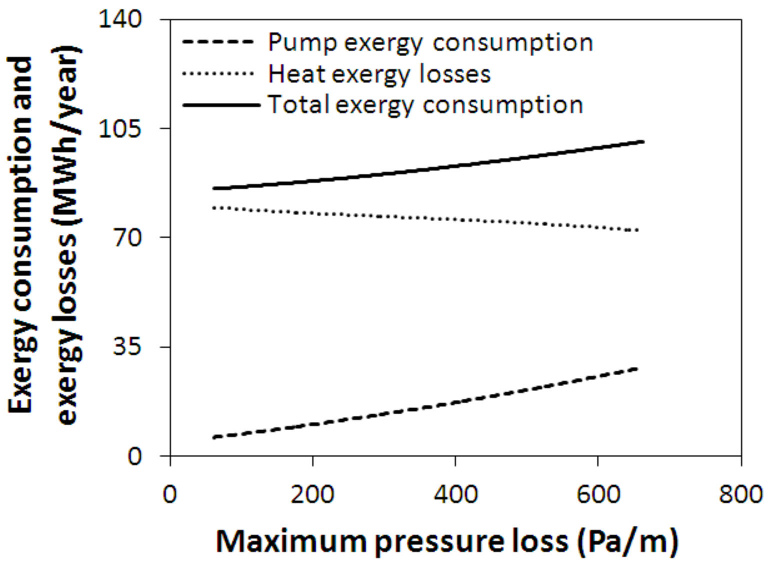

Figure 4-9 Annual exergy consumption and losses, low temperature district heating

The annual total exergy consumption is minimum for the design case based on MPL of 62 Pa/m. As MPL increases, the annual total exergy consumption increases. The obtained physical and heating parameters of the design case are presented in Table B4-5 (appendix B).

C. Minimisation of the equivalent annual cost

For minimisation of the annualised cost, the impact of the heat source was taken into account. The *ideal-DH*, *boiler-DH* and *CHP-DH* were investigated. Investigation was carried out using the objective function given in equation 4.11. Results are presented in Figure 4-10.

For low temperature DH, the heat source does not affect the EAC. It is evident that as MPL increases, EAC of the heat network installation and its operation reduces substantially. Therefore, design cases based on larger MPL values are less expensive. Using low temperature DH, the design case based on MPL of 662 Pa/m has the minimum EAC. The obtained physical and heating parameters of the design case are given in Table B4-6 (appendix B).

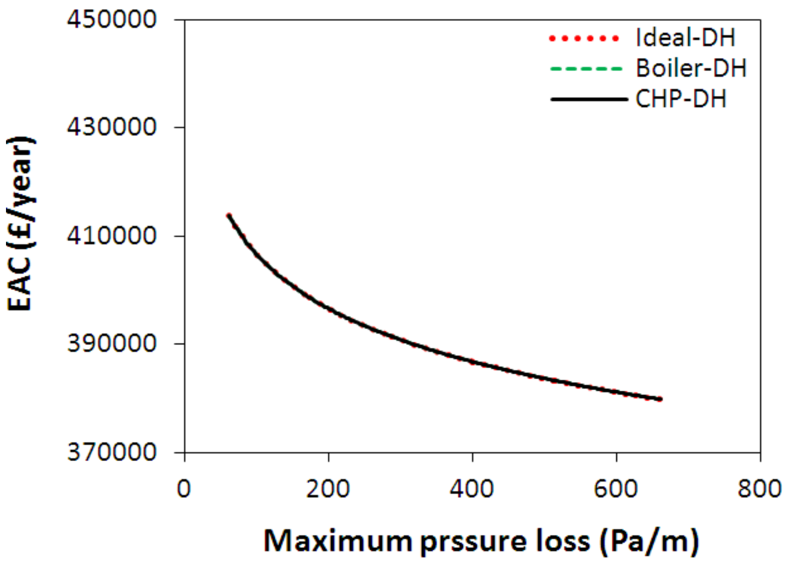

Figure 4-10 Equivalent annual cost, low temperature district heating

4.3.3 Comparison

The DH design cases with minimum annual total energy consumption, minimum annual total exergy consumption and minimum EAC using high and low temperatures DH were summarised and compared. The summaries of the results are presented in Table 4-1, Table 4-2 and Table 4-3.

Table 4-1 Design cases with minimum annual total energy consumption

District heating temperature	High	Low
MPL (Pa/m)	709	662
E_p (MWh/year)	40	33
Share of total energy demand (%)	0.6	0.5
E_{loss} (MWh/year)	753	519
Share of total energy demand (%)	11	8
$E_{T,min}$ (MWh/year)	794	552
Share of total energy demand (%)	12	8

From Table 4-1, it can be seen that the share of annual pump energy consumption to the annual total energy demand (6893 MWh/year) is very small while the share of annual heat energy losses to the annual total energy demand is rather high. A substantial reduction in the heat losses is achieved by switching to low temperature DH. Using low temperature DH, the annual heat energy losses is reduced by 31%, and annual pump energy consumption by about 18% compared to the high temperature DH. Overall, minimum annual total energy consumption is reduced by 30% using low temperature DH in comparison to the high temperature DH.

Since heat losses in both high and low temperature DH are more significant than the pump energy consumption, the design cases based on large pressure losses have a better energy performance. Using a large pressure loss in a DH network, smaller diameters of pipes can be used which reduce heat losses in the network.

Table 4-2 Design cases with minimum annual total exergy consumption

District heating temperature	High	Low
MPL (Pa/m)	126	62
Ex_p (MWh/year)	13	5
Share of total energy demand (%)	0.2	0.1
Ex_{loss} (MWh/year)	152	80
Share of total energy demand (%)	2	1
$Ex_{T,min}$ (MWh/year)	165	85
Share of total energy demand (%)	2	1

Table 4-2 shows that using minimisation of the annual total exergy consumption, for both high and low temperatures DH, the obtained results are different from those found using minimisation of the annual total energy consumption (Table 4-1). Using minimisation of the annual total exergy consumption, the design cases with larger pipe diameters and smaller pressure losses were found for both high and low temperatures DH. The reason is related to the fact that pump exergy consumption is more important than heat exergy losses. Therefore, for the design cases based on larger pressure losses the impact of pump exergy consumption becomes more significant. As a result, design cases with smaller pressure losses were found.

Through using low temperature DH, the minimum annual total exergy consumption is reduced by around 48% in comparison to higher temperature.

Table 4-3 Design cases with minimum EAC

System	*Ideal-DH*		*Boiler-DH*		*CHP-DH*	
District heating temperature	**MPL(Pa/m)**	EAC_{min} **(£/year)**	**MPL(Pa/m)**	EAC_{min} **(£/year)**	**MPL(Pa/m)**	EAC_{min} **(£/year)**
High	709	406597	709	406718	709	410312
Low	662	379576	662	379576	662	379576

Table 4-3 summarises results found using the minimisation of EAC. For the high temperature DH, the obtained design case does not depend upon the energy source (*ideal-DH*, boiler-DH and *CHP-DH*). However, due to the impact of the electricity generation in *CHP-DH*, the EAC is slightly higher than that using the *ideal-DH* and *boiler-DH*. For low temperature DH, the obtained results for the *ideal-DH*, *Boiler-DH,* and *CHP-DH* are the same.

Using the *ideal-DH* and *boiler-DH* the reduction of the EAC is about 7% for low temperature DH compared to high temperature DH. For *CHP-DH* the EAC is reduced by 8% by switching to the low temperature DH.

The cost of heat transmission was calculated for each design case and the design cases with minimum cost of heat transmission (excluding the capital and operating costs of the heat source) are shown in Table 4-4.

Table 4-4 Design cases with minimum cost of heat transmission

System	***Ideal-DH***		***Boiler-DH***		***CHP-DH***	
District heating temperature	**MPL(Pa/m)**	**Cost (£/MWh)**	**MPL(Pa/m)**	**Cost (£/MWh)**	**MPL(Pa/m)**	**Cost (£/MWh)**
High	709	58.99	709	59.00	709	59.53
Low	662	55.07	662	55.07	662	55.07

A comparison of results presented in Table 4-1, Table 4-2 and Table 4-3 shows that there are considerable benefits of using low temperature DH. The annual total energy consumption, annual total exergy consumption and the EAC of DH were reduced. However, the obtained design cases for the low temperature DH have larger pipe sizes and smaller pressure losses in comparison with those found for the high temperature DH. This is related to a larger flow rate for the low temperature DH.

Comparison of the results of two investigated case studies, Barry Island and Ebbw Vale's DH networks (see chapter 2 and chapter 3), shows a significant difference in annual total energy consumption and annualised cost. This reason is that both cases studies have a different network configuration and heat density. In addition, different operating methods and temperature regimes had impacts on the results. Therefore, every single case study has to be examined individually.

Finally, it was observed in Table 2-5, Table 3-3 and Table 4-4 that although heat demand is much higher for the Ebbw Vale's DH, the cost of heat transmission is much less in Ebbw Vale compared to the Barry Island's DH. This is associated to the high heat density and less pipe connection for the Ebbw Vale's DH compared to the Barry Island, which has less heat density and a larger piping network.

4.4 Conclusions

A two-stage programming model which combined designs and optimal operation of a DH network was developed. The objective of the optimisation was to obtain optimal flow, supply temperature, pipe and pump sizes in a DH network. Optimal flow, supply temperature, pipe and pump sizes were found based on the minimisation of the annual total energy consumption, minimisation of the annual total exergy consumption or minimisation of the EAC, using high and low temperature DH.

The objectives of the optimisation and temperature regime had impacts on the optimal results. Using minimisation of the annual total energy consumption and the annualised cost, selection of pipe and pump sizes were based on relatively large pressure losses for both high and low temperature DH. However, using minimisation of the annual total exergy consumption, selection of pipe and pump sizes were based on smaller pressure losses for both high and low temperature DH, due to the importance of the pump exergy consumption to the heat exergy losses.

Using minimisation of the annualised cost, it was shown that the impact of the heat source on the optimal results was negligible. However, using high temperature DH, the design case found for the *CHP-DH* had slightly larger annualised cost compared to the results found for the *ideal-DH* and *boiler-DH,* due to the impact of the electricity generation in *CHP-DH*.

The annual total energy consumption, annual total exergy consumption and the EAC were reduced substantially using low temperature DH compared with high temperature DH. While design cases with slightly larger pipe sizes and less pressure drops were found for the low temperature DH due to the larger flow rate in comparison to the design cases found for the high temperature DH.

Finally, DH is more cost effective in an area with high heat density. DH in area with high heat density means to serve more consumers with less pipe connection. Therefore, pipe investment costs and costs associated with heat losses reduce, which in turn leads to decrease in the annualised cost of the heat network installation and operation.

CHAPTER 5- Conclusions

5.1 Conclusions

Modelling and analysis of a DH network was conducted. Different design cases of the DH network were modelled and simulated. Design cases were operated using different operating strategies and supply and return temperature regimes. The annual total energy consumption (heat energy losses and pump energy consumption), annual total exergy consumptions (heat exergy losses and pump exergy consumption) and the EAC of the design cases were calculated and compared. Following the analysis, a two-stage programming model which synthesises design and optimal operation of a DH pipe network was developed.

Using the two-stage model, first a number of DH design cases were designed and simulated at the maximum heating load. Then their operation was optimised for one year according to the annual heat demand. The objective of the optimisation was to minimise the annual total energy consumption, annual total exergy consumption and/or annualised cost of the heat network.

The two-stage programming model is able to accommodate various types of heat sources such as ideal heat sources, boilers and CHP units connected to a DH network.

Moreover, several supply and return temperature regimes and analysis methods such as energy, exergy and cost analyses were investigated. Using this model, the optimal flow, supply temperature, pipe and pump sizes were determined and the minimum annual total energy consumption, annual total exergy consumption and minimum annualised cost were calculated.

Based on the modelling and analysis it is concluded:

- Pipe sizes in a DH network have a considerable impact on capital investment, heat energy and exergy losses, and pump energy consumption. Therefore, the determination of the optimal pipe and pump sizes is crucial in designing the most effective DH network. It was shown that as the pipe diameters decrease, heat losses and pipe investment costs decrease while pump investment and operating costs increase. It was found that the minimum annual total energy consumption and the minimum EAC were obtained using rather small pipe sizes with large pressure drops in the DH pipe network. Using exergy analysis, a DH pipe network with rather larger pipe diameters and smaller pressure drop was found to be desirable.
- There is a relation between the design supply and return temperatures, and the chosen operating regime which both affect the desirable variations of flow rate. Pump energy consumption and heat losses vary depending on the operating regime and heat demand. It was shown that using a low temperature DH system, the annual total energy consumption, annual total exergy consumption and the EAC of the heat network were reduced compared to high temperature DH. Furthermore, it was seen that by designing the DH pipe network with higher temperature difference between supply and return pipes (reducing the flow rate), the annual total energy consumption, annual total exergy consumption and the EAC were reduced.
- The DH operating strategy is a means of controlling flow rate and supply temperature to maintain stable indoor temperatures during operation. The DH operating method affects the heat energy losses and pump energy consumption. For high temperature DH networks, it was observed that the VF-VT operating method had a better performance compared to the CF-VT and VF-CT methods. Using the VF-VT operating method, the annual total

energy consumption, annual total exergy consumption and the EAC of DH were reduced compared to the other operating methods. For the low temperature DH network, the system temperature was reduced to the minimum level, close to the temperature of a domestic hot water system. Therefore, the VF-CT operating method was used.

- It was found that for the VF-VT operating method, the type of heat source had an impact on the selection of the optimal flow and supply temperature during operation, based on minimisation of the annual total operating costs. Consequently, to minimise the annualised cost the obtained design cases were dissimilar for different types of heat sources. For example, for the *CHP-DH* (Ebbw Vale's DH network), due to the impact of electricity generation in CHP, it was economically beneficial to have larger pipe diameters and smaller size pump compared with the *ideal-DH* and *boiler-DH.* For the Barry Island DH network, the impact of the heat source on the optimal solution of the flow and supply temperature was found to be negligible.
- Different DH networks have different network configurations and annual heat loads. The results obtained from the two case studies, one with high heat density and another with low heat density, showed a major difference in annual total energy consumption and annualised cost. It was shown that DH in an area with high heat density is comparatively more energy efficient and cost effective.

5.2 Contributions of the thesis

- Modelling and analysis of a DH network was conducted, using different temperature regimes, TPL and operating strategies. A method was formulated to obtain the most energy, exergy and cost effective design of a DH pipe network.
- A two-stage optimisation model was developed to obtain optimal flow, supply temperature, pipe and pump sizes in a DH network. The optimisation model was based on minimisation of the annual total energy consumption,

annual total exergy consumption or annualised cost of the heat network, according to the annual heat demand.

- Two case studies with different heat density were examined using energy, cost and exergy analyses.

5.3 Future work

Recommendations for further work are divided into the following areas:

- Temperature change in a DH network is usually slower than flow and pressure change. In bigger systems temperature change can take up to 10-12 hours before reaching the most distant consumer. In this research, system temperature and heat losses were calculated at a steady state condition. Calculation of the heat losses taking into account the dynamic performance of the temperature results in a more accurate investigation.
- In a DH pipe network with loops, calculation of pressure loss in the network becomes more challenging. In this research, only radial networks were investigated. Therefore, further analyses are required to optimise the design of DH networks with loops.
- Thermal load in a DH network changes over the year. Also, it is not expected that consumers will consume heat at a full demand level, or at exactly the same time. Therefore, more investigations on variations of heat demand are required taking into account the occupancy type, consumer behaviour, diversity factor and outside temperature.
- Return temperature in a DH network changes nonlinearly according to thermal demand, consumer behaviour and supply temperature. Therefore, calculation of the return temperature in a DH network is challenging. For simplicity, return temperature was assumed to be known at the consumer’s heating substations. Further analyses are needed, to develop more accurate model of the consumer and the return temperature.
- In a DH network pumps are sized to overcome pressure loss along the route with maximum pressure drop. Branches or pipe sections which are located

closer to the heat source experience a much higher differential pressure. Therefore, pipe diameters of these branches can be reduced further to match the differential pressure available at the branch connection to the main pipeline point. Consequently, the capital investment and heat losses of the DH pipe network decrease. Due to the different differential pressure at the connection point to each branch, the TPL used for the selection of branch pipes can be different. In this study for the sake of simplicity, a single TPL was assumed for all the pipe sections of the network. Hence, the investigation of how to implement the additional option to choose different TPL for different sections into the existing model is needed.

References

[1] G. Davies and P. Woods, "The potential and costs of district heating network: A report to the department of energy and climate change." Pöyry Energy (Oxford) Ltd, pp. 1–134, 2009.

[2] "The Carbon Plan: Delivering our low carbon future." Department of Energy & Climate Change, pp. 3–4, 2011.

[3] "UK renewable energy roadmap." Department of Energy & Climate Change, pp. 3–8, 2011.

[4] "The Renewable Heat Incentive: consultation on interim cost control." Department of Energy & Climate Change, pp. 9–14, 2012.

[5] H. Lund, B. Möller, B. V. Mathiesen, and A. Dyrelund, "The role of district heating in future renewable energy systems," *Energy*, vol. 35, no. 3, pp. 1381–1390, Mar. 2010.

[6] H. Lund, "Renewable energy strategies for sustainable development," *Energy*, vol. 32, no. 6, pp. 912–919, Jun. 2007.

[7] H. Lund and B. V. Mathiesen, "Energy system analysis of 100% renewable energy systems—The case of Denmark in years 2030 and 2050," *Energy*, vol. 34, no. 5, pp. 524–531, May 2009.

[8] H. Lund and F. Hvelplund, "The economic crisis and sustainable development: The design of job creation strategies by use of concrete institutional economics," *Energy*, vol. 43, no. 1, pp. 192–200, Jul. 2012.

[9] K. Routledge and J. Williams, "District heating - Heat metering cost benefit analysis," BRE Client report number 278-408, Building Research Establishment Ltd, 2012.

[10] "The Future of Heating: A strategic framework for low carbon heat in the UK." Department of Energy and Climate Change, Crown copyright, pp. 59–73, 2012.

[11] I. M. Austin, "Potential for district heating as a solution to fuel poverty in the UK," [Master thesis], Faculty of Earth Sciences, University of Iceland, 2010.

[12] "Annual report on fuel poverty statistics." Department of Energy and Climate Change,Crown Copyright. URN 12D/069, pp. 64–79, 2012.

[13] "London Heat Map," *Centre for Sustainable Energy*, 2010. [Online]. Available: http://www.londonheatmap.org.uk/Mapping/. [Accessed: 15-Aug-2012].

[14] "Code for Sustainable Homes: A step-change in sustainable home building practice." Department for Communities and Local Government, pp. 1–28, 2006.

[15] O. Jangsten, A. Aguiló-rullán, J. Williams, and R. Wiltshire, "The performance of district heating in new development: Application guidance." BRE Press, pp. 1–10, 2011.

[16] A. Rytoft and L. Strömberg, "Industrial landscaping of district heating - Opportunities for knowledge transfer to the UK market," [Master Thesis], Department of Environmental and Energy systems studies & Department of business administration, Lund University, 2009.

[17] D. J. C. Hawkey, "Will district heating come to town? Analysis of current opportunities and challenge in the UK," [Master Thesis], Environmental Sustainability School of Geosciences, University of Edinburgh, 2009.

[18] R. Wiltshire, "Low temperature district energy systems," in *16th, Building Services, Mechanical and Building Industry Days, International Conference, 14-15 October, Debrecen, Hungary*, 2011, pp. 1–13.

[19] B. Rezaie and M. A. Rosen, "District heating and cooling: Review of technology and potential enhancements," *Applied Energy*, vol. 93, pp. 2–10, May 2012.

[20] D. Connolly, B. V. Mathiesen, P. A. Østergaard, B. Möller, S. Nielsen, H. Lund, U. Persson, D. Nilsson, S. Werner, and D. Trier, "Heat road map EUROPE 2050." Euroheat & Power, pp. 30–32, 2012.

[21] S. Werner and N. Constantinescu, "The European heat market." Ecoheatcool and Euroheat & Power, pp. 58–62, 2006.

[22] "District heating and cooling statistics," *Euroheat & Power*, 2009. [Online]. Available: http://www.euroheat.org/Statistics-69.aspx. [Accessed: 15-Aug-2012].

[23] S. Landolina, "Strategic research priorities for cross-cutting technology." European Technology Platform on Renewable Heating and Cooling, pp. 12–15, 2012.

[24] P.K.Olsen, H. Lambertsen, R. Hummelshøj, B. Bøhm, C. H. Christiansen, S. Svendsen, C. T. Larsen, and J. Worm, "A new low temperature district heating system for low energy buildings," in *The 11th International Symposium on*

District Heating and Cooling, August 31 to September 2, Reykjavik, ICELAND, 2008, pp. 1–8.

[25] M. Pachocki, "Akureyri's district heating system: An optimisation study-optimisation of supply temperature," [Master Thesis], School for Renewable Energy Science, University of Iceland & the University of Akureyri, 2009.

[26] M. F. Demirbas, M. Balat, and H. Balat, "Potential contribution of biomass to the sustainable energy development," *Energy Conversion and Management*, vol. 50, no. 7, pp. 1746–1760, Jul. 2009.

[27] "Catalogue of CHP technologies." U.S. Environmental Protection Agency Combined Heat and Power Partnership, pp. 1–14, 2008.

[28] "District heating system in the Copenhagen Region," *Ramboll Group*. [Online]. Available: http://www.ramboll.com/projects/viewproject?projectid=4ADA954D-BA15-4AB1-904D-267567A04CF9. [Accessed: 15-Aug-2012].

[29] B. Skagestad and P. Mildenstein, *District heating and cooling connection handbook*. IEA District Heating and Cooling, 1999, pp. 12–86.

[30] "Advantages & benefits of a district heating network," *Combined Heat & Power Association*. [Online]. Available: http://www.chpa.co.uk/advantages--benefits_192.html. [Accessed: 06-Sep-2012].

[31] "Energy efficiency best practice in housing, benefits of best practice: Community Heating," Energy Saving Trust (EST), 2003.

[32] "Community heating- a guide." CE55 © Energy Saving Trust, pp. 13–15, 2004.

[33] T. Savola and I. Keppo, "Off-design simulation and mathematical modeling of small-scale CHP plants at part loads," *Applied thermal engineering*, vol. 25, no. 8–9, pp. 1219–1232, 2005.

[34] H. Zinko, B. Bøhm, H. Kristjansson, U. Ottosson, M. Rämä, and K. Sipilä, "District heating distribution in areas with low heat demand density." IEA R&D Program on District Heating and Cooling, including the integration of CHP, SenterNovem, pp. 5–11, 2008.

[35] A. Dalla Rosa and J. E. Christensen, "Low-energy district heating in energy-efficient building areas," *Energy*, vol. 36, no. 12, pp. 6890–6899, Dec. 2011.

[36] H. İ. Tol and S. Svendsen, "Improving the dimensioning of piping networks and network layouts in low-energy district heating systems connected to low-energy buildings: A case study in Roskilde, Denmark," *Energy*, vol. 38, no. 1, pp. 276–290, Feb. 2012.

[37] N. Yildirim, M. Toksoy, and G. Gokcen, “Piping network design of geothermal district heating systems: Case study for a university campus,” *Energy*, vol. 35, no. 8, pp. 3256–3262, Aug. 2010.

[38] A. Hlebnikov, A. Siirde, and A. Paist, “Basics of optimal design of district heating pipelines diameters and design examples of Estonian old non-optimised district heating networks,” in *Doctoral school of energy- and geo-technology, January 15–20, Kuressaare, Estonia*, 2007, pp. 149–153.

[39] A. Hlebnikov, N. Dementjeva, and A. Siirde, “Optimization of Narva district heating network and analysis of competitiveness of Oil Shale CHP building in Narva,” *Oil Shale*, vol. 26, no. 3, pp. 269–282, 2009.

[40] P. Ulloa, “Potential for combined heat and power and district heating and cooling from waste-to- energy facilities in the U.S. – Learning from the Danish experience,” [Master thesis], Department of Earth and Environmental Engineering, Columbia University, 2007.

[41] X. Li, L. Duanmu, and H. Shu, “Optimal design of district heating and cooling pipe network of seawater-source heat pump,” *Energy and Buildings*, vol. 42, no. 1, pp. 100–104, Jan. 2010.

[42] O. Gudmundsson, A. Nielsen, and J. Iversen, “The effects of lowering the network temperatures in existing networks,” in *DHC13, the 13th International Symposium on District Heating and Cooling, September 3rd to September 4th, Copenhagen, Denmark*, 2012, pp. 116–121.

[43] G. Phetteplace, “Optimal design of piping systems for district heating,” U.S. Army Corps of Engineers-Cold Regions Research & Engineering Laboratory CRREL Report 95-17, 1995.

[44] K. Sipilä, E. Pursiheimo, T. Savola, C. J. Fogelholm, I. Keppo, and P. Ahtila, “Small-scale biomass CHP plant and district heating.” VTT Tiedotteita – Research Notes 2301, pp. 35–52, 2005.

[45] I. Vallios, T. Tsoutsos, and G. Papadakis, “Design of biomass district heating systems,” *Biomass and Bioenergy*, vol. 33, no. 4, pp. 659–678, Apr. 2009.

[46] H. Li, A. D. Rosa, and S. Svendsen, “Design of low temperature district heating network with supply water recirculation,” in *The 12th International Symposium on District Heating and Cooling, September 5th to September 7th, Tallinn, Estonia*, 2010, pp. 73–80.

[47] M. T. Rees, J. Wu, B. Awad, J. Ekanayake, and N. Jenkins, “A total energy approach to integrated community infrastructure design,” in *2011 IEEE Power and Energy Society General Meeting*, 2011, pp. 1–8.

[48] B. Hutt, J. Field, D. Hobbs, T. Johnson, J. Palmer, and A. Watson, *Energy efficiency in buildings: CIBSE Guide F*. CIBSE, 2004, pp. Part A: 10–1–13–4.

[49] C. Beggs, *Energy management supply and conservation*, Second edi. Elsevier Ltd, 2009, pp. 135–140.

[50] T. Day, *Degree-days theory: and application*. CIBSE, 2006, pp. 1–23.

[51] "Heating degree days (HDD)." [Online]. Available: http://www.degreedays.net/. [Accessed: 30-Jul-2012].

[52] B. Bøhm, S. Ha, W. Kim, B. Kim, T. Koljonen, H. V. Larsen, M. Lucht, Y. Park, K. Sipilä, M. Wigbels, and M. Wistbacka, "Simple models for operational optimisation." IEA District Heating and Cooling , Annex VI: Report 2002: S1, NOVEM, pp. 1–132, 2002.

[53] C. Snoek, L. Yang, T. Onno, S. Frederiksen, and H. Korsman, "Optimization of district heating systems by maximizing building heating system temperature difference." International Energy Agency (IEA), pp. 88–90, 1999.

[54] S. Schofield, "Variable speed driven pumps: Best practice guide," British Pump Manufacturers' Association (BPMA).

[55] "Grundfos data booklet- NB, NBE, NK, NKE: Single-stage end-suction pumps according to EN 733, 50 Hz," GRUNDFOS A/S . DK-8850 Bjerringbro . Denmark.

[56] J. Gustafsson, J. Delsing, and J. van Deventer, "Improved district heating substation efficiency with a new control strategy," *Applied Energy*, vol. 87, no. 6, pp. 1996–2004, Jun. 2010.

[57] "PSS®SINCAL 6.5 Heating: Heating calculations in flow networks," SIEMENS AG, 2010.

[58] H. Cross, "Analysis of flow in networks of conduits or conductors," *University of Illinois Bulletin*, vol. XXXIV, no. 22, pp. 7–28, 1936.

[59] A. Dalla Rosa, H. Li, and S. Svendsen, "Method for optimal design of pipes for low-energy district heating, with focus on heat losses," *Energy*, vol. 36, no. 5, pp. 2407–2418, May 2011.

[60] "Met Office-Wales: climate." [Online]. Available: http://www.metoffice.gov.uk/climate/uk/wl/print.html. [Accessed: 30-Jul-2012].

[61] D. Dobersek and D. Goricanec, "Optimisation of tree path pipe network with nonlinear optimisation method," *Applied Thermal Engineering*, vol. 29, no. 8–9, pp. 1584–1591, Jun. 2009.

[62] "Pre-insulated steel pipe catalogue." Logstor, 2004.

[63] "District heating substations design and installation," *Technical requirements F:101*. Svensk Fjärrvärme AB, pp. 8–10, 2004.

[64] "Pre insulated pipe- price list." PPSL District Energy, 2010.

[65] "Environment, planning and housing." [Online]. Available: http://www.local.gov.uk/environment-planning-and-housing. [Accessed: 30-Jul-2012].

[66] "Cost of district heating." [Online]. Available: http://chp.decc.gov.uk/cms/cost-of-district-heating/. [Accessed: 30-May-2012].

[67] "Grundfos Industrial Products- Price list October 2010, Category 2," Grundfos, 2010.

[68] "Inverter drive supermarket, variable speed drives (VFD), soft starter, motor and component." [Online]. Available: http://www.inverterdrive.com/group/AC-Inverter-Drives-400V/Siemens-Micromaster-430-11kW-400V-EMC/default.aspx. [Accessed: 30-May-2012].

[69] C. Weber and N. Shah, "Optimisation based design of a district energy system for an eco-town in the United Kingdom," *Energy*, vol. 36, no. 2, pp. 1292–1308, Feb. 2011.

[70] "Office for national statistic." [Online]. Available: http://www.ons.gov.uk/ons/rel/cpi/consumer-price-indices/september-2011/index.html. [Accessed: 18-Sep-2011].

[71] "Europe Energy's portal." [Online]. Available: http://www.energy.eu/#Industrial-Elec. [Accessed: 30-May-2012].

[72] A. Benonysson, B. Bøhm, and H. F. Ravn, "Operational optimization in a district heating system," *Energy Conversion and Management*, vol. 36, no. 5, pp. 297–314, May 1995.

[73] B. Bøhm and H. V. Larsen, "Simple models of district heating systems for load and demand side management and operational optimisation." Department of Mechanical Engineering, Technical University of Denmark & Risø National Laboratory, Systems Analysis Department, pp. 1–25, 2004.

[74] H. Pálsson, H. V. Larsen, B. Bøhm, H. F. Ravn, and J. Zhou, "Equivalent models of district heating systems for on-line minimization of operational costs of the complete district heating system," *Department of Energy Engineering Technical, University of Denmark & RISØ National Laboratory ,Systems Analysis Department*. Department of Energy Engineering, Technical

University of Denmark & Risø National Laboratory, Systems Analysis Department, pp. 1–126, 1999.

[75] M. Wighbels, B. Bøhm, and K. Sipilae, “Dynamic heat storage optimisation and demand side management.” IEA R&D Programme on District Heating and Cooling, Annex VII 2005:8DHC-05-06 , SenterNovem, pp. 15–69, 2005.

[76] B. Awad, “Operation of energy Micro Grids,” [PhD thesis], Institute of Energy, Cardiff University, 2010.

[77] B. Rolfsman, “Combined heat-and-power plants and district heating in a deregulated electricity market,” *Applied Energy*, vol. 78, no. 1, pp. 37–52, May 2004.

[78] “Analytical Annex to the Renewable Heat Incentive Impact Assessment: Assumptions used in the analysis underpinning the RES,” Department of Energy & Climate Change, 2010.

[79] I. Ben Hassine and U. Eicker, “Simulation and optimization of the district heating network in Scharnhauser Park,” in *2nd European Conference on Polygeneration, 30th March-1st April , Tarragona, Spain*, 2011, pp. 1–12.

[80] M. J. Moran, H. N. Shapiro, B. R. Munson, and D. P. DeWitt, *Introduction to thermal systems engineering: Thermodynamic, Fluid Mechanic, and Heat Transfer*. John Wiley & Sons, Inc., 2003, pp. 313–341.

[81] “Fico Xpress optimization suite: User Guides.” [Online]. Available: http://www.fico.com/en/Products/DMTools/xpress-overview/Pages/Xpress-Documentation.aspx. [Accessed: 30-Jul-2012].

[82] M. J. Moran and H. N. Shapiro, *Fundamentals of engineering thermodynamics*, 5th editio. John Wiley & Sons, Inc., 2006, pp. 272–324.

[83] R. Zmeureanu and X. Yu Wu, “Energy and exergy performance of residential heating systems with separate mechanical ventilation,” *Energy*, vol. 32, no. 3, pp. 187–195, Mar. 2007.

[84] K. Çomaklı, B. Yüksel, and Ö. Çomaklı, “Evaluation of energy and exergy losses in district heating network,” *Applied Thermal Engineering*, vol. 24, no. 7, pp. 1009–1017, May 2004.

[85] H. Li and S. Svendsen, “Exergy and energy analysis of low temperature district heating network,” in *Proceedings of ECOS2011, 24th International Conference on Efficiency, Cost, Optimisation, Simulation and Environmental Impact of Energy Systems, Novi Sad, Serbia, July 4-7*, 2011, pp. 3034–3045.

[86] H. Torío and D. Schmidt, "Development of system concepts for improving the performance of a waste heat district heating network with exergy analysis," *Energy and Buildings*, vol. 42, no. 10, pp. 1601–1609, Oct. 2010.

[87] A. Hepbasli, "A key review on exergetic analysis and assessment of renewable energy resources for a sustainable future," *Renewable and Sustainable Energy Reviews*, vol. 12, no. 3, pp. 593–661, Apr. 2008.

[88] M. Shukuya and A. Hammache, "Introduction to the concept of exergy- for a better understanding of low temperature-heating and high temperature-cooling systems." VTT Research note 2158, ESPOO2002, pp. 8–39, 2002.

[89] I. Dincer, "The role of exergy in energy policy making," *Energy Policy*, vol. 30, no. 2, pp. 137–149, Jan. 2002.

[90] T. Hunt and N. Vaughan, *Hydraulic handbook*, 9th editio. Elsevier Science LTD, 1996, pp. 265–275.

[91] Y. Xing, A. Bagdanavicius, S. Lannon, M. Pirouti, and T. Bassett, "Low temperature district heating network planning with focus on distribution energy losses," in *International Conference on Applied Energy, ICAE 2012 - 5-8 July, Suzhou, China*, 2012, pp. 1–10.

Appendix

Appendix A: Calculation of heat flow

Procedure for heat flow calculation for two simple district heating networks (a radial network and a loop network)

Example 1: Single pipe of supply and return in a district heating

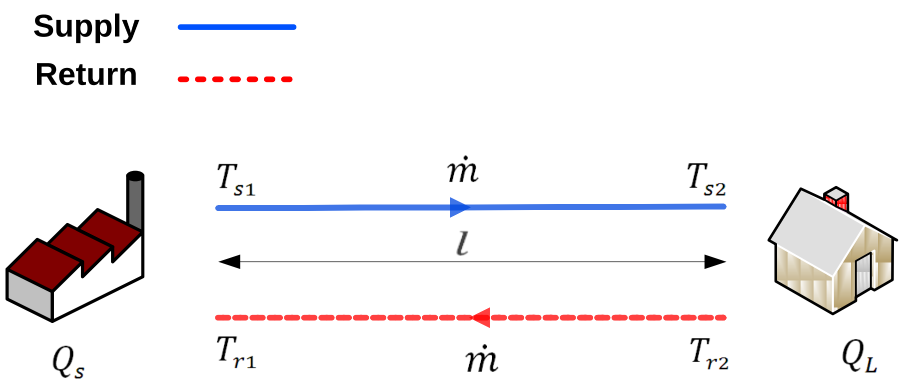

Known variables:

Thermal load (Q_L)	5000 kW
Pipe length (l)	500 m
Pipe diameter (d)	200 mm
Pipe roughness (ε)	0.4 mm
Heat transition coefficient (U)	0.455 W/mK
kinematic viscosity (v)	0.294×10^{-6} m^2/s
Specific heat capacity (c_p)	4.182 KJ/KgK
Water density (ρ)	960 kg/m^3
Supply temperature (T_{s1})	120 °C
Return temperature (T_{r2})	70 °C
Ground temperature (T_g)	7 °C

Unknown variables:

Mass flow rate ($\dot{m}$)	Kg/s
Supply temperature (T_{s2})	℃
Return temperature (T_{r1})	℃
Supply , heat loss ($Q_{s,loss}$)	kW
Return, heat loss ($Q_{r,loss}$)	kW
Water velocity (u)	m/s
Pressure drop (p)	Pascal (Pa)

Equations 1:

Heat supply	$Q_S = c_p \dot{m}\,(T_{s1} - T_{r1})$	(A.1)
Heat load	$Q_L = c_p \dot{m}\,(T_{s2} - T_{r2})$	(A.2)
Supply , heat loss	$Q_{s,loss} = c_p \dot{m}\,(T_{s1} - T_{s2})$	(A.3)
Return, heat loss	$Q_{r,loss} = c_p \dot{m}\,(T_{r2} - T_{r1})$	(A.4)
Heat balance	$Q_S = Q_{s,loss} + Q_L + Q_{r,loss}$	(A.5)
Water velocity	$u = \dfrac{4\dot{m}}{\pi \rho d^2}$	(A.6)
Supply, temperature drop	$T_{s2} = \left(T_{s1} - T_g\right) e^{-\frac{lU}{c_p \dot{m}}} + T_g$	(A.7)
Return, temperature drop	$T_{r1} = \left(T_{r2} - T_g\right) e^{-\frac{lU}{c_p \dot{m}}} + T_g$	(A.8)
Friction factor	$\dfrac{1}{\sqrt{f}} = -2log_{10}\left(\dfrac{\varepsilon}{3.71d} + \dfrac{2.51}{Re}\dfrac{1}{\sqrt{f}}\right)$	(A.9)
Reynolds number	$Re = \dfrac{ud}{v} \qquad Re > 4000$	(A.10)
Pressure drop	$\Delta p = 8f\,\dfrac{l}{d^5}\dfrac{\dot{m}^2}{\rho \pi^2}$	(A.11)

Solution

1st iteration:

Initial guess of supply temperature (T_{s2})	118 ℃
Initial guess of return temperature (T_{r1})	68 ℃

$$\dot{m} = \frac{Q_L}{c_p(T_{s2}-T_{r2})} = \frac{5000}{4.18\times(118-70)} = 24.92 \text{ Kg/s}$$

$$T_{s2} = (T_{s1} - T_g)e^{-\frac{lU}{c_p\dot{m}}} + T_g = (120-7)\, e^{-\frac{500\times0.455}{4182\times24.41}} + 7 = 119.75 \text{ ℃}$$

$$T_{r1} = (T_{r2} - T_g)e^{-\frac{lU}{c_p\dot{m}}} + T_g = (70-7)e^{-\frac{500\times0.455}{4182\times24.41}} + 7 = 69.86 \text{ ℃}$$

2nd iteration:

From 1st iteration :Supply temperature (T_{s2})	119.75 ℃
From 1st iteration : Return temperature (T_{r1})	69.86 ℃

$$\dot{m} = \frac{Q_L}{c_p(T_{s2}-T_{r2})} = \frac{5000}{4.18\times(119.75-70)} = 24.04 \text{ Kg/s}$$

$$T_{s2} = (T_{s1} - T_g)e^{-\frac{lU}{c_p\dot{m}}} + T_g = (120-7)\, e^{-\frac{500\times0.455}{4182\times24.04}} + 7 = 119.74 \text{ ℃}$$

$$T_{r1} = (T_{r2} - T_g)e^{-\frac{lU}{c_p\dot{m}}} + T_g = (70-7)e^{-\frac{500\times0.455}{4182\times24.04}} + 7 = 69.85 \text{ ℃}$$

3rd iteration:

From 2nd iteration :Supply temperature (T_{s2})	119.74 ℃
From 2nd iteration : Return temperature (T_{r1})	69.85 ℃

$$\dot{m} = \frac{Q_L}{c_p(T_{s2}-T_{r2})} = \frac{5000}{4.18\times(119.74-70)} = 24.04 \text{ Kg/s}$$

$$T_{s2} = \left(T_{s1} - T_g\right)e^{-\frac{lU}{c_p\dot{m}}} + T_g = (120\text{-}7)\, e^{-\frac{500\times0.455}{4182\times24.04}} + 7 = 119.74\ ℃$$

$$T_{r1} = \left(T_{r2} - T_g\right)e^{-\frac{lU}{c_p\dot{m}}} + T_g = (70 - 7)e^{-\frac{500\times0.455}{4182\times24.04}} + 7 = 69.85\ ℃$$

Final results:

Supply temperature (T_{s2})	119.74 ℃
Return temperature (T_{r1})	69.85 ℃
Mass flow rate ($\dot{m}$)	24.04 Kg/s

$$Q_{s,loss} = c_p\dot{m}\,(T_{s1} - T_{s2}) = 4.182 \times 24.04 \times (120 - 119.74) = 26.13 \quad \text{kW}$$

$$Q_{r,loss} = c_p\dot{m}\,(T_{r2} - T_{r1}) = 4.182 \times 24.04 \times (70 - 69.85) = 15.08 \quad \text{kW}$$

$$Q_S = c_p\dot{m}\,(T_{s1} - T_{r1}) = 4.182 \times 24.04 \times (120 - 69.85) = 5041.2 \quad \text{kW}$$

$$Q_S = Q_{s,loss} + Q_L + Q_{r,loss} = 26.13 + 5000 + 15.08 = 5041.2 \quad \text{kW}$$

$$u = \frac{4\dot{m}}{\pi\rho d^2} = \frac{4\times24.04}{3.14\times960\times0.2^2} = 0.79 \quad \text{m/s}$$

$$Re = \frac{ud}{v} = \frac{0.79\times0.2}{0.294\times10^{-6}} = 537410 \qquad \text{Turbulent flow},\ Re > 4000$$

$$\frac{1}{\sqrt{f}} = -2log_{10}\left(\frac{\varepsilon}{3.71d} + \frac{2.51}{Re}\frac{1}{\sqrt{f}}\right) \qquad f = 1/\left(-2log_{10}\left(\frac{0.0004}{3.71 \times 0.2}\right)\right)^2 = 0.0234$$

$$\Delta p = 8f\,\frac{l}{d^5}\frac{\dot{m}^2}{\rho\pi^2} = 8 \times 0.0234 \times \frac{500}{0.2^5} \times \frac{24.04^2}{960 \times 3.14^2} = 17859 \quad \text{Pa}$$

Example 2: District heating with loop

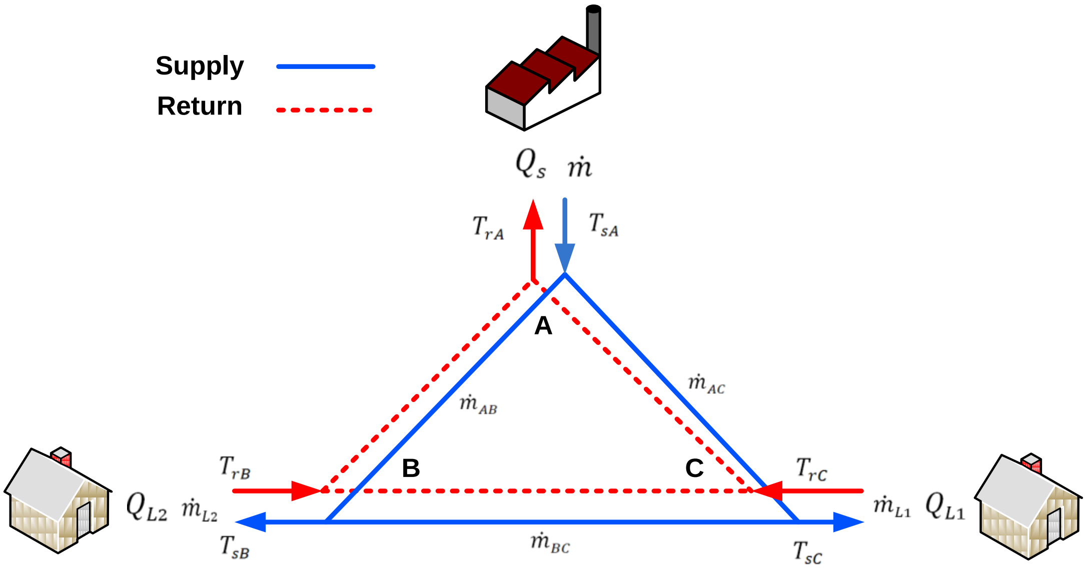

Known variables:

Thermal load (Q_{L1})	3000 kW
Thermal load (Q_{L2})	4000 kW
Pipe length (l_{AB})	300 m
Pipe length (l_{AC})	300 m
Pipe length (l_{BC})	300 m
Pipe diameter (d_{AB})	100 mm
Pipe diameter (d_{AC})	100 mm
Pipe diameter (d_{BC})	100 mm
Pipe roughness (ε)	0.4 mm
Heat transition coefficient (U)	0.327 W/mK
kinematic viscosity (v)	0.294×10^{-6} m^2/s
Specific heat capacity (c_p)	4.182 KJ/KgK
Water density (ρ)	960 kg/m^3
Supply temperature (T_{sA})	120 ℃
Return temperature (T_{rL1})	70 ℃
Return temperature (T_{rL2})	70 ℃
Ground temperature (T_g)	7 ℃

Unknown variables:

Mass flow rate ($\dot{m}$)	Kg/s
Mass flow rate ($\dot{m}_{L1}$)	Kg/s
Mass flow rate ($\dot{m}_{L2}$)	Kg/s
Mass flow rate ($\dot{m}_{AB}$)	Kg/s
Mass flow rate ($\dot{m}_{AC}$)	Kg/s
Mass flow rate ($\dot{m}_{BC}$)	Kg/s
Supply temperature (T_{sB})	℃
Supply temperature (T_{sC})	℃
Return temperature (T_{rA})	℃
Return temperature (T_{rB})	℃
Return temperature (T_{rC})	℃
Supply , heat loss ($Q_{s,loss}$)	kW
Return, heat loss ($Q_{r,loss}$)	kW
Water velocity (u)	m/s
Pressure drop (p)	Pascal (Pa)

Equations 2:

The equations were used for the example 1 (Equations 1) are used. In addition:

Temperature mixture in node with more than one incoming flow:

$$T_{n1} = \frac{\dot{m}_1 T_{1,outl} + \dot{m}_2 T_{2,outl}}{\dot{m}_1 + \dot{m}_2} \tag{A.12}$$

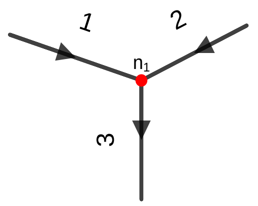

$T_{1,outl}$: Outlet temperautreof the pipe 1

$T_{2,outl}$: Outlet temperautre of the pipe 2

Solution

1st iteration:

Initial guess of supply temperature (T_{sB} & T_{sC})   118 ℃

Initial guess of return temperature (T_{rA})	68 ℃

$$\dot{m}_{L1} = \frac{Q_{L1}}{c_p(T_{sC}-T_{rC})} = \frac{3000}{4.18\times(118-70)} = 14.94 \text{ Kg/s}$$

$$\dot{m}_{L2} = \frac{Q_{L2}}{c_p(T_{sB}-T_{rB})} = \frac{4000}{4.18\times(118-70)} = 19.92 \text{ Kg/s}$$

$$\dot{m} = \dot{m}_{L1} + \dot{m}_{L2} = 14.94 + 19.92 = 34.86 \text{ Kg/s}$$

Hydraulic calculation-Hardy Cross method:

Assuming highly turbulent flow:

$$f = 1/\left(-2log_{10}\left(\frac{\varepsilon}{3.71d}\right)\right)^2 = 1/\left(-2log_{10}\left(\frac{0.4}{3.71\times100}\right)\right)^2 = 0.0284$$

$$\Delta p = 8f\frac{l}{d^5}\frac{\dot{m}^2}{\rho\pi^2} = 8\times0.0284\times\frac{300}{0.1^5}\times\frac{\dot{m}^2}{960\times3.14^2} = 720\dot{m}^2$$

$$\sum\Delta p = \sum(\Delta p_{AB} + \Delta p_{AC} + \Delta p_{BC}) = \sum(720\dot{m}_{AB}^2 + 720\dot{m}_{AC}^2 + 720\dot{m}_{BC}^2) = 0$$

First trial:

Flow
Anti- clockwise (-)
Clockwise (+)

Pipe	$\dot{m}$ (kg/s)	Δp (Pa)	H (m)	$\Delta p/\dot{m}$
AB	-19.92	-285700.61	-29.76	14342.40
AC	14.94	160706.59	16.74	10756.80
BC	0	0.00	0.00	0.00
Σ		-124994.02	-13.020	25099.20

$\sum H > 0.05$ hence, correction has to be applied

$$\Delta\dot{m} = -\frac{\sum\Delta p}{2\times\sum\frac{\Delta p}{\dot{m}}} = -\frac{-124994.02}{2\times25099.20} = 2.49 \text{ Kg/s}$$

Second trial:

Pipe	$\dot{m}$ (kg/s)	Δp (Pa)	H (m)	$\Delta p/\dot{m}$
AB	-17.43	-218739.53	-22.79	12549.60
AC	17.43	218739.53	22.79	12549.60
BC	2.49	4464.07	0.47	1792.80
Σ		4464.07	0.465	26892.00

$\sum H > 0.05$, hence, correction has to be applied

$$\Delta\dot{m} = -\frac{\sum \Delta p}{2\times\sum\frac{\Delta p}{\dot{m}}} = -\frac{4464.07}{2\times 26892.00} = -0.08 \quad \text{Kg/s}$$

Third trial:

Pipe	$\dot{m}$ (kg/s)	Δp (Pa)	H (m)	$\Delta p/\dot{m}$
AB	-17.51	-220752.07	-23.00	12607.20
AC	17.35	216736.20	22.58	12492.00
BC	2.41	4181.83	0.44	1735.20
Σ		165.96	0.017	26834.40

$\sum H \leq 0.05$, then it is OK!

$$T_{sC} = \left(T_{sA} - T_g\right)e^{-\frac{lU}{c_p\dot{m}_{AC}}} + T_g = (120-7)e^{-\frac{300\times 0.327}{4182\times 17.35}} + 7 = 119.84\ ℃$$

$$T_{sCB,outl} = \left(T_{sC} - T_g\right)e^{-\frac{lU}{c_p\dot{m}_{CB}}} + T_g = (119.84-7)e^{-\frac{300\times 0.327}{4182\times 2.41}} + 7 = 118.74\ ℃$$

$$T_{sAB,outl} = \left(T_{sA} - T_g\right)e^{-\frac{lU}{c_p\dot{m}_{AB}}} + T_g = (120-7)e^{-\frac{300\times 0.327}{4182\times 17.51}} + 7 = 119.84\ ℃$$

$$T_{sB} = \frac{\dot{m}_{AB}T_{sAB,outl} + \dot{m}_{CB}T_{sCB,outl}}{\dot{m}_{AB} + \dot{m}_{CB}} = \frac{17.51\times 119.84 + 2.41\times 118.74}{17.51 + 2.41} = 119.7\ ℃$$

$$T_{rB} = T_{rL2} = 70\ ℃$$

$$T_{rBC,outl} = \left(T_{rB} - T_g\right)e^{-\frac{lU}{c_p\dot{m}_{BC}}} + T_g = (70-7)e^{-\frac{300\times 0.327}{4182\times 2.41}} + 7 = 69.38\ ℃$$

$$T_{rC} = \frac{\dot{m}_{L1}T_{rL1} + \dot{m}_{BC}T_{rBC,outl}}{\dot{m}_{L1} + \dot{m}_{BC}} = \frac{14.94 \times 70 + 2.41 \times 69.38}{14.94 + 2.41} = 69.9\ ℃$$

$$T_{rCA,outl} = \left(T_{rC} - T_g\right)e^{-\frac{lU}{c_p\dot{m}_{CA}}} + T_g = (69.9 - 7)e^{-\frac{300\times0.327}{4182\times17.35}} + 7 = 69.81\ ℃$$

$$T_{rBA,outl} = \left(T_{rB} - T_g\right)e^{-\frac{lU}{c_p\dot{m}_{BA}}} + T_g = (70 - 7)e^{-\frac{300\times0.327}{4182\times17.51}} + 7 = 69.91\ ℃$$

$$T_{rA} = \frac{\dot{m}_{BA}T_{rBA,outl} + \dot{m}_{CA}T_{rCA,outl}}{\dot{m}_{BA} + \dot{m}_{CA}} = \frac{17.35 \times 69.81 + 17.51 \times 69.91}{17.35 + 17.51} = 69.86\ ℃$$

2nd iteration:

Supply temperature from previous iteration (T_{sA})	120 ℃
Supply temperature from previous iteration (T_{sB})	119.7 ℃
Supply temperature from previous iteration (T_{sC})	119.84 ℃
Return temperature from previous iteration (T_{rA})	69.86 ℃
Return temperature from previous iteration (T_{rC})	69.9 ℃
Return temperature from previous iteration (T_{rB})	70 ℃

$$\dot{m}_{L1} = \frac{Q_{L1}}{c_p(T_{sC} - T_{rC})} = \frac{3000}{4.18\times(119.84 - 69.9)} = 14.37\ \text{Kg/s}$$

$$\dot{m}_{L2} = \frac{Q_{L2}}{c_p(T_{sB} - T_{rB})} = \frac{4000}{4.18\times(119.7 - 70)} = 19.25\ \text{Kg/s}$$

$$\dot{m} = \dot{m}_{L1} + \dot{m}_{L2} = 14.37 + 19.25 = 33.62\ \text{Kg/s}$$

Hydraulic calculation-Hardy Cross method:

Assuming highly turbulent flow :

$$f = 1/\left(-2log_{10}\left(\frac{\varepsilon}{3.71d}\right)\right)^2 = 1/\left(-2log_{10}\left(\frac{0.4}{3.71\times100}\right)\right)^2 = 0.0284$$

$$\Delta p = 8f\frac{l}{d^5}\frac{\dot{m}^2}{\rho\pi^2} = 8\times0.0284\times\frac{300}{0.1^5}\times\frac{\dot{m}^2}{960\times3.14^2} = 720\dot{m}^2$$

$$\sum\Delta p = \sum(\Delta p_{AB} + \Delta p_{AC} + \Delta p_{BC}) = \sum(720\dot{m}_{AB}^2 + 720\dot{m}_{AC}^2 + 720\dot{m}_{BC}^2) = 0$$

First trial:

Flow
Anti- clockwise (-)
Clockwise (+)

Pipe	$\dot{m}$ (kg/s)	Δp (Pa)	H (m)	$\Delta p/\dot{m}$
AB	-19.25	-266805	-27.79	13860.0
AC	14.37	148677.77	15.49	10346.4
BC	0	0	0.00	0.0
Σ		-118127.23	-12.30	24206.4

$\sum H > 0.05$, hence, correction has to be applied

$$\Delta\dot{m} = -\frac{\sum\Delta p}{2\times\sum\frac{\Delta p}{\dot{m}}} = -\frac{-118127.23}{2\times24206.4} = 2.44 \quad \text{Kg/s}$$

Second trial:

Pipe	$\dot{m}$ (kg/s)	Δp (Pa)	H (m)	$\Delta p/\dot{m}$
AB	-16.81	-203454.79	-21.19	12103.2
AC	16.81	203454.79	21.19	12103.2
BC	2.44	4286.59	0.45	0.0
Σ		4286.59	0.45	24206.4

$\sum H > 0.05$, hence, correction has to be applied

$$\Delta\dot{m} = -\frac{\sum\Delta p}{2\times\sum\frac{\Delta p}{\dot{m}}} = -\frac{4286.59}{2\times24206.4} = -0.088 \quad \text{Kg/s}$$

Third trial:

Pipe	$\dot{m}$ (kg/s)	Δp (Pa)	H (m)	$\Delta p/\dot{m}$
AB	-16.89	-205590.53	-21.42	12166.6
AC	16.72	201330.20	20.97	12039.8
BC	2.35	3982.97	0.41	0.0
Σ		-277.36	-0.03	24206.4

$\sum H \leq 0.05$, then it is OK!

$$T_{sC} = (T_{sA} - T_g)e^{-\frac{lU}{c_p\dot{m}_{AC}}} + T_g = (120 - 7)e^{-\frac{300\times0.327}{4182\times16.72}} + 7 = 119.84\ ℃$$

$$T_{sCB,outl} = (T_{sC} - T_g)e^{-\frac{lU}{c_p\dot{m}_{CB}}} + T_g = (119.84 - 7)e^{-\frac{300\times0.327}{4182\times2.35}} + 7 = 118.71\ ℃$$

$$T_{sAB,outl} = (T_{sA} - T_g)e^{-\frac{lU}{c_p\dot{m}_{AB}}} + T_g = (120 - 7)e^{-\frac{300\times0.327}{4182\times16.89}} + 7 = 119.84\ ℃$$

$$T_{sB} = \frac{\dot{m}_{AB}T_{sAB,outl} + \dot{m}_{CB}T_{sCB,outl}}{\dot{m}_{AB} + \dot{m}_{CB}} = \frac{16.89\times119.84 + 2.35\times118.71}{16.89 + 2.35} = 119.7\ ℃$$

$$T_{rB} = T_{rL2} = 70\ ℃$$

$$T_{rBC,outl} = (T_{rB} - T_g)e^{-\frac{lU}{c_p\dot{m}_{BC}}} + T_g = (70 - 7)e^{-\frac{300\times0.327}{4182\times2.35}} + 7 = 69.37\ ℃$$

$$T_{rC} = \frac{\dot{m}_{L1}T_{rL1} + \dot{m}_{BC}T_{rBC,outl}}{\dot{m}_{L1} + \dot{m}_{BC}} = \frac{14.37\times70 + 2.35\times69.37}{14.37 + 2.35} = 69.91\ ℃$$

$$T_{rCA,outl} = (T_{rC} - T_g)e^{-\frac{lU}{c_p\dot{m}_{CA}}} + T_g = (69.91 - 7)e^{-\frac{300\times0.327}{4182\times16.72}} + 7 = 69.82\ ℃$$

$$T_{rBA,outl} = (T_{rB} - T_g)e^{-\frac{lU}{c_p\dot{m}_{BA}}} + T_g = (70 - 7)e^{-\frac{300\times0.327}{4182\times16.89}} + 7 = 69.91\ ℃$$

$$T_{rA} = \frac{\dot{m}_{BA}T_{rBA,outl} + \dot{m}_{CA}T_{rCA,outl}}{\dot{m}_{BA} + \dot{m}_{CA}} = \frac{16.72\times69.82 + 16.89\times69.91}{16.72 + 16.89} = 69.86\ ℃$$

Final results :

Mass flow rate ($\dot{m}_{L1}$)	14.37 Kg/s
Mass flow rate ($\dot{m}_{L2}$)	19.25 Kg/s
Mass flow rate ($\dot{m}$)	33.62 Kg/s
Mass flow rate ($\dot{m}_{sAB}$)	-16.89 (anti-clockwise) Kg/s
Mass flow rate ($\dot{m}_{sAC}$)	16.72 (clockwise) Kg/s
Mass flow rate ($\dot{m}_{sBC}$)	2.35 (clockwise) Kg/s
Mass flow rate ($\dot{m}_{rAB}$)	16.89 (clockwise) Kg/s
Mass flow rate ($\dot{m}_{rAC}$)	-16.72 (anti-clockwise) Kg/s
Mass flow rate ($\dot{m}_{rBC}$)	-2.35 (anti-clockwise) Kg/s
Supply temperature (T_{sA})	120 ℃
Supply temperature (T_{sB})	119.7 ℃
Supply temperature (T_{sC})	119.84 ℃
Return temperature (T_{rA})	69.86 ℃
Return temperature (T_{rB})	70 ℃
Return temperature (T_{rC})	69.91 ℃
Supply, heat loss (AC)	$Q_{sAC,loss} = c_p \dot{m}_{AC} \, (T_{sA} - T_{sC}) = 11.18$ kW
Supply, heat loss (AB)	$Q_{sAB,loss} = c_p \dot{m}_{AB} \, (T_{sA} - T_{sB}) = 21.19$ kW
Supply, heat loss (CB)	$Q_{sCB,loss} = c_p \dot{m}_{CB} \, (T_{sC} - T_{sB}) = 1.37$ kW
Return, heat loss (CA)	$Q_{rCA,loss} = c_p \dot{m}_{AC} \, (T_{rC} - T_{rA}) = 3.49$ kW

Return, heat loss (BA)	$Q_{rBA,loss} = c_p \dot{m}_{AB}\ (T_{rB} - T_{rA}) = 9.88$ kW
Return, heat loss (BC)	$Q_{rBC,loss} = c_p \dot{m}_{CB}\ (T_{rB} - T_{rC}) = 0.88$ kW
Total losses	$Q_{loss} = 11.18 + 21.19 + 1.37 + 3.49 + 9.88 + 0.88 = 47.99$ kW
Heat supply	$Q_s = c_p \dot{m}(T_{sA} - T_{rA}) = 4.182 \times 33.62 \times (120 - 69.86) = 7049$ kW $Q_s = Q_{L1} + Q_{L2} + Q_{loss} = 7048$ kW
Water velocity (AB)	$u_{AB} = \frac{4\dot{m}_{AB}}{\pi\rho d^2} = \frac{4\times16.89}{3.14*960*0.1^2} = 2.24$ m/s
Water velocity (AC)	$u_{AC} = \frac{4\dot{m}_{AC}}{\pi\rho d^2} = \frac{4\times16.72}{3.14*960*0.1^2} = 2.21$ m/s
Water velocity (BC)	$u_{BC} = \frac{4\dot{m}_{BC}}{\pi\rho d^2} = \frac{4\times2.35}{3.14*960*0.1^2} = 0.31$ m/s

Appendix B

- ***Standard pipe size:***

Table B2-1 Standard size of pre-insulated steel pipe

d (mm)	*U* (W/mK)
15	0.122
20	0.155
25	0.18
32	0.189
40	0.21
50	0.219
65	0.236
80	0.278
100	0.327
125	0.321
150	0.367
200	0.455
250	0.549
300	0.631
350	0.576
400	0.62

- ***District heating design cases:***

Table B2-2 Physical and heating parameters of district heating design cases

	Pipe No.	From node	To node	DH1	DH2	DH3	DH4	DH5	DH6	DH7	DH8	DH9	DH10	DH11	DH12	DH13	DH14	DH15	DH16	DH17	DH18
				d (mm)	d (mm)	d (mm)	d (mm)	d (mm)	d (mm)	d (mm)	d (mm)	d (mm)	d (mm)	d (mm)	d (mm)	d (mm)	d (mm)	d (mm)	d (mm)	d (mm)	d (mm)
$T_{s,max}/T_{r,max}$: 120/70 °C	1	1	2	250	250	250	200	200	200	200	150	200	200	150	200	150	150	150	150	150	150
	2	2	3	125	125	100	100	100	100	100	80	80	80	80	80	80	80	80	80	80	80
	3	2	4	250	250	200	200	200	200	200	200	150	150	150	150	150	150	150	150	125	125
	4	4	5	150	125	100	100	100	100	100	100	80	80	80	80	80	80	80	80	80	80
	5	4	6	250	200	200	200	200	150	150	150	150	150	150	150	150	150	125	125	125	125
	6	6	7	125	125	100	100	100	100	100	100	100	100	100	80	80	80	80	80	80	80
	7	6	8	200	150	150	150	125	150	125	125	150	125	125	125	125	125	125	125	125	100
	8	8	9	150	125	125	100	100	100	100	100	100	100	100	100	100	80	100	80	80	80
	9	8	10	125	100	100	100	80	80	80	80	80	80	80	65	65	65	65	65	65	65
	10	8	11	125	125	100	100	100	100	100	100	80	80	80	80	80	80	80	80	80	80
	12	11	12	100	80	80	65	65	65	65	65	65	65	65	50	50	50	50	50	50	50
	12	11	13	100	100	100	80	80	80	80	80	80	80	80	65	65	65	65	65	65	65
	d_{eq} (mm)			176	159	143	136	134	127	126	122	115	114	111	109	106	104	102	100	96	95
	$\dot{V}_{max}$ (m^3/s)			0.057	0.057	0.057	0.057	0.057	0.057	0.057	0.057	0.057	0.057	0.057	0.057	0.057	0.057	0.057	0.057	0.057	0.057
	u_{max} (m/s)			1.25	1.72	1.72	1.95	2.48	2.3	2.48	3.48	2.91	2.91	3.47	2.91	3.47	3.47	3.47	3.47	4.2	4.2
	$\Delta p_{p,max}$ (kPa)			108	158	222	285	232	384	423	498	543	581	657	701	777	919	982	1125	1454	1593
	$P_{p,max}$ (kW)			8	12	17	22	25	30	32	38	42	45	50	54	60	71	75	86	112	122
	$Q_{loss,max}$ (kW)			88	82	80	78	77	75	74	73	70	70	69	67	66	65	65	63	62	62

	Pipe No.	From node	To node	DH19	DH20	DH21	DH22	DH23	DH24	DH25	DH26	DH27	DH28	DH29	DH30	DH31	DH32	DH33	DH34	DH35	DH36
				d (mm)	d (mm)	d (mm)	d (mm)	d (mm)	d (mm)	d (mm)	d (mm)	d (mm)	d (mm)	d (mm)	d (mm)	d (mm)	d (mm)	d (mm)	d (mm)	d (mm)	d (mm)
$T_{s,max}/T_{r,max}$: 110/70 °C	1	1	2	300	250	250	250	200	200	200	200	200	200	150	150	200	200	150	150	150	150
	2	2	3	150	125	100	100	100	100	100	100	100	100	100	100	80	80	80	80	80	80
	3	2	4	300	250	250	200	200	200	200	200	200	200	200	200	150	150	150	150	150	150
	4	4	5	150	125	125	100	100	100	100	100	100	100	100	100	100	100	100	100	100	100
	5	4	6	250	250	200	200	200	200	200	150	150	150	150	150	150	150	150	150	150	125

6	6	7	150	125	125	125	100	100	100	100	100	100	100	100	100	100	100	100	80	80
7	6	8	250	200	150	150	150	200	150	150	150	125	150	125	150	125	150	125	125	125
8	8	9	150	125	125	125	125	100	100	125	100	100	100	100	100	100	100	100	100	100
9	8	10	125	100	100	100	100	80	80	100	80	80	80	80	80	80	80	80	80	80
10	8	11	150	125	100	100	100	80	80	100	100	100	100	100	100	100	100	80	80	80
12	11	12	100	100	80	80	80	80	80	65	65	65	65	65	65	65	65	65	65	65
12	11	13	125	100	100	100	80	80	80	80	80	80	80	80	80	80	80	80	65	65
d_{eq} (mm)			196	170	157	146	139	137	135	131	127	126	124	123	118	116	114	113	109	105
$\dot{V}_{max}$ (m^3/s)			0.071	0.071	0.071	0.071	0.071	0.071	0.071	0.071	0.071	0.071	0.071	0.071	0.071	0.071	0.071	0.071	0.071	0.071
u_{max} (m/s)			1.08	1.55	2.13	2.13	2.42	2.48	2.48	2.85	2.85	3.07	4.31	4.31	3.61	3.61	4.31	4.31	4.31	4.31
$\Delta p_{p,max}$ (kPa)			100	159	218	266	338	385	414	492	567	627	684	743	813	873	930	989	1175	1493
$P_{p,max}$ (kW)			10	15	21	25	32	37	39	47	54	60	65	71	78	83	89	94	112	142
$Q_{loss,max}$ (kW)			89	81	77	75	74	73	73	71	71	70	70	70	68	68	67	66	64	63

$T_{s,max}/T_{r,max}$: 100/70 °C

Pipe No.	**From node**	**To node**	**DH37** d (mm)	**DH38** d (mm)	**DH39** d (mm)	**DH40** d (mm)	**DH41** d (mm)	**DH42** d (mm)	**DH43** d (mm)	**DH44** d (mm)	**DH45** d (mm)	**DH46** d (mm)	**DH47** d (mm)	**DH48** d (mm)	**DH49** d (mm)	**DH50** d (mm)	**DH51** d (mm)	**DH52** d (mm)	**DH53** d (mm)	**DH54** d (mm)
1	1	2	350	300	250	250	250	250	250	200	200	200	200	150	200	200	150	150	200	200
2	2	3	150	125	125	125	125	100	100	125	100	100	100	80	100	100	100	100	100	100
3	2	4	300	250	250	250	250	200	200	200	200	200	200	200	200	200	200	200	150	150
4	4	5	150	150	150	125	125	125	125	125	100	100	100	100	100	100	100	100	100	100
5	4	6	300	250	250	200	200	200	200	200	200	200	200	200	150	150	150	150	150	150
6	6	7	150	150	125	125	125	125	125	125	100	100	100	100	100	100	100	100	100	100
7	6	8	250	250	200	200	150	200	150	150	150	200	150	200	150	125	150	125	150	125
8	8	9	200	150	150	150	125	125	125	125	125	100	100	100	100	100	100	100	100	100
9	8	10	150	125	125	100	100	100	100	100	100	80	80	80	80	80	80	80	80	80
10	8	11	150	150	125	125	125	125	100	100	100	100	100	100	100	100	100	100	100	100
12	11	12	125	100	100	80	80	80	80	80	80	80	80	65	65	65	65	65	65	65
12	11	13	125	125	100	100	100	100	100	100	80	80	80	80	80	80	80	80	80	80
d_{eq} (mm)			214	186	176	164	159	151	148	146	139	138	135	134	127	126	124	123	118	117
$\dot{V}_{max}$ (m^3/s)			0.094	0.094	0.094	0.094	0.094	0.094	0.094	0.094	0.094	0.094	0.094	0.094	0.094	0.094	0.094	0.094	0.094	0.094
u_{max} (m/s)			1.19	1.72	2.05	2.12	2.82	2.69	2.82	3.21	3.21	3.21	3.21	5.70	3.78	4.07	5.70	5.70	4.78	4.78
$\Delta p_{p,max}$ (kPa)			107	161	207	260	345	379	430	470	558	640	690	845	961	1066	1167	1271	1395	1500
$P_{p,max}$ (kW)			13	20	26	33	44	48	54	59	70	81	87	107	121	134	147	160	176	189
$Q_{loss,max}$ (kW)			87	81	78	74	72	71	70	70	69	69	69	68	66	66	66	65	64	64

$T_{s,max}/T_{r,max}$: 90/70 °C	Pipe No.	From node	To node	DH55 d (mm)	DH56 d (mm)	DH57 d (mm)	DH58 d (mm)	DH59 d (mm)	DH60 d (mm)	DH61 d (mm)	DH62 d (mm)	DH63 d (mm)	DH64 d (mm)	DH65 d (mm)	DH66 d (mm)	DH67 d (mm)	DH68 d (mm)	DH69 d (mm)	DH70 d (mm)	DH71 d (mm)	DH72 d (mm)
	1	1	2	400	300	300	300	300	250	300	250	250	250	200	250	200	200	250	200	200	200
	2	2	3	200	150	150	150	150	125	125	125	125	125	125	125	125	125	125	100	100	100
	3	2	4	350	300	300	300	250	250	250	250	250	250	250	200	200	200	200	200	200	200
	4	4	5	200	200	150	150	150	150	125	125	125	125	125	125	125	125	125	125	125	125
	5	4	6	300	300	250	250	250	250	250	250	200	200	200	200	200	200	200	200	200	200
	6	6	7	200	200	150	150	150	125	125	125	125	125	125	125	125	125	100	100	100	100
	7	6	8	300	250	250	200	200	200	200	200	200	200	200	200	200	150	150	150	200	150
	8	8	9	200	200	200	150	150	150	125	125	150	125	125	125	125	125	125	125	100	100
	9	8	10	150	150	125	125	125	125	100	100	100	100	100	100	100	100	100	100	100	100
	10	8	11	200	150	150	150	150	125	125	125	125	125	125	125	125	125	100	100	100	100
	12	11	12	125	125	100	100	100	100	100	80	80	80	80	80	80	80	80	80	65	65
	12	11	13	150	150	125	125	125	100	100	100	100	100	100	100	100	100	100	100	100	100
	d_{eq}(mm)			244	223	201	193	185	176	173	169	164	161	158	152	149	147	146	142	142	139
	$\dot{V}_{max}$ (m^3/s)			0.14	0.14	0.14	0.14	0.14	0.14	0.14	0.14	0.14	0.14	0.14	0.14	0.14	0.14	0.14	0.14	0.14	0.14
	u_{max} (m/s)			1.40	2.12	2.12	2.36	2.56	3.05	2.65	3.05	3.16	3.16	4.77	4	4.77	4.77	4.2	4.77	4.77	4.77
	$\Delta p_{p,max}$ (kPa)			111	153	217	266	318	400	453	478	517	595	685	783	873	986	1092	1182	1365	1477
	$P_{p,max}$ (kW)			21	29	41	50	60	75	85	90	97	112	128	147	164	185	205	222	256	277
	$Q_{loss,max}$ (kW)			88	87	80	77	75	73	72	71	70	68	68	66	66	65	66	65	66	65

- ***Price of pipe:***

Table B2-3 Prices of pipes excluding associated civil works

Size (mm)	Price (£/m)
DN[1]25/90	126
DN 32/110	134
DN 40/110	140
DN 50/125	146
DN 65/140	151
DN 80/160	161
DN 100/200	182
DN 125/225	209
DN 150/250	259
DN 200/315	325
DN 250/400	488
DN 300/450	626
DN 400/520	765
DN 500/710	897
DN 600/800	1040

- ***Price of pump and variable frequency drive:***

Table B2-4 a) Price of pump and variable speed drive, $T_{s,max}/T_{r,max}$: 120/70 ℃

TPL (Pa/m)	Flow rate (m^3/s)	Pump differential pressure (Pa)	Pump size (kW)	Pump investment cost (£)	Variable frequency drive investment cost (£)
50	0.057	107714	8	2915	956
100	0.057	158466	12	3475	1190
150	0.057	221731	17	4145	1450
200	0.057	284914	22	5070	1648
250	0.057	323297	25	5971	1916
300	0.057	384126	30	7542	1916
350	0.057	422504	32	7542	2439
400	0.057	497816	38	8700	2822
450	0.057	543079	42	9859	3267
500	0.057	581433	45	9859	3267
550	0.057	656701	50	10845	4004
600	0.057	701445	54	11609	4004
700	0.057	776677	60	15288	4004
800	0.057	919391	71	15812	4004
900	0.057	981999	75	15812	4717
1000	0.057	1124643	86	12854	5436
1100	0.057	1453724	112	16045	5936
1200	0.057	1593455	122	16045	5936

[1] Diametre Nominal

Table B2-4 b) Price of pump and variable speed drive, $T_{s,max}/T_{r,max}$: 110/70 ℃

TPL (Pa/m)	Flow rate (m^3/s)	Pump differential pressure (Pa)	Pump size (kW)	Pump investment cost (£)	Variable frequency drive investment cost (£)
50	0.071	99665	10	3112	956
100	0.071	159179	15	3820	1450
150	0.071	217840	21	5119	1648
200	0.071	265787	25	5971	1916
250	0.071	338425	32	6484	2439
300	0.071	384904	37	6680	2439
350	0.071	413588	39	7542	2822
400	0.071	492101	47	8700	3246
450	0.071	567231	54	9859	3246
500	0.071	626660	60	9859	3662
550	0.071	683887	65	11609	4717
600	0.071	743307	71	15288	4717
700	0.071	813475	78	15288	4717
800	0.071	872876	83	15812	5436
900	0.071	930081	89	15812	5436
1000	0.071	989432	94	16884	5436
1100	0.071	1175237	112	14295	5936
1200	0.071	1493271	142	16045	7916

Table B2-4 c) Price of pump and variable speed drive, $T_{s,max}/T_{r,max}$: 100/70 ℃

TPL (Pa/m)	Flow rate (m^3/s)	Pump differential pressure (Pa)	Pump size (kW)	Pump investment cost (£)	Variable frequency drive investment cost (£)
50	0.094	106568	13	4225	1190
100	0.094	160722	20	4893	1648
150	0.094	207068	26	5854	1916
200	0.094	259799	33	7740	2439
250	0.094	345488	44	8997	2822
300	0.094	379365	48	8997	3246
350	0.094	429952	54	10353	3246
400	0.094	469948	59	11512	3662
450	0.094	557840	70	11512	3662
500	0.094	639822	81	15912	4310
550	0.094	690359	87	16884	5436
600	0.094	845469	107	16440	6280
700	0.094	961050	121	19372	6280
800	0.094	1065770	134	19372	7916
900	0.094	1166643	147	19372	7972
1000	0.094	1271350	160	19372	7972
1100	0.094	1394980	176	19372	7972
1200	0.094	1499658	189	19372	7972

Table B2-4 d) Price of pump and variable speed drive, $T_{s,max}/T_{r,max}$: 90/70 ℃

TPL (Pa/m)	Flow rate (m^3/s)	Pump differential pressure (Pa)	Pump size (kW)	Pump investment cost (£)	Variable frequency drive investment cost (£)
50	0.14	110621	21	5854	1648
100	0.14	153107	29	5854	1916
150	0.14	216819	41	8898	2822
200	0.14	266391	50	10253	3246
250	0.14	318427	60	10353	3662
300	0.14	399671	75	11512	4310
350	0.14	453340	85	11512	4310
400	0.14	477954	90	15388	4310
450	0.14	517188	97	15388	5134
500	0.14	595451	112	15912	6670
550	0.14	684677	128	17871	7916
600	0.14	783784	147	20063	7972
700	0.14	872981	164	20063	7972
800	0.14	985736	185	20160	7972
900	0.14	1092328	205	31093	9087
1000	0.14	1181504	222	31093	9087
1100	0.14	1364521	256	31093	9987
1200	0.14	1477215	277	31093	9987

- ***Estimated cost of pipe and pump:***

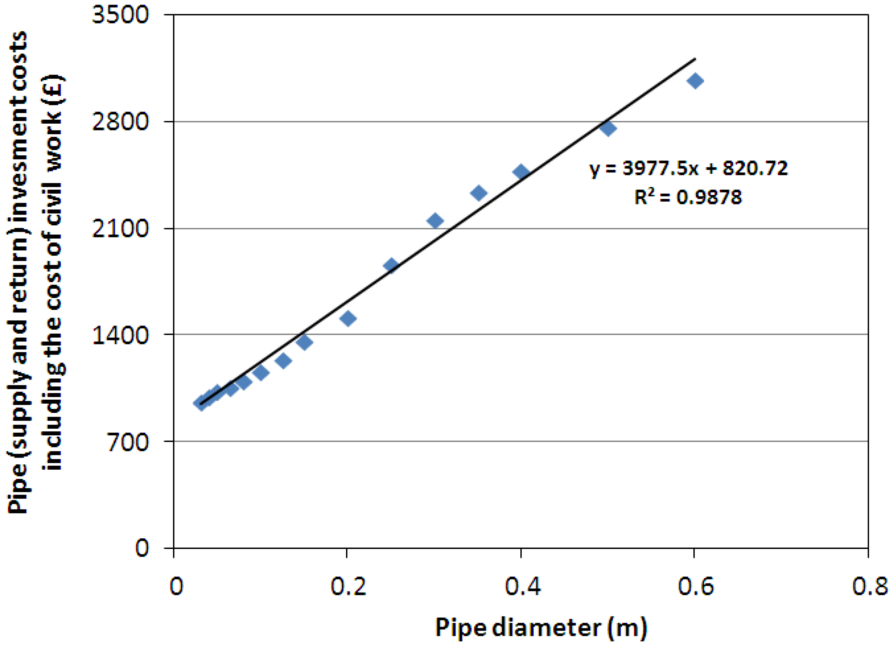

Figure B4-1 Estimation of pipe (supply and return) investment costs including the cost of civil work

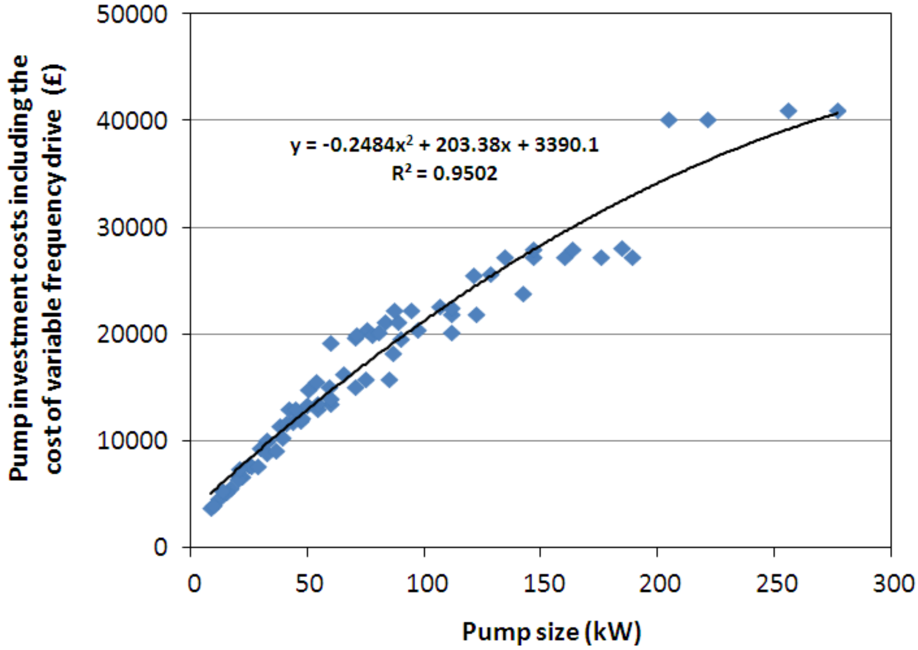

Figure B4-2 Estimation of pump investment costs including the cost of variable frequency drive

- **High temperature district heating**

A. Minimisation of the annual total energy consumption:

Table B4-1 Obtained physical and heating parameters of the design case with minimum annual total energy consumption, high temperature district heating

Pipe No.	From node	To node	d (m)	Maximum velocity (m/s)	Maximum pressure loss (Pa)	Maximum pressure loss per meter (Pa/m)
Pipe01	Node01	Node02	0.08	2.16	227745	884
Pipe02	Node02	Node03	0.025	1.07	100127	1027
Pipe03	Node02	Node04	0.032	0.87	24623	483
Pipe04	Node02	Node05	0.08	1.92	41784	702
Pipe05	Node05	Node06	0.032	0.70	84291	311
Pipe06	Node05	Node07	0.05	1.11	102671	436
Pipe07	Node07	Node08	0.032	0.70	55680	314
Pipe08	Node07	Node09	0.032	0.68	30786	299
Pipe09	Node07	Node10	0.032	0.72	81277	328
Pipe10	Node05	Node11	0.08	1.39	59139	368
Pipe11	Node11	Node12	0.025	1.11	142442	1103
Pipe12	Node11	Node13	0.065	1.76	143392	771
Pipe13	Node13	Node14	0.065	1.76	104944	771
Pipe14	Node14	Node15	0.032	1.06	30288	725
Pipe15	Node15	Node16	0.025	0.87	78791	675
Pipe16	Node15	Node17	0.025	0.88	93528	686
Pipe17	Node14	Node18	0.025	0.87	91943	674
Pipe18	Node14	Node19	0.065	1.27	18131	404
Pipe19	Node19	Node20	0.025	0.88	94408	692
Pipe20	Node19	Node21	0.025	0.88	92639	691
Pipe21	Node19	Node22	0.05	1.74	44319	1063
Pipe22	Node22	Node23	0.032	0.71	52046	323
Pipe23	Node22	Node24	0.032	0.71	42627	318
Pipe24	Node22	Node25	0.05	1.16	24587	472
Pipe25	Node25	Node26	0.032	0.71	43603	321
Pipe26	Node25	Node27	0.032	0.71	39214	318
Pipe27	Node25	Node28	0.04	0.91	23970	388
Pipe28	Node28	Node29	0.032	0.71	30327	319
Pipe29	Node28	Node30	0.032	0.71	33693	321
Average pressure drop in route with maximum pressure loss (Pa/m)						709
Maximum flow (kg/s)						10.85
Maximum pump differential pressure (kPa)						1638
Maximum pump power (kW)						22

B. *Minimisation of the annual total exergy consumption:*

Table B4-2 Obtained physical and heating parameters of the design case with minimum annual total exergy consumption, high temperature district heating

Pipe No.	From node	To node	d (m)	Maximum velocity (m/s)	Maximum pressure loss (Pa)	Maximum pressure loss per meter (Pa/m)
Pipe01	Node01	Node02	0.125	0.88	21458	83
Pipe02	Node02	Node03	0.04	0.42	8092	83
Pipe03	Node02	Node04	0.04	0.56	7471	146
Pipe04	Node02	Node05	0.1	1.23	12812	215
Pipe05	Node05	Node06	0.04	0.45	25576	94
Pipe06	Node05	Node07	0.065	0.66	25432	108
Pipe07	Node07	Node08	0.04	0.45	16895	95
Pipe08	Node07	Node09	0.04	0.44	9341	91
Pipe09	Node07	Node10	0.04	0.46	24662	100
Pipe10	Node05	Node11	0.1	0.89	18134	113
Pipe11	Node11	Node12	0.04	0.43	11512	89
Pipe12	Node11	Node13	0.1	0.74	14606	78
Pipe13	Node13	Node14	0.1	0.74	10689	78
Pipe14	Node14	Node15	0.04	0.68	9190	220
Pipe15	Node15	Node16	0.032	0.53	20986	180
Pipe16	Node15	Node17	0.032	0.53	24911	183
Pipe17	Node14	Node18	0.032	0.53	24489	180
Pipe18	Node14	Node19	0.08	0.84	6023	134
Pipe19	Node19	Node20	0.032	0.54	25145	184
Pipe20	Node19	Node21	0.032	0.54	24674	184
Pipe21	Node19	Node22	0.08	0.68	3647	87
Pipe22	Node22	Node23	0.04	0.46	15792	98
Pipe23	Node22	Node24	0.04	0.45	12934	96
Pipe24	Node22	Node25	0.065	0.69	6090	117
Pipe25	Node25	Node26	0.04	0.45	13230	97
Pipe26	Node25	Node27	0.04	0.45	11899	97
Pipe27	Node25	Node28	0.05	0.58	7294	118
Pipe28	Node28	Node29	0.04	0.45	9202	97
Pipe29	Node28	Node30	0.04	0.45	10223	97
Average pressure drop in route with maximum pressure loss (Pa/m)					126	
Maximum flow (kg/s)					10.85	
Maximum pump differential pressure (kPa)					296	
Maximum pump power (kW)					4	

C. Minimisation of the equivalent annual cost:

Table B4-3 Obtained physical and heating parameters of the design case with minimum EAC, *Ideal-DH*, *Boiler-DH* and *CHP-DH*, high temperature district heating

Pipe No.	From node	To node	d (m)	Maximum velocity (m/s)	Maximum pressure loss (Pa)	Maximum pressure loss per meter (Pa/m)
Pipe01	Node01	Node02	0.08	2.16	227745	884
Pipe02	Node02	Node03	0.025	1.07	100127	1027
Pipe03	Node02	Node04	0.032	0.87	24623	483
Pipe04	Node02	Node05	0.08	1.92	41784	702
Pipe05	Node05	Node06	0.032	0.70	84291	311
Pipe06	Node05	Node07	0.05	1.11	102671	436
Pipe07	Node07	Node08	0.032	0.70	55680	314
Pipe08	Node07	Node09	0.032	0.68	30786	299
Pipe09	Node07	Node10	0.032	0.72	81277	328
Pipe10	Node05	Node11	0.08	1.39	59139	368
Pipe11	Node11	Node12	0.025	1.11	142442	1103
Pipe12	Node11	Node13	0.065	1.76	143392	771
Pipe13	Node13	Node14	0.065	1.76	104944	771
Pipe14	Node14	Node15	0.032	1.06	30288	725
Pipe15	Node15	Node16	0.025	0.87	78791	675
Pipe16	Node15	Node17	0.025	0.88	93528	686
Pipe17	Node14	Node18	0.025	0.87	91943	674
Pipe18	Node14	Node19	0.065	1.27	18131	404
Pipe19	Node19	Node20	0.025	0.88	94408	692
Pipe20	Node19	Node21	0.025	0.88	92639	691
Pipe21	Node19	Node22	0.05	1.74	44319	1063
Pipe22	Node22	Node23	0.032	0.71	52046	323
Pipe23	Node22	Node24	0.032	0.71	42627	318
Pipe24	Node22	Node25	0.05	1.16	24587	472
Pipe25	Node25	Node26	0.032	0.71	43603	321
Pipe26	Node25	Node27	0.032	0.71	39214	318
Pipe27	Node25	Node28	0.04	0.91	23970	388
Pipe28	Node28	Node29	0.032	0.71	30327	319
Pipe29	Node28	Node30	0.032	0.71	33693	321
Average pressure drop in route with maximum pressure loss (Pa/m)						709
Maximum flow (kg/s)						10.85
Maximum pump differential pressure (kPa)						1638
Maximum pump power (kW)						22

- **Low temperature district heating**

A. Minimisation of the annual total energy consumption:

Table B4-4 Obtained physical and heating parameters of the design case with minimum annual total energy consumption, low temperature district heating

Pipe No.	From node	To node	d (m)	Maximum velocity (m/s)	Maximum pressure loss (Pa)	Maximum pressure loss per meter (Pa/m)
Pipe01	Node01	Node02	0.1	1.97	141801	550
Pipe02	Node02	Node03	0.032	0.94	54964	564
Pipe03	Node02	Node04	0.032	1.26	51740	1015
Pipe04	Node02	Node05	0.1	1.74	25689	432
Pipe05	Node05	Node06	0.032	0.97	162170	598
Pipe06	Node05	Node07	0.05	1.56	202312	859
Pipe07	Node07	Node08	0.032	0.98	109071	615
Pipe08	Node07	Node09	0.032	0.97	61712	600
Pipe09	Node07	Node10	0.032	0.99	155902	629
Pipe10	Node05	Node11	0.08	1.96	117083	728
Pipe11	Node11	Node12	0.032	0.95	75126	582
Pipe12	Node11	Node13	0.08	1.62	92649	498
Pipe13	Node13	Node14	0.08	1.62	67807	498
Pipe14	Node14	Node15	0.04	0.94	17669	423
Pipe15	Node15	Node16	0.032	0.77	44806	384
Pipe16	Node15	Node17	0.032	0.78	52755	387
Pipe17	Node14	Node18	0.032	0.74	47371	347
Pipe18	Node14	Node19	0.065	1.78	35270	786
Pipe19	Node19	Node20	0.032	0.74	47466	348
Pipe20	Node19	Node21	0.032	0.74	46619	348
Pipe21	Node19	Node22	0.065	1.42	20897	501
Pipe22	Node22	Node23	0.032	0.98	98617	612
Pipe23	Node22	Node24	0.032	0.97	81430	607
Pipe24	Node22	Node25	0.05	1.60	46816	899
Pipe25	Node25	Node26	0.032	0.98	82920	610
Pipe26	Node25	Node27	0.032	0.97	74864	607
Pipe27	Node25	Node28	0.04	1.25	45610	738
Pipe28	Node28	Node29	0.032	1.02	63571	668
Pipe29	Node28	Node30	0.032	1.02	70404	670
Average pressure drop in route with maximum pressure loss (Pa/m)					662	
Maximum flow (kg/s)					15.47	
Maximum pump differential pressure (kPa)					1511	
Maximum pump power (kW)					29	

B. Minimisation of the annual total exergy consumption:

Table B4-5 Obtained physical and heating parameters of the design case with minimum annual total exergy consumption, low temperature district heating

Pipe No.	From node	To node	d (m)	Maximum velocity (m/s)	Maximum pressure loss (Pa)	Maximum pressure loss per meter (Pa/m)
Pipe01	Node01	Node02	0.15	0.88	16640	65
Pipe02	Node02	Node03	0.05	0.38	5075	52
Pipe03	Node02	Node04	0.065	0.31	1183	23
Pipe04	Node02	Node05	0.15	0.78	3015	51
Pipe05	Node05	Node06	0.05	0.40	14973	55
Pipe06	Node05	Node07	0.08	0.61	16648	71
Pipe07	Node07	Node08	0.05	0.40	10071	57
Pipe08	Node07	Node09	0.05	0.40	5698	55
Pipe09	Node07	Node10	0.05	0.41	14395	58
Pipe10	Node05	Node11	0.125	0.80	11032	69
Pipe11	Node11	Node12	0.05	0.39	6936	54
Pipe12	Node11	Node13	0.125	0.66	8729	47
Pipe13	Node13	Node14	0.125	0.66	6389	47
Pipe14	Node14	Node15	0.065	0.36	1332	32
Pipe15	Node15	Node16	0.05	0.32	4137	35
Pipe16	Node15	Node17	0.05	0.32	4871	36
Pipe17	Node14	Node18	0.05	0.30	4374	32
Pipe18	Node14	Node19	0.125	0.48	1104	25
Pipe19	Node19	Node20	0.05	0.30	4383	32
Pipe20	Node19	Node21	0.05	0.30	4304	32
Pipe21	Node19	Node22	0.1	0.60	2129	51
Pipe22	Node22	Node23	0.05	0.40	9105	57
Pipe23	Node22	Node24	0.05	0.40	7519	56
Pipe24	Node22	Node25	0.08	0.62	3852	74
Pipe25	Node25	Node26	0.05	0.40	7656	56
Pipe26	Node25	Node27	0.05	0.40	6912	56
Pipe27	Node25	Node28	0.065	0.47	3438	56
Pipe28	Node28	Node29	0.05	0.42	5870	62
Pipe29	Node28	Node30	0.05	0.42	6500	62
Average pressure drop in route with maximum pressure loss (Pa/m)					62	
Maximum flow (kg/s)					15.47	
Maximum pump differential pressure (kPa)					188	
Maximum pump power (kW)					4	

C. Minimisation of the equivalent annual cost:

Table B4-6 Obtained physical and heating parameters of the design case with minimum EAC, *Ideal-DH*, *Boiler-DH* and *CHP-DH*, low temperature district heating

Pipe No.	From node	To node	d (m)	Maximum velocity (m/s)	Maximum pressure loss (Pa)	Maximum pressure loss per meter (Pa/m)
Pipe01	Node01	Node02	0.1	1.97	142033	551
Pipe02	Node02	Node03	0.032	0.94	55071	565
Pipe03	Node02	Node04	0.032	1.26	51859	1017
Pipe04	Node02	Node05	0.1	1.75	25730	432
Pipe05	Node05	Node06	0.032	0.97	162324	598
Pipe06	Node05	Node07	0.05	1.56	202590	861
Pipe07	Node07	Node08	0.032	0.98	109213	616
Pipe08	Node07	Node09	0.032	0.97	61819	601
Pipe09	Node07	Node10	0.032	0.99	156042	630
Pipe10	Node05	Node11	0.08	1.96	117280	729
Pipe11	Node11	Node12	0.032	0.96	75277	583
Pipe12	Node11	Node13	0.08	1.62	92827	499
Pipe13	Node13	Node14	0.08	1.62	67937	499
Pipe14	Node14	Node15	0.04	0.95	17736	424
Pipe15	Node15	Node16	0.032	0.74	40663	348
Pipe16	Node15	Node17	0.032	0.74	47884	351
Pipe17	Node14	Node18	0.032	0.74	47466	348
Pipe18	Node14	Node19	0.065	1.78	35342	787
Pipe19	Node19	Node20	0.032	0.74	47556	349
Pipe20	Node19	Node21	0.032	0.74	46708	348
Pipe21	Node19	Node22	0.065	1.42	20941	502
Pipe22	Node22	Node23	0.032	0.98	98812	613
Pipe23	Node22	Node24	0.032	0.98	81604	608
Pipe24	Node22	Node25	0.05	1.60	46913	900
Pipe25	Node25	Node26	0.032	0.98	83090	611
Pipe26	Node25	Node27	0.032	0.98	75023	608
Pipe27	Node25	Node28	0.04	1.25	45705	740
Pipe28	Node28	Node29	0.032	1.02	63723	669
Pipe29	Node28	Node30	0.032	1.03	70568	671
Average pressure drop in route with maximum pressure loss (Pa/m)					662	
Maximum flow (kg/s)					15.47	
Maximum pump differential pressure (kPa)					1511	
Maximum pump power (kW)					29	